EFFECTS OF FORMULATION AND PROCESSING PARAMETERS ON SODIUM AVAILABILITY IN A MODEL LIPOPROTEIC EMULSION GEL

BY

KYLE SATOSHI OKADA

THESIS

Submitted in partial fulfilliment of the requirements
for the degree of Master of Science in Food Science and Human Nutrition
with a concentration in Food Science
in the Graduate College of the
University of Illinois at Urbana-Champaign, 2016

Urbana, Illinois

Adviser:

Assistant Professor Youngsoo Lee

Abstract

Sodium reduction in processed foods is a high priority in the food industry due to the health implications of excessive dietary sodium consumption. Foods with a lipid/protein-based (lipoproteic) emulsion structure (such as processed cheeses and meats) are of particular interest because of their contribution to dietary sodium and the role of sodium in desired sensory and textural properties. When reducing sodium content in these food systems, it is crucial to understand the physicochemical and matrix properties contributing to sodium availability and saltiness perception.

The overall objective of this study was to characterize chemical and rheological influences on sodium availability in a model lipoproteic emulsion gel. There were three specific aims to accomplish the overall objective. The first aim was to characterize the effects of formulation and processing parameters on sodium ion molecular mobility and binding in the model gel system. The second aim was to characterize how altering formulation and processing parameters affected rheological and structural properties. The third aim was to correlate the measured mobility and rheological properties with sensory perceived saltiness and texture attributes.

To accomplish these objectives, model lipoproteic gels formulated with varying protein, fat, and NaCl content and processed with varying homogenization pressure were prepared. Sodium ion molecular activity was characterized with ^{23}Na nuclear magnetic resonance (NMR) spectroscopy. Single quantum (SQ) experiments were used to characterize the mobility of overall sodium in the system, while double quantum filtered (DQF) experiments were used to characterize sodium in a restricted mobility ('bound') state and quantify relative 'bound' sodium. Formulation and processing parameters were found to influence gel structure and sodium matrix-

interactions. Increasing protein or fat content reduced sodium mobility, and increasing protein or fat content or homogenization pressure increased the amount of relative 'bound' sodium. Rheological and structural properties were characterized with small deformation oscillatory rheometry and creep compliance/recovery rheometry. Gel mechanical behavior was successfully modeled with a four-component Burgers model, and it was found that increasing protein, fat, or salt content or homogenization pressure resulted in a stronger and more solid protein network structure. The results from the ^{23}Na NMR and rheometry experiments were correlated with sensory taste and texture properties obtained by quantitative descriptive analysis (QDA). Salty taste and syneresis texture correlated positively with sodium mobility and elastic compliance, and correlated negatively with dry matter content, relative 'bound' sodium, and gel firmness.

This study found that formulation and homogenization pressure significantly influence sodium behavior and rheology in lipoproteic emulsion gels, which may have significant implications for saltiness perception and sodium reduction. The results suggest that saltiness perception can be influenced by altering sodium availability via modulation of molecular interactions, texture, and sodium release. Future research could explore increasing saltiness perception by introducing species that compete with sodium for binding sites to increase sodium availability.

Acknowledgements

This research would not have been possible without the support and input of many others. I would like to thank my adviser, Dr. Youngsoo Lee, for his continuing guidance in my development as a researcher, academic, and professional. I would also like to thank the members of my thesis committee, Dr. Shelly Schmidt and Dr. Graciela Padua, for their feedback regarding my research and their tutelage as instructors. My graduate pursuits were supported by the Jeannette Chu and Winston Y. Lo Endowed Fellowship in Food Science and Human Nutrition. This material is based upon work that is supported by the National Institute of Food and Agriculture, U.S. Department of Agriculture, under award number 2015-67017-23089.

I would like to give special thanks to several people who were essential to the completion of this research. Dr. Wan-Yuan Kuo, of the Dr. Youngsoo Lee laboratory, was key in the development of the model gel system and researching other properties beyond the scope of my experiments. Emily Defnet, formerly of the Dr. Shelly Schmidt laboratory, and Dr. Lingyang Zhu, of the NMR Lab of the School of Chemical Sciences, were instrumental in adapting the NMR data collection and analysis methodologies. Brian Jacobson and Scott Buchanon, of the UIUC Pilot Plant, maintained the APV homogenizer and ensured safe and successful homogenization operations. Thank you to all of these valued contributors.

I would like to also thank my labmates from the Dr. Youngsoo Lee and Dr. Soo-Yeun Lee laboratories for welcoming and supporting me with their friendship and fellowship. Some of my fondest, most enduring memories will be lunches with my FSHN family at the Bevier Café. Finally, I would like to thank my family, friends, and especially my girlfriend, Wendy Chen, for their love and encouragement on this journey of exploration and growth. You are the inspiration of my aspirations, the motivation of my perspiration.

Table of Contents

List of Tables

List of Figures

Chapter 1. Introduction

1.1 Motivation

In the United States, 81-97% of males and 63-91% of females had usual dietary sodium intakes above the upper limit for their age and gender (Dietary Guidelines Advisory Committee 2015). Excessive dietary sodium consumption is associated with risks for increased blood pressure, cardiovascular damage, stroke, and other health issues(de Wardener and MacGregor 2002). High blood pressure is the single largest risk factor for cardiovascular-related mortality, and high blood pressure and excessive salt consumption accounted for approximately 400,000 and 100,000 deaths in US adults in 2005, respectively (Danaei et al. 2009). It has been estimated that reducing dietary sodium consumption by 400 mg/day could prevent up to 28,000 deaths and save up to $7 billion annually, not including additional long-term benefits resulting from reduced intake by children (Dietary Guidelines Advisory Committee 2010).

Sodium added during processing accounts for approximately 75% of dietary sodium, making processed foods major targets for sodium reduction efforts (Mattes and Donnelly 1991; Dietary Guidelines Advisory Committee 2010). Food products containing lipid/protein-based (lipoproteic) emulsion food matrices (i.e. processed meats and cheeses) in particular are prevalent and substantial sources of dietary sodium, with over 36% of dietary sodium coming from bread and rolls, cold cuts/cured meats, pizza, fresh and processed poultry, sandwiches like cheeseburgers, cheese, pasta mixed dishes, and meat mixed dishes (Centers for Disease Control and Prevention 2012). In processed foods, sodium salts contribute to salty taste, flavor balance, structure and texture, stability, enzyme activity, and leavening (Busch et al. 2013).

Sodium reduction strategies aim to reduce sodium content while maintaining desired properties and consumer acceptance. Many strategies focus on optimizing sodium availability or

distribution by modifying food composition and structure, with the hypothesis that increasing sodium availability increases saltiness perception (Busch et al. 2013; Guodjonsdottir et al. 2013; Kuo and Lee 2014a). For the purposes of this research, sodium availability refers to the accessibility and behavior of sodium; i.e. sodium ions that are more mobile and less restricted have more availability. Matrix composition and structure may influence sodium mobility and binding via ionic interactions with the matrix components (Rosett et al. 1994; Picouet et al. 2012; Mosca et al. 2015), and matrix diffusivity and sodium release from the food structure (Lauverjat et al. 2009; Boisard et al. 2013; Kuo and Lee 2014a; Kuo and Lee 2014b). Sensory saltiness perception may also be influenced by texture effects on mastication, salivation, and cross-modal taste-texture interactions (Busch et al. 2013; Mosca et al. 2015).

1.2 Overall Hypothesis and Goal

The ***hypothesis*** of this research is that increasing interfacial protein interactions in a model lipoproteic emulsion gel creates a highly structured protein network and decreases sodium availability, contributing to reduced saltiness perception. The ***goal*** is to characterize chemical and rheological influences on sodium availability and saltines perception in a model lipoproteic emulsion gel.

1.3 Specific Objectives

The ***specific objectives*** of this research:

1) Characterize the effects of varying formulation and processing parameters on sodium mobility in a model lipoproteic emulsion gel**.**

The hypothesis of this objective is that increasing protein, fat, or salt concentration, or increasing homogenization pressure increases interprotein interactions and results in reduced sodium mobility. Particle size distribution was measured by laser diffraction. Sodium mobility and binding in model lipoproteic emulsion gels were characterized by ^{23}Na nuclear magnetic resonance (NMR) spectroscopy. The sodium mobility and binding properties were compared between samples prepared with varying formulations and homogenization pressures to validate the hypothesis.

2) Characterize the effects of varying formulation and processing parameters on the rheological properties of a model lipoproteic emulsion gel.

The hypothesis of this objective is that increasing protein, fat, or salt concentration, or increasing homogenization pressure increases interprotein interactions and results in a more rigid and less compliant matrix. Intrinsic rheological properties of model lipoproteic emulsion gels were measured by small deformation oscillatory rheometry and mechanical modeling of creep compliance rheometry behavior. The rheological and mechanical properties were compared between samples prepared with varying formulations and homogenization pressures to validate the hypothesis.

3) Correlate sodium mobility, rheological, and sensory properties of a model lipoproteic emulsion gel.

The hypothesis of this objective is that salty taste correlates positively with sodium mobility and negatively with sodium binding. Sensory taste and texture properties of model lipoproteic emulsion gels were obtained from quantitative descriptive analysis (QDA) data

collected by Kuo (2016). Results from the ^{23}Na NMR spectroscopy and rheometry experiments were correlated with QDA sensory data to validate the hypothesis.

1.4 Literature Cited

Boisard L, Andriot I, Arnould C, Achilleos C, Salles C, Guichard E. 2013. Structure and composition of model cheeses influence sodium NMR mobility, kinetics of sodium release and sodium partition coefficients. Food Chem. 136(2):1070–1077.

Busch JLHC, Yong FYS, Goh SM. 2013. Sodium reduction: Optimizing product composition and structure towards increasing saltiness perception. Trends Food Sci. Technol. 29(1):21–34.

Centers for Disease Control and Prevention. 2012. Vital Signs: Food Categories Contributing the Most to Sodium Consumption - United States, 2007-2008. MMWR 61(5):92–98.

Danaei G, Ding EL, Mozaffarian D, Taylor B, Rehm J, Murray CJL, Ezzati M. 2009. The preventable causes of death in the United States: Comparative risk assessment of dietary, lifestyle, and metabolic risk factors. PLoS Med. 6(4):1–23.

de Wardener H, MacGregor G. 2002. Harmful effects of dietary salt in addition to hypertension. J. Hum. Hypertens. 16(4):213–223.

Dietary Guidelines Advisory Committee. 2010. Report of the Dietary Guidelines Advisory Committee on the Dietary Guidelines for Americans, 2010. Washington, DC: United States Department of Agriculture.

Dietary Guidelines Advisory Committee. 2015. Scientific Report of the 2015 Dietary Guidelines Advisory Committee. Washington, DC: United States Department of Agriculture.

Gobet M, Mouaddab M, Cayot N, Bonny J-M, Guichard E, Le Quéré J-L, Moreau C, Foucat L. 2009. The effect of salt content on the structure of iota-carrageenan systems: 23 Na DQF NMR and rheological studies. Magn. Reson. Chem. 47(4):307–12.

Guodjonsdottir M, Traore A, Renou J-P. 2013. The effect of crystal size and encapsulation of salt on sodium distribution and mobility in bread as studied with 23Na double quantum filtering NMR. In: van Duynhoven J, Van As H, Belton P, Webb G, editors. Magnetic Resonance in Food Science: Food for Thought. Cambridge, UK: RSC Publishing. p. 35–43.

Kuo W-Y. 2016. Relating structural properties to saltiness perception of model lipoproteic gels. Doctoral dissertation. University of Illinois at Urbana-Champaign.

Kuo W-Y, Lee Y. 2014a. Effect of Food Matrix on Saltiness Perception-Implications for Sodium Reduction. Compr. Rev. Food Sci. Food Saf. 13(5):906–923.

Kuo W-Y, Lee Y. 2014b. Temporal Sodium Release Related to Gel Microstructural Properties

— Implications for Sodium Reduction. J.Food Sci. 79(11):2245–2252.

Lauverjat C, Déléris I, Tréléa IC, Christian S, Isabelle S. 2009. Salt and aroma compound release in model cheeses in relation to their mobility. J. Agric. Food Chem. 57(21):9878–9887.

Mattes RD, Donnelly D. 1991. Relative contributions of dietary sodium sources. J. Am. Coll. Nutr. 10(4):383–393.

Mosca AC, Andriot I, Guichard E, Salles C. 2015. Binding of Na^+ ions to proteins: Effect on taste perception. Food Hydrocoll. 51:33–40.

Picouet P a., Sala X, Garcia-Gil N, Nolis P, Colleo M, Parella T, Arnau J. 2012. High pressure processing of dry-cured ham: Ultrastructural and molecular changes affecting sodium and water dynamics. Innov. Food Sci. Emerg. Technol. 16:335–340.

Rosett TR, Shirley L, Schmidt SJ, Klein BP. 1994. Na+ binding as measured by 23Na nuclear magnetic resonance spectroscopy influences the perception of saltiness in gum solutions. J.Food Sci. 59(1):206–210.

Chapter 2. Literature Review

2.1 Introduction

Excessive dietary sodium is a significant problem due to the associated health risks. Higher levels of sodium intake are commonly associated with increased blood pressure and incidence of strokes and cardiovascular disease (de Wardener and MacGregor 2002; Dietary Guidelines Advisory Committee 2010). Additional health risks that can result from high salt intake include renal function deterioration and reduction of bone density (de Wardener and MacGregor 2002). The 2010 Dietary Guidelines for Americans recommended a daily sodium intake of less than 2300 mg for adults and 1500 mg for middle-aged and older adults, hypertensive individuals, and African-Americans, though the average daily intake exceeded these limits at over 3200 mg (individuals at least 2 years old, 2007-2008) (Dietary Guidelines Advisory Committee 2010; Centers for Disease Control and Prevention 2012). When considering sources of dietary sodium, approximately 75% of dietary sodium is from salt added to food during processing (Mattes and Donnelly 1991; Dietary Guidelines Advisory Committee 2010), and over 36% of dietary sodium is from processed food categories containing lipid/protein-based (lipoproteic) emulsion matrices (including bread and rolls, cold cuts/cured meats, pizza, fresh and processed poultry, sandwiches like cheeseburgers, cheese, pasta mixed dishes, and meat mixed dishes) (Centers for Disease Control and Prevention 2012). Therefore, foods with lipoproteic emulsion matrices have the potential for significant impact as targets of sodium reduction efforts.

Methods of sodium reduction can be based on principles of cognitive mechanisms, chemical mechanisms, or product structure design (Busch et al. 2013). Efforts based on cognitive mechanisms involve influencing awareness or sensory stimuli, and include increasing sodium

reduction awareness, stealth reduction (gradual stepwise reduction in salt content), or altering saltiness perception by manipulating other sensory modalities. Sodium reduction methods using chemical mechanisms aim to enhance salty perception at the chemical level with less sodium, such as by using salt replacers (such as potassium chloride) or salt boosters which increase receptor sensitivity (Busch et al. 2013). Finally, food products can be designed to optimize salt release or saltiness perception (Busch et al. 2013; Kuo and Lee 2014). The formulation and structure of materials with a lipid/protein-based matrix (including model dairy products) influences sodium-matrix interactions, sodium mobility, mastication behavior, and saltiness perception (Panouillé et al. 2011; Kuo and Lee 2014). Understanding the relationship between sodium ions, the food matrix, and sensory saltiness perception is critical for reducing sodium content in processed foods while maintaining desired characteristics.

2.2 Model Lipoproteic Emulsion Gels

Protein and salt interactions

Behavior of lipoproteic emulsion foods has been explored and conceptualized using model emulsion gels based on food proteins such as milk proteins. Solid-like gel structure can be obtained by altering protein interactions via acidification or enzyme, heat, or high pressure treatment (Van Vliet et al. 2004; Dickinson 2006; Dickinson 2012). These gelation methods induce the formation of molecular crosslinks or disrupt colloidal protein particles for reorganization into gel networks (Dickinson 2006). Acidification induces protein aggregation by lowering the pH towards the isoelectric point of the protein to reduce electrostatic repulsion between protein molecules. Enzyme treatment catalyzes the formation of covalent cross-links between protein groups, resulting in the formation of elastic gels (Dickinson 2012). High pressure and heat gelation induce protein conformational changes, exposing hydrophobic

portions of the proteins which interact to irreversibly form protein networks upon removal of the pressure or heat (Dickinson 2006).

Salt type and concentration also affect gel formation and physical properties. Ionic salt species can act as ionic bridges and stabilize electrostatic repulsion between protein groups allowing for protein network formation. Consequently, gel strength and rheological properties are influenced by ionic strength and aggregation (McClements et al. 1993; Chen and Dickinson 1998; Kinekawa et al. 1998). In heat-set whey protein gels, it has been found that increasing ionic strength increased gel strength until a critical salt concentration was reached (McClements et al. 1993; Kinekawa et al. 1998). Gel strength then decreased above the critical salt concentration, which was attributed to protein aggregation and the formation of a coarser, less continuous gel structure. In protein-based matrices, salty taste perception may be influenced by sodium binding to negatively charged groups in proteins and matrix rheological properties (Mosca et al. 2015).

Fat inclusion and homogenization pressure

The structural and sensory properties of lipoproteic emulsion gels are affected by the presence of fat particles and the processes used to incorporate the fat. The inclusion of fat has been used as a sodium reduction strategy by contributing to inhomogeneous salt distribution, as inert fillers can occupy volume and increase salt concentration in the aqueous phase (Busch et al. 2013). Dispersed lipid particles are typically classified as active or inactive fillers depending on the type of emulsifying agent at the emulsion interface and their effect on gel strength (McClements et al. 1993; Chen and Dickinson 1998; Dickinson 2012). Dispersed lipid droplets with emulsifying agents such as non-ionic surfactants, which have minimal or no interaction with

the gel matrix, function as inactive filler particles that do not strengthen the gel. Active fillers, such as lipid droplets emulsified by milk proteins, exhibit strong interactions between the filler particles and the gel matrix and result in an increase in gel strength. Figure 2.1 illustrates the formation of a lipoproteic emulsion gel, with interfacial protein molecules stabilizing the emulsion interface after dispersion (i.e. homogenization), then interacting with aqueous protein molecules during the gelation step (i.e. heat treatment) to form a three-dimensional protein network (Jost et al. 1989).

In addition to the inclusion of fat particles and the surface character of the emulsifiers, processing methods such as high pressure homogenization also influence emulsion gel properties. High pressure homogenization uses shear forces to disrupt the lipid phase and create smaller fat particles, which are then stabilized by surfactants adsorbing to the emulsion interface (Kuhn and Cunha 2012). The distribution of the lipid phase affects gel behavior, with smaller droplets resulting in stronger gels, less oil released during oral and gastric processing, and less protein hydrolysis (Guo et al. 2014). Beyond changing the particle size distribution, high pressure homogenization also influences interfacial protein interactions. A study on whey protein-stabilized emulsions found that increasing homogenization pressure resulted in increased interfacial protein interactions and less adsorbed protein, creating a more rigid, compact interfacial protein layer (Lee et al. 2009). The structure and physicochemical properties of lipoproteic emulsion gels are strongly influenced by intermolecular interactions, which can be modified by varying composition and processing parameters.

2.3 ^{23}Na Nuclear Magnetic Resonance Spectroscopy

Nuclear magnetic resonance spectroscopy

Nuclear magnetic resonance (NMR) spectroscopy is a useful tool for characterizing molecular mobility and intermolecular interactions. It is a non-invasive and non-destructive technique, and thus does not inherently affect molecular mobility during measurement and allows for further characterization (Rosett et al. 1994). Sodium mobility and binding interactions are valuable parameters for sodium reduction because they may affect the availability of sodium ions for sensory saltiness perception (Rosett et al. 1994; Lauverjat et al. 2009; Boisard et al. 2014; Kuo and Lee 2014).

NMR spectroscopy is based on the quantum mechanics concepts of nuclear spin and quantized energy levels. In a constant, homogeneous magnetic field, B_0, nuclei with nuclear spin have a discrete number of quantized energy states and orientations available. ^{23}Na is a spin-3/2 nucleus with four available energy states (-3/2, -1/2, 1/2, 3/2) with three allowable energy level transitions (-3/2 → -1/2, -1/2 → 1/2, 1/2 → 3/2) (Mouaddab et al. 2007). In an applied magnetic field, nuclei with spin have angular momentum and a magnetic moment which is expressed as a magnetization vector that precesses around the applied field (Figure 2.2) at a frequency proportional to B_0 (Levitt 2008). For simplicity, many similar magnetization vectors can be summed and expressed as an equilibrium net magnetization vector, M_0 (Figure 2.3), which follows classical mechanical behavior (Claridge 1999).

Single quantum longitudinal (T_1) and transverse (T_2) relaxation times

A second applied magnetic field resonant with the nuclei of interest, B_1, can be applied as a pulse to torque the net magnetization vector, M, exciting the nuclei and inducing phase coherence (Claridge 1999). For example, a 90° B_1 pulse would rotate M into the xy-plane (perpendicular to B_0), with an equal number of spins aligned in the high and low energy state

relative to B_0 (Figure 2.4). When the B_1 pulse ends, the excited nuclei will release energy and the magnetization will recover to equilibrium by longitudinal (in the direction of B_0) and transverse (perpendicular to B_0) relaxation. Longitudinal (spin-lattice) relaxation is the transfer of energy from the spins into the surroundings as heat. This can be characterized from recovery of the net magnetization vector in the z-direction (M_z) to equilibrium over time, described by:

$$\frac{dM_z}{dt} = \frac{\left(M_{z_0} - M_z\right)}{T_1} \tag{1}$$

where T_1 is the first-order time constant for this recovery process. Starting from an excited state with no net longitudinal magnetization ($M_{z_0} = 0$), the longitudinal magnetization as a function of time follows:

$$M_z = M_{z_0}\left(1 - e^{-\frac{t}{T_1}}\right) \tag{2}$$

(Claridge 1999; Levitt 2008) T_1 is the time for M_z to recover by a factor of e, and is referred to as the longitudinal relaxation time. Longitudinal relaxation time provides information on total sodium ion mobility, with longer relaxation time corresponding to more mobile sodium ions (Rosett et al. 1994). Conversely, sodium ions in a restricted mobility state relax faster due to the stronger association with the surrounding matrix. Transverse (spin-spin) relaxation is the dephasing of magnetization vectors as individual spins experience different magnetic fields (Levitt 2008). This can be characterized from the recovery of the net magnetization vector in the transverse direction (M_{xy}) as a function of time, described by:

$$M_{xy} = M_{xy_0}\left(e^{-\frac{t}{T_2}}\right) \tag{3}$$

where T_2 is the time constant for this recovery process and is referred to as the transverse relaxation time (Claridge 1999; Levitt 2008).

Double quantum filtered ^{23}NMR spectroscopy

The double quantum filtered (DQF) pulse sequence selectively characterizes the behavior of nuclei in a restricted mobility ('bound') state by eliminating SQ coherences. The phase-cycled pulse sequence used for the DQF experiment is:

$$(\pi/2)_{\varphi} - \frac{\tau}{2} - (\pi)_{\varphi+90} - \frac{\tau}{2} - \left(\frac{\pi}{2}\right)_{\varphi} - \delta - \left(\frac{\pi}{2}\right)_{0} - \mathrm{Acq}(t)_{\varphi'} \quad (4)$$

where τ is the creation time and δ is the DQ evolution time. DQ coherences were isolated using a four-step phase cycle of $\varphi = 0°, 90°, 180°, 270°$; $\varphi' = 2(0°, 180°)$ (Kemp-Harper et al. 1997; Mouaddab et al. 2007). The DQF signal is maximized at creation time τ^{opt} (Figure 2.5), which can be found by first fitting the maximum signal intensity of each DQF spectrum (I_{DQ}) to the three parameter function:

$$I_{DQ} = k * \left[\exp\left(-\frac{\tau}{T_{2s}^{DQ}}\right) - \exp\left(-\frac{\tau}{T_{2f}^{DQ}}\right)\right] \quad (5)$$

where T_{2s}^{DQ} and T_{2f}^{DQ} are the DQF relaxation times for the 'slow' (-1/2 → 1/2) and 'fast' (-3/2 → -1/2, 1/2 → 3/2) transitions, respectively (Pekar and Leigh 1986). τ^{opt} can then be calculated as follows:

$$\tau^{opt} = \frac{\ln\left(T_{2s}^{DQ}/T_{2f}^{DQ}\right)}{\left(1/T_{2f}^{DQ} - 1/T_{2s}^{DQ}\right)} \quad (6)$$

with smaller τ^{opt} values corresponding to a higher degree of order around the 'bound' sodium (Boisard et al. 2013). The DQF signal is the sum of two lines with equal areas but different widths (Figure 2.6). The area of the DQF signal can be defined as the integral of the lineshape function between the zero derivative points (Allis et al. 1991; Mouaddab et al. 2007), and the relative 'bound' sodium fraction can be calculated by comparing the areas of the DQF and SQ peaks (Gobet et al. 2010).

^{23}Na NMR spectroscopy food applications

^{23}Na NMR SQ NMR experiments have been used to characterize sodium mobility (in terms of SQ relaxation times T_1 and/or T_2) in food systems including gum solutions (Rosett et al. 1994), protein matrices (Mosca et al. 2015), model emulsion (model Ranch dressing) solutions (Defnet et al. 2016), cheese and model cheese (Gobet, Foucat, et al. 2009; Gobet et al. 2010; Andriot et al. 2011; Boisard et al. 2013; Boisard et al. 2014), and dry-cured ham (Picouet et al. 2012). Many of these studies found that interactions between food matrix components and sodium reduced sodium mobility which correlated with reduced perceived saltiness.

In a previous study on sodium binding in gum solutions, ionic gum solutions had relatively lower total sodium mobility and corresponding perceived saltiness than nonionic gum solutions (Rosett et al. 1994). This was attributed to binding interactions between sodium ions and ionic matrix components. As sodium concentration was increased, however, overall sodium mobility and associated saltiness perception equalized between ionic and nonionic systems. It was concluded that above a critical sodium concentration, the available sodium ions exceeded the number of anionic binding sites and additional added sodium would have increased mobility and availability for sensory perception. Andriot et al. (2011) and Boisard et al. (2013) investigated the effects of structure and composition on sodium mobility in model cheeses with varying protein/fat ratios and added salt (NaCl). Andriot et al. found that total sodium mobility was lower in samples with added NaCl, while Boisard et al. found that total mobility increased in samples with added NaCl. Both studies found overall sodium mobility decreased with increased protein/fat ratio. These changes in composition resulted in varying structural and rheological properties, and lower sodium mobility was exhibited in model cheeses with increasing firmness and stronger protein networks. These studies concluded that differences in chemical,

microstructural, and rheological properties may affect overall sodium mobility and sensory saltiness perception.

^{23}Na NMR DQF NMR experiments have been used to characterize mobility and binding of 'bound' sodium in food systems including protein matrices (Mosca et al. 2015), iota-carrageenan systems (Gobet et al. 2009; Defnet 2015), model emulsion (model Ranch dressing) solutions (Defnet et al. 2016), cheese and model cheese (Gobet et al. 2009a; Gobet et al. 2010; Andriot et al. 2011; Boisard et al. 2013; Boisard et al. 2014), bread (Guodjonsdottir et al. 2013), and meat products (Foucat et al. 2003; Picouet et al. 2012). Commonly measured or calculated parameters include the relaxation time of the 'bound' sodium fraction (T_{2s}^{DQ}, T_{2f}^{DQ}), the DQ creation time (τ^{opt}), and the relative 'bound' fraction (ratio of the DQF and SQ peak areas). Mouaddab et al. (2007) used a model cationic exchange resin system with a known, controlled number of binding sites to derive a calculation method for absolute quantification of 'bound' sodium. The absolute quantification method was later cited and used in several ensuing studies (Guodjonsdottir et al. 2013; Boisard et al. 2014; Mosca et al. 2015), though in other subsequent DQF experiments exploring sodium binding the absolute binding calculation was absent (Gobet, Foucat, et al. 2009; Gobet, Mouaddab, et al. 2009; Gobet et al. 2010; Picouet et al. 2012; Boisard et al. 2013) or found to produce inaccurate results (Defnet 2015) indicating the absolute quantification method may not be suitable for all food materials.

Several experiments studied the effects of formulation and structure on sodium binding in cheeses and model cheeses (Gobet, Foucat, et al. 2009; Gobet et al. 2010; Andriot et al. 2011; Boisard et al. 2013; Boisard et al. 2014), food systems featuring lipid/protein-based emulsion matrices. There was a strong dependence of mobility and binding parameters on water content (Gobet, Foucat, et al. 2009), and samples with increased water content had less order around

'bound' sodium (larger τ^{opt}) and increased sodium mobility (T_{2s}^{DQ}, T_{2f}^{DQ}). Gobet et al. (2010) and Andriot et al. (2011) found that higher salt content resulted in more 'bound' sodium and lower 'bound' sodium mobility, suggesting that this may be caused by increased sodium-protein interactions and/or increases in matrix viscosity. Increasing the ratio of protein/fat content similarly resulted in a firmer gel and lower 'bound' sodium mobility, as well as a larger 'bound' sodium fraction (Boisard et al. 2013; Boisard et al. 2014). Sensory saltiness perception correlated strongly with 'free' sodium concentration ([Na] free, $r^2 = 0.98$), lack of order around 'bound' sodium (τ^{opt}, $r^2 = 0.82$), and sodium mobility ($T_1/10$, $r^2 = 0.71$; T_{2s}^{DQ}, $r^2 = 0.51$; T_{2f}^{DQ}, $r^2 = 0.84$) (Boisard et al. 2014).

Beyond formulation considerations, sodium binding can also be influenced by altering processing parameters. In a study investigating sodium binding and distribution in breads with different salt types (varied crystal size, liquid salt, or encapsulated salt) and incorporation methods (salt added at beginning or end of kneading), it was found that adding salt later in processing resulted in more 'free' (less 'bound') sodium (Guodjonsdottir et al. 2013). Incorporating encapsulated salt resulted in more 'free' sodium and more order around 'bound' sodium (smaller τ^{opt}) relative to samples using unencapsulated crystalline salt. It was hypothesized that between bread samples with the same sodium content, those with more 'free' sodium would have higher sensory saltiness. A different study explored the effects of high pressure processing (HPP) on sodium mobility in dry-cured ham (Picouet et al. 2012). Increasing HPP pressure increased the order around 'bound' sodium, while decreasing the total amount of 'bound' sodium. It was hypothesized that increasing HPP pressure altered conformation, releasing some 'bound' sodium ions to the 'free' state via structural disruption while simultaneously increasing binding strength between sodium ions and HPP-modified proteins.

DQF ^{23}Na NMR experiments allow for selective analysis of sodium in limited mobility states, and results can be compared to SQ experiment results to determine the relative amounts of 'bound' and 'free' sodium. Sodium binding in food systems has been previously measured, related to molecular interactions, and correlated to saltiness perception.

2.4 Rheometry

Small deformation oscillatory rheometry

Small deformation (or amplitude) oscillatory rheometry is a common method for characterizing rheological properties or viscoelastic behavior of foods (Steffe 1996; Rao 2007). Common testing set-ups for analyzing fluids or gels are parallel plate geometries with the sample placed between the test fixtures. Tests are conducted in the linear viscoelastic range (determined from experimental data) where an applied stress results in a proportional strain response and material functions are independent of applied stress or strain (Steffe 1996).

Small deformation oscillatory rheometry typically involves applying a small sinusoidally oscillating shear strain or deformation, which causes stress to be transferred through the sample. The stress has an elastic component (in line with the applied strain) and a viscous component (90° out of phase with the applied strain). Within the linear viscoelastic range, the elastic stress component is expressed by the elastic (or storage) modulus, G', while the viscous stress component is expressed by the viscous (or loss) modulus, G'' (Rao 2007). G' and G'' are measures of the energy stored and lost, respectively, during deformation, and can be related by the equation:

$$\tan\delta = \frac{G''}{G'} \tag{7}$$

where δ is the phase shift or phase angle. In polymer systems, dilute solutions will have very high $\tan\delta$ values (indicating more viscous character and more energy lost) while gels will have very low $\tan\delta$ (indicating more elastic character and more energy stored) (Steffe 1996).

Viscoelastic theory and creep compliance

Massless mechanical models are valuable tools in explaining modeling viscoelastic behavior (Van Wazer et al. 1963; Steffe 1996), some examples of which are shown in Figure 2.7. Elastic components are represented by Hookean springs (ideal solid elements following Hooke's law), while viscous components are represented by Newtonian dashpots (ideal fluid elements following Newton's law). Rheological behavior of viscoelastic materials is commonly modeled using Maxwell (a spring and dashpot in series) or Kelvin-Voigt (a spring and dashpot in parallel) elements. A Maxwell element can be placed in series with at least one Kelvin-Voigt element to form a Burgers model, which is useful for modeling viscoelastic creep behavior (response to application and removal of a constant stress) (Guinee 2011). Under a constant applied stress (in the linear viscoelastic region below a critical stress threshold to avoid irreversible structure disruption), a Burgers body will exhibit instantaneous elastic response, retarded elastic response, and Newtonian compliance (long time viscous flow) (Figure 2.8). Between application and removal of the stress, experimental creep response data can be modeled as creep compliance as a function of time, $J(t)$, following:

$$J(t) = \frac{\gamma}{\sigma_0} = J_0 + \sum_{i=1}^{m} J_i \left(1 - e^{-\frac{t}{\tau_i}}\right) + \frac{\tau}{\eta_N} \quad (8)$$

where γ is the measured strain, σ_0 is the constant applied stress, J_0 is the instantaneous elastic compliance of the Maxwell spring component, m is the number of Kelvin-Voigt elements, J_i and

τ_i are the retarded elastic compliance and the retardation time, respectively, associated with each Kelvin-Voigt element, and η_N is the Newtonian viscosity of the Maxwell dashpot component (Steffe 1996). Creep compliance/recovery rheometry is valuable for determining intrinsic elastic and viscous character, which can then be used to gain insight on structural properties and matrix interactions (Olivares et al. 2009; Guinee 2011).

Mechanical modeling with the Burgers model has been an effective method for conceptualizing rheological behavior and structural properties of food systems. Creep compliance has been previously measured in model oil-based spreads (Ojijo et al. 2004), whey protein emulsion gels (Chen et al. 2000), and cheese samples (Ma et al. 1996; Ma et al. 1997; Subramanian and Gunasekaran 1997; Subramanian et al. 2003; Olivares et al. 2009). In a whey protein-based emulsion gel, the incorporation of active fat filler particles resulted in firmer gels with less elastic compliance and less non-recoverable viscous compliance than gels with inactive filler particles (Chen et al. 2000). The measured increase in gel strength was attributed to interactions between the protein molecules/aggregates and emulsion interfacial protein molecules in the gels with active filler particles. In a study on mozzarella cheese samples, a four-component Burgers model was used to model compliance behavior and evaluate matrix changes over different ripening times (Olivares et al. 2009). Cheeses with longer ripening times were found to have greater deformation when subjected to creep strain, which was associated with proteolysis weakening protein network strength and cheese structure. Matrix textural properties may influence mastication processes and sensory perception (Panouillé et al. 2011; Busch et al. 2013), and mechanical modeling is a useful tool for characterizing texture and the contributing molecular interactions.

2.5 Literature Cited

Allis JL, Seymour AML, Radda GK. 1991. Absolute quantification of intracellular Na+ using triple-quantum-filtered sodium-23 NMR. J. Magn. Reson. 93(1):71–76.

Andriot I, Boisard L, Vergoignan C, Salles C, Guichard E. 2011. Sodium Ions in Model Cheeses at Molecular and Macroscopic Levels. In: Renou J-P, Belton PS, Webb GA, editors. Magnetic Resonance in Food Science: An Exciting Future. Vol. 53. p. 67–70.

Boisard L, Andriot I, Arnould C, Achilleos C, Salles C, Guichard E. 2013. Structure and composition of model cheeses influence sodium NMR mobility, kinetics of sodium release and sodium partition coefficients. Food Chem. 136(2):1070–1077.

Boisard L, Andriot I, Martin C, Septier C, Boissard V, Salles C, Guichard E. 2014. The salt and lipid composition of model cheeses modifies in-mouth flavour release and perception related to the free sodium ion content. Food Chem. 145:437–444.

Busch JLHC, Yong FYS, Goh SM. 2013. Sodium reduction: Optimizing product composition and structure towards increasing saltiness perception. Trends Food Sci. Technol. 29(1):21–34.

Centers for Disease Control and Prevention. 2012. Vital Signs: Food Categories Contributing the Most to Sodium Consumption - United States, 2007-2008. MMWR 61(5):92–98.

Chen J, Dickinson E. 1998. Viscoelastic Properties of Heat-Set Whey Protein Emulsion Gels. J. Texture Stud. 29(3):285–304.

Chen J, Dickinson E, Langton M, Hermansson A-M. 2000. Mechanical properties and microstructure of heat-set whey protein emulsion gels: effect of emulsifiers. LWT-Food Sci. Technol. 307:299–307.

Claridge TDW. 1999. Introducing high-resolution NMR. In: Baldwin J, Williams RM, editors. High-Resolution NMR Techniques in Organic Chemistry. Kidlington, Oxford, UK: Elsevier Science Ltd. p. 13–44.

de Wardener H, MacGregor G. 2002. Harmful effects of dietary salt in addition to hypertension. J. Hum. Hypertens. 16(4):213–223.

Defnet E. 2015. Investigation of sodium binding through implementation and application of single- and double-quantum filtered 23Na NMR spectroscopy. Master's thesis. University of Illinois at Urbana-Champaign.

Defnet E, Zhu L, Schmidt SJ. 2016. Characterization of sodium mobility, binding, and apparent viscosity in full-fat and reduced-fat model emulsion systems. J. Food Meas. Charact.:1–9.

Dickinson E. 2006. Structure formation in casein-based gels, foams, and emulsions. Colloids Surfaces A Physicochem. Eng. Asp. 288:3–11.

Dickinson E. 2012. Emulsion gels: The structuring of soft solids with protein-stabilized oil droplets. Food Hydrocoll. 28(1):224–241.

Dietary Guidelines Advisory Committee. 2010. Report of the Dietary Guidelines Advisory Committee on the Dietary Guidelines for Americans, 2010. Washington, DC: United States Department of Agriculture.

Foucat L, Donnat J, Renou J. 2003. 23Na and 35Cl NMR Studies of the Interactions of Sodium and Chloride Ions with Meat Products. In: Belton P, Gil A, Webb G, Rutledge D, editors. Magnetic Resonance in Food Science: Latest Developments. Cambridge, UK: RSC Publishing. p. 180–185.

Gobet M, Foucat L, Moreau C. 2009. Investigation of sodium ions in cheeses by 23Na NMR spectroscopy. In: Guodjonsdottir M, Belton P, Webb G, editors. Magnetic Resonance in Food Science: Challenges in a Changing World. Cambridge, UK: RSC Publishing. p. 57–64.

Gobet M, Mouaddab M, Cayot N, Bonny J-M, Guichard E, Le Quéré J-L, Moreau C, Foucat L. 2009. The effect of salt content on the structure of iota-carrageenan systems: 23 Na DQF NMR and rheological studies. Magn. Reson. Chem. 47(4):307–12.

Gobet M, Rondeau-Mouro C, Buchin S, Le Quéré JL, Guichard E, Foucat L, Moreau C. 2010. Distribution and mobility of phosphates and sodium ions in cheese by solid-state 31P and double-quantum filtered 23Na NMR spectroscopy. Magn. Reson. Chem. 48(4):297–303.

Guinee TP. 2011. Cheese Rheology. In: Fuquay JW, Fox PF, McSweeney PLH, editors. Encyclopedia of Dairy Sciences. 2nd ed. Elsevier. p. 685–697.

Guo Q, Ye A, Lad M, Dalgleish D, Singh H. 2014. Behaviour of whey protein emulsion gel during oral and gastric digestion: effect of droplet size. Soft Matter 10(23):4173–83.

Guodjonsdottir M, Traore A, Renou J-P. 2013. The effect of crystal size and encapsulation of salt on sodium distribution and mobility in bread as studied with 23Na double quantum filtering NMR. In: van Duynhoven J, Van As H, Belton P, Webb G, editors. Magnetic Resonance in Food Science: Food for Thought. Cambridge, UK: RSC Publishing. p. 35–43.

Jost R, Dannenberg F, Rosset J. 1989. Heat-set gels based on oil/water emulsions: an application of whey protein functionality. Food Microstruct. 8(1):23–28.

Kemp-Harper R, Brown SP, Hughes CE, Styles P, Wimperis S. 1997. 23Na NMR methods for selective observation of sodium ions in ordered environments. Prog. Nucl. Magn. Reson. Spectrosc. 30:157–181.

Kinekawa Y-I, Fuyuki T, Kitabatake N. 1998. Effects of Salts on the Properties of Sols and Gels Prepared from Whey Protein Isolate and Process Whey Protein. J. Dairy Sci. 81(6):1532–1544.

Kuhn KR, Cunha RL. 2012. Flaxseed oil – Whey protein isolate emulsions: Effect of high pressure homogenization. J.Food Eng. 111(2):449–457.

Kuo W-Y, Lee Y. 2014. Effect of Food Matrix on Saltiness Perception-Implications for Sodium Reduction. Compr. Rev. Food Sci. Food Saf. 13(5):906–923.

Lauverjat C, Déléris I, Tréléa IC, Christian S, Isabelle S. 2009. Salt and aroma compound release in model cheeses in relation to their mobility. J. Agric. Food Chem. 57(21):9878–9887.

Lee S-H, Lefèvre T, Subirade M, Paquin P. 2009. Effects of ultra-high pressure homogenization on the properties and structure of interfacial protein layer in whey protein-stabilized emulsion. Food Chem. 113(1):191–195.

Levitt MH. 2008. Spin Dynamics: Basics of Nuclear Magnetic Resonance. 2nd ed. Chichester, West Sussex, England: John Wiley & Sons Ltd.

Ma L, Drake MA, Barbosa-Canovas G V, Swanson BG. 1996. Viscoelastic Properties of Reduced-fat and Full-fat Cheddar Cheeses. J.Food Sci. 61(4):821–823.

Ma L, Drake MA, Barbosa-Canovas GV, Swanson BG. 1997. Rheology of Full-fat and Low-fat Cheddar Cheeses as Related to Type of Fat Mimetic. J.Food Sci. 62(4):748–752.

Mattes RD, Donnelly D. 1991. Relative contributions of dietary sodium sources. J. Am. Coll. Nutr. 10(4):383–393.

McClements DJ, Monahan FJ, Kinsella JE. 1993. Effect of emulsion droplets on the rheology of whey protein isolate gels. J. Texture Stud. 24(4):411–422.

Mosca AC, Andriot I, Guichard E, Salles C. 2015. Binding of Na^+ ions to proteins: Effect on taste perception. Food Hydrocoll. 51:33–40.

Mouaddab M, Foucat L, Donnat JP, Renou JP, Bonny JM. 2007. Absolute quantification of Na+ bound fraction by double-quantum filtered 23Na NMR spectroscopy. J. Magn. Reson. 189(1):151–5.

Ojijo NKO, Kesselman E, Shuster V, Eichler S, Eger S, Neeman I, Shimoni E. 2004. Changes in microstructural, thermal, and rheological properties of olive oil/monoglyceride networks during storage. Food Res. Int. 37(4):385–393.

Olivares ML, Zorrilla SE, Rubiolo AC. 2009. Rheological properties of mozzarella cheese determined by creep/recovery tests: Effect of sampling direction,test temperature and ripening time. J. Texture Stud. 40(3):300–318.

Panouillé M, Saint-Eve A, de Loubens C, Déléris I, Souchon I. 2011. Understanding of the influence of composition, structure and texture on salty perception in model dairy products. Food Hydrocoll. 25(4):716–723.

Pekar J, Leigh JS. 1986. Detection of biexponential relaxation in sodium-23 facilitated by double-quantum filtering. J. Magn. Reson. 69(3):582–584.

Picouet P a., Sala X, Garcia-Gil N, Nolis P, Colleo M, Parella T, Arnau J. 2012. High pressure processing of dry-cured ham: Ultrastructural and molecular changes affecting sodium and water dynamics. Innov. Food Sci. Emerg. Technol. 16:335–340.

Rao MA. 2007. Influence of food microstructure on food rheology. In: McClements DJ, editor. Understanding and controlling the microstructure of complex foods. Boca Raton, FL: CRC Press LLC. p. 411–424.

Rosett TR, Shirley L, Schmidt SJ, Klein BP. 1994. Na+ binding as measured by 23Na nuclear

magnetic resonance spectroscopy influences the perception of saltiness in gum solutions. J.Food Sci. 59(1):206–210.

Steffe JF. 1996. Rheological Methods in Food Process Engineering. 2nd ed. East Lansing, MI: Freeman Press.

Subramanian R, Gunasekaran S. 1997. Small Amplitude Oscillatory Shear Studies on Mozzarella Cheese Part II. Relaxation Spectrum. J. Texture Stud. 28(6):643–656.

Subramanian R, Muthukumarappan K, Gunasekaran S. 2003. Effect of methocel as a water binder on the linear viscoelastic properties of Mozzarella cheese during early stages of maturation. J. Texture Stud. 34(4):361–380.

Van Vliet T, Lakemond CMM, Visschers RW. 2004. Rheology and structure of milk protein gels. Curr. Opin. Colloid Interface Sci. 9(5):298–304.

Van Wazer JR, Lyons JW, Kim KY, Colwell RE. 1963. Viscosity and Flow Measurement: A Laboratory Handbook of Rheology. New York, NY: John Wiley & Sons.

2.6 Tables and Figures

Figure 2.1 Protein-stabilized emulsion gel formation.

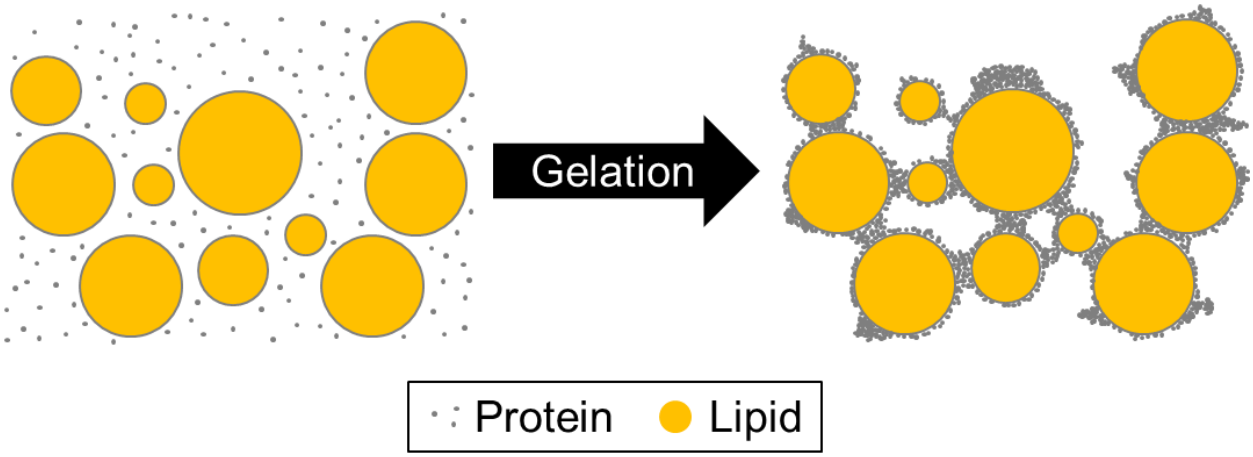

Illustration depicting the formation of a three-dimensional protein network between interfacial proteins (stabilizing the dispersed lipid droplets) and proteins in solution during gelation.

Figure 2.2 Spin precession of a magnetization vector around the applied magnetic field (B_0).

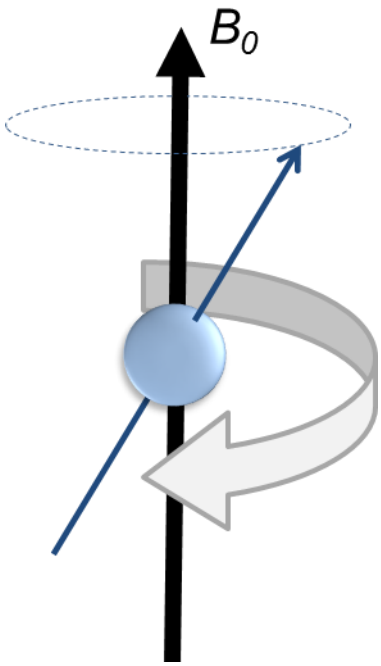

Figure 2.3 NMR spin vectors expressed as an equilibrium magnetization vector (M_0).

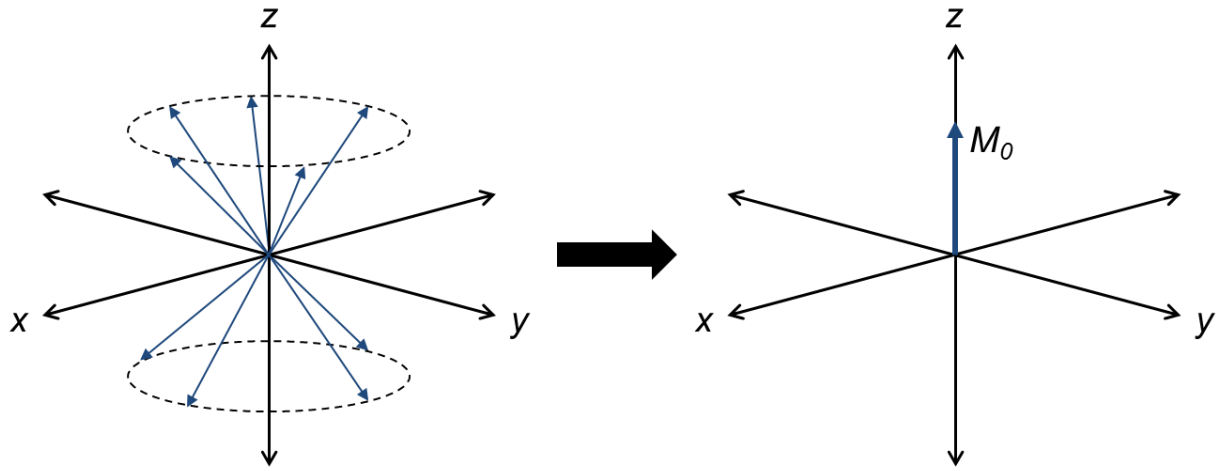

Multiple magnetization vectors can be expressed as a net magnetization vector for simplicity. An excess of spins in the positive z-direction (aligned with the applied magnetic field) results in a net magnetization vector parallel to +z-axis (Claridge 1999).

Figure 2.4 Magnetization vectors following a 90° pulse.

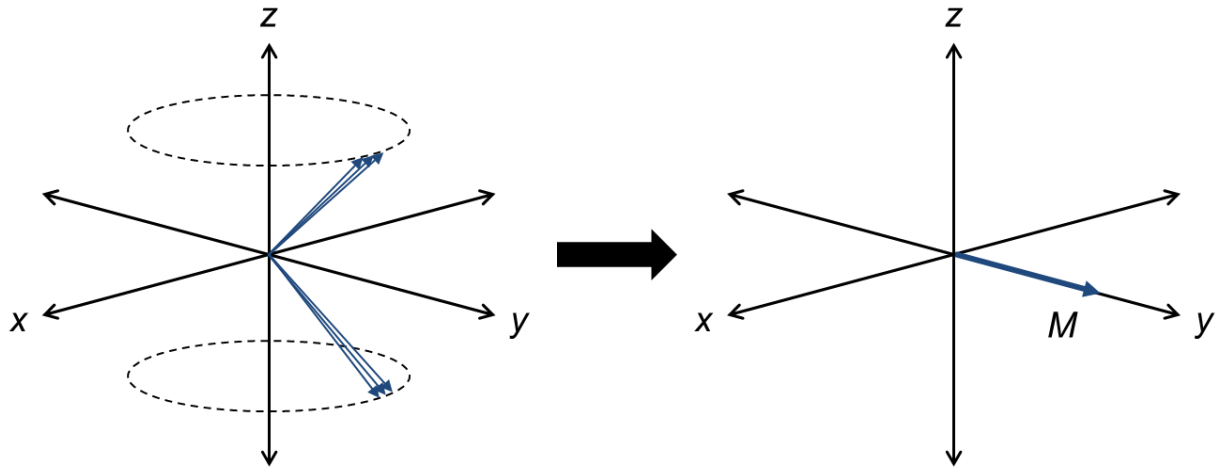

A representative NMR vector model after application of a 90° B_1 pulse, with the spin vectors aligned along the y-axis in phase coherence and the net magnetization vector (M) lying perpendicular to the B_0 field (Claridge 1999).

Figure 2.5 Representative curve of DQF spectrum peak intensity as a function of creation time.

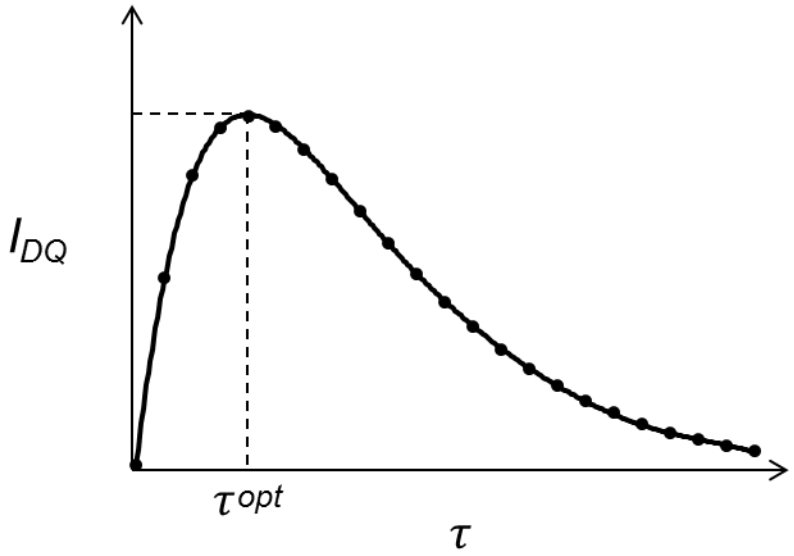

DQF spectrum peak intensity (I_{DQ}) as a function of DQ creation time (τ), where τ^{opt} is the creation time at which the DQF signal is maximized.

Figure 2.6 Representative DQF spectrum and A_{DQ} determination.

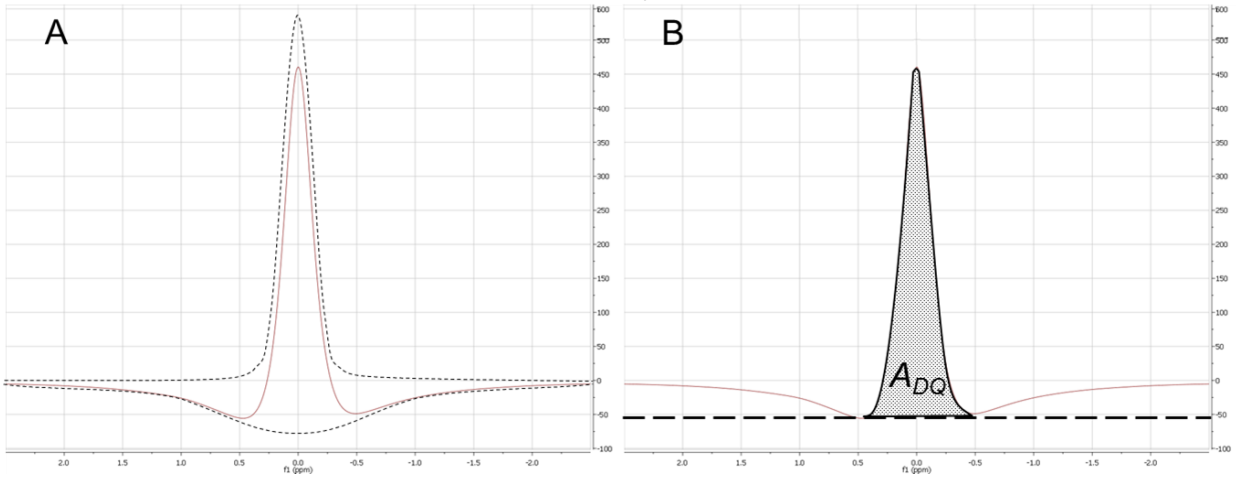

Representative DQF spectrum of a lipoproteic emulsion gel sample. (A) Depiction of the two lines (dashed) which sum to the DQF lineshape (solid). (B) The area of the DQF spectrum (A_{DQ}) is estimated by the area of the lineshape between the zero derivative points.

Figure 2.7 Mechanical model examples.

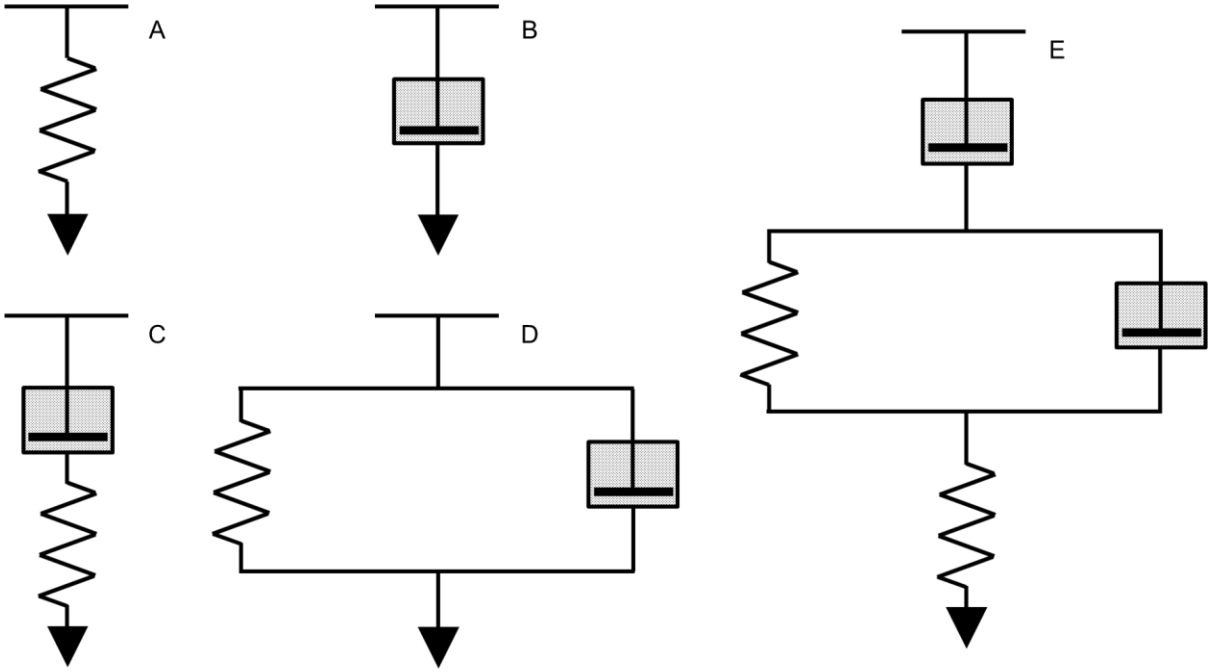

Mechanical model elements: (A) spring, (B) dashpot, (C) Maxwell model, (D) Kelvin-Voigt model, and (E) four-component Burgers model.

Figure 2.8 Representative creep compliance and recovery curve.

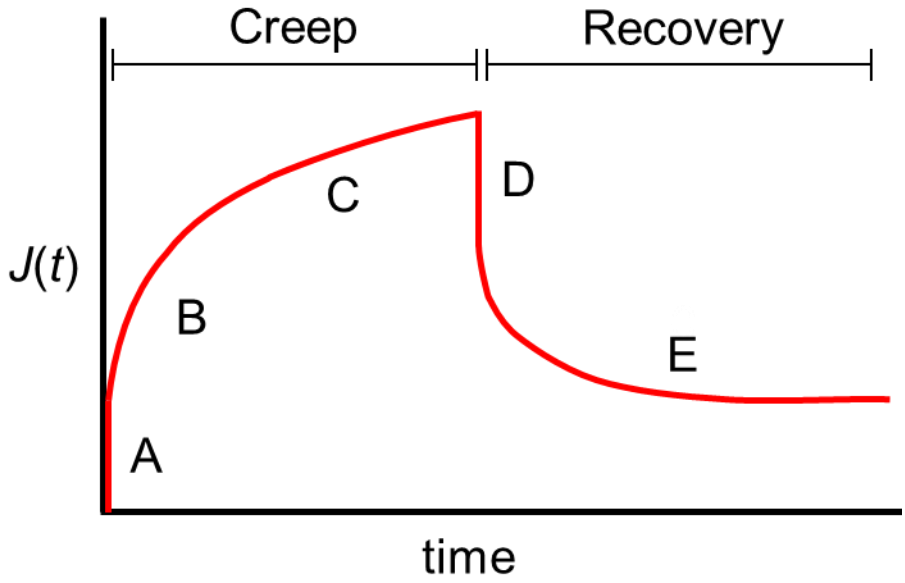

Creep compliance/recovery curve exhibiting (A) instantaneous elastic compliance, (B) retarded elastic compliance, (C) long-term viscous flow, (D) instantaneous elastic recovery, and (E) delayed elastic recovery (Steffe 1996; Guinee 2011).

Chapter 3. Characterization of Sodium Mobility and Binding in a Model Lipoproteic Emulsion Gel by ^{23}Na NMR Spectroscopy

3.1 Abstract

The effects of varying formulation and processing parameters on sodium ion mobility and binding in a model lipid/protein-based (lipoproteic) emulsion gel were studied. Heat-set model lipoproteic emulsion gels were prepared with varying levels of protein (whey protein isolate, 8 and 16 % w/w), lipid (anhydrous milk fat, 0, 11, and 22 % w/w), and NaCl (1.5 and 3.5 % w/w), homogenized under different levels of high pressure homogenization (14 and 55 MPa). Single quantum (SQ) and double quantum filtered (DQF) ^{23}Na NMR spectroscopy was used to analyze total sodium and sodium in a restricted mobility state ('bound' sodium) and characterize sodium mobility (relaxation times, T_1 and T_2), degree of structural order around 'bound' sodium (creation time, τ_{opt}), and sodium binding (relative 'bound' sodium fraction, A_{DQ}/A_{SQ}), which have been correlated to saltiness perception in food systems previously. The mobility of total sodium ion was decreased (lower T_1 and T_2) in gels with higher protein or fat content, while changing homogenization pressure did not have an effect. The gels with increased protein, fat, or homogenization pressure had a more ordered structure surrounding 'bound' sodium (lower τ_{opt}) and more relative 'bound' sodium (higher A_{DQ}/A_{SQ}). Increasing NaCl concentration in the range of 1.5 to 3.5 % (w/w) did not have a statistically significant effect on mobility or binding which may be attributed to the system being at sodium binding saturation. This study highlighted how the mobility of sodium ions is affected by formulation and processing parameters. The data obtained in this study provide information on factors affecting sodium mobility and availability, which can be applied towards sodium reduction in lipid/protein-based foods.

3.2 Introduction

Salt has an important role in foods, contributing to sensory, structural, and stability properties. However, excessive dietary sodium intake presents a major health concern in the United States and throughout other parts of the world (de Wardener and MacGregor 2002). Foods with a lipoproteic emulsion matrix, such as processed cheeses and meats, are of great interest in sodium reduction research. This interest is due to their prevalence in the diet, their relative contribution to dietary sodium, and the role of sodium in sensory properties and stability (Dietary Guidelines Advisory Committee 2010; National Cancer Institute 2016).

Strategies to reduce sodium content include sodium availability and perception by incorporating fillers or modulating textural properties (Busch et al. 2013). These strategies change intermolecular interactions which affect sodium concentration, release, and availability. Past studies have found that increasing homogenization pressure applied to lipid/protein-based emulsions decreased particle size, increased interfacial protein interactions, and reduced protein-lipid interactions (Lee et al. 2009; Kuhn and Cunha 2012). It has also been found that altering formulation and processing parameters affected emulsion gel microstructure and sodium release during large deformation (Kuo and Lee 2014). There have not been studies exploring intrinsic sodium behavior in model lipid/protein-based emulsion gels and the effects of modulating formulation and homogenization conditions.

^{23}Na nuclear magnetic resonance (NMR) spectroscopy has been used to characterize the mobility and dynamics of sodium in food systems. Single quantum (SQ) experiments provide information about the mobility of the total sodium population, while double quantum filtered (DQF) experiments isolate the signal of sodium ions in a restricted mobility (‘bound’) state. Previous studies in literature used NMR to characterize the effects of composition (Gobet et al.

2009; Andriot et al. 2011; Boisard et al. 2013) and high pressure processing (Picouet et al. 2012) on sodium behavior in food systems, and sodium mobility measurements have been correlated to saltiness perception (Rosett et al. 1994; Boisard et al. 2014).

The objective of this study was to determine how formulation and processing parameters affect sodium ion mobility in a model lipid/protein-based emulsion gel. Model emulsion gels were prepared with varying formulation (% Protein, % Fat, % NaCl) and processing (homogenization pressure) conditions, and sodium behavior (overall sodium mobility, order of system around 'bound' sodium, and relative 'bound' sodium fraction) was characterized with ^{23}Na NMR spectroscopy. It was hypothesized that increasing interfacial protein interactions (by increasing protein, fat, or salt content or homogenization pressure) would create a more highly ordered protein network and reduce sodium mobility. Characterizing how sodium behavior is affected by changes to the food matrix is an important step in understanding the relationship between sodium, food microstructure, and saltiness perception, which can then be applied toward sodium reduction.

3.3 Materials and Methods

Emulsion gel preparation

The model gel formulation and preparation procedures were adapted from the method developed by Kuo and Lee (2014). Whey protein isolate (WPI, Hilmar 9000) was donated by Hilmar Ingredients (Hilmar, CA), anhydrous milkfat (AMF) was purchased from Danish Maid Butter Company (Chicago, IL), and sodium chloride (NaCl, Crystalline/Certified ACS) was purchased from Fisher Scientific (Fair Lawn, NJ). Table 3.1 lists the formulation and homogenization pressures used for each emulsion gel, which were selected for overlap with prior

research by Kuo and Lee (focusing on microstructure, sodium release, mass deformation texture analysis, and sensory analysis) for potential data correlation. Samples were coded by their formulation and homogenization pressures in the format of: [Protein (% w/w)]-[Fat (% w/w)]-[NaCl (% w/w)]-[Homogenization pressure (MPa)]. For example, a sample containing 8% protein, 11% fat, and 3.5% NaCl homogenized at 55 MPa would have the code 8-11-3.5-55. An incomplete factorial structure resulted due to samples with simultaneous higher protein and fat levels (16% Protein and 22% Fat) forming viscous, aerated gels unsuitable for NMR sample preparation following high pressure homogenization. The 8-11-0.5-55 sample formulation was added later to explore for potential sodium saturation in the sample matrix.

WPI suspensions were prepared by slowly adding WPI into NaCl solution and stirring for 10 minutes at room temperature on a stirplate. WPI suspensions were incubated at 45 °C for 20 minutes, then stored at 4°C overnight to hydrate the WPI suspension. Following the overnight storage, WPI suspensions were incubated at 45 °C for 20 minutes and AMF was heated to 45 °C to prevent solidification and separation of AMF during prehomogenization. Emulsion solutions were prepared by adding AMF into the WPI suspensions over 15 seconds while prehomogenizing at 9600 rpm with an IKA T-25 Digital High-Speed Homogenizer (IKA Works Inc., Wilmington, NC), then prehomogenizing at 11600 rpm for 3 minutes. Prehomogenized emulsion solutions were then pressure homogenized using an APV 2 stage homogenizer (SPX Flow Technology, Charlotte, NC) for 3 minutes (~3 passes), with the first stage at 14 or 55 MPa and the second stage at 3.4 MPa. Following pressure homogenization, emulsion solutions were degassed under 170 mm Hg vacuum for 20 minutes to improve final gel consistency. Three batch replicates were prepared for each sample.

NMR analysis samples were gelled in NMR tubes *in situ* to prevent possible sample matrix disruption occurring during cutting and loading of set gels into NMR tubes. Samples were loaded by gently pipetting emulsion solutions into 177.8 mm length, 5 mm outer diameter NMR tubes (528-PP-7, Wilmad-LabGlass, Vineland, NJ) to at least half full to ensure sufficient sample presence in the measuring frame of the NMR spectrometer used. NMR tubes were sealed and placed in Teflon tubes (228.6 mm length, 25.4 mm inner diameter) filled with water, and Teflon tubes were heated in a 90 °C water bath for 30 minutes to induce gelation. Sample tubes were removed and stored overnight at 4 °C until NMR analysis. The samples for NMR analysis were prepared in this manner to parallel the gelation conditions of emulsion gels filled directly into Teflon tubes, and allow for accurate comparison between NMR tube gels and Teflon tube gels. Initial testing with thermocouples in Teflon tubes filled with emulsion solution or water verified compatible temperature changes during heating at 90 °C for 30 minutes. One NMR sample was prepared from each batch replicate.

Emulsion particle size analysis

The average dispersed particle size (d_{43}) of the emulsified milkfat was measured in the fat-containing emulsions by laser diffraction using a Shimadzu SALD-2300 Laser Diffraction Particle Size Analyzer equipped with a SALD-MS23 Sampler (Shimadzu Scientific Instruments, Inc., Columbia, MD). Measurements were conducted at room temperature following high pressure homogenization and vacuum treatment. 3 to 12 drops of emulsion solution were dispensed into the sampler bath (circulating deionized water solvent) to achieve absorbance values in the acceptable range for the instrument. A refractive index of 1.45±0.01i for the

emulsified AMF was used for all samples (Michalski et al. 2001). Triplicate measurements were averaged for each emulsion batch replicate.

^{23}Na NMR spectroscopy and data processing

Sodium mobility was measured at the molecular level using ^{23}Na NMR spectroscopy using procedures adapted from the method used by Defnet et al. (Defnet 2015; Defnet et al. 2016) which can be found in Appendix A. ^{23}Na NMR experiments were conducted at room temperature (22 °C) and recorded at 158.660 MHz on a Varian Unity Inova 600 MHz (14.09 T) NMR instrument equipped with a 5 mm Varian AutoTuneX ^{1}H/^{23}Na probe (Agilent Technologies, Santa Clara, CA) using a $\pi/2$ pulse length ranging from 14.35 to 19.40 ms (optimized for each sample).

Single quantum (SQ) sequence experiments were used to measure the ^{23}Na SQ longitudinal (T_1) and transverse (T_2) relaxation times and characterize the mobility of total sodium nuclei. SQ relaxation times provide information on how long it takes total sodium nuclei to relax to equilibrium following excitation, with longer relaxation times corresponding to increased nuclei mobility. T_1 measurements were obtained by fitting recovery curves from inversion-recovery (IR) pulse sequence experiments (15 inter-pulse delays from 0.125 to 2048 ms), and T_2 measurements were obtained from Carr-Purcel-Meiboom-Gil (CPMG) pulse sequence experiments (31 echo times from 0.375 to 1536 ms with a 200 μs echo time). T_1 and T_2 measurements were taken in triplicate and averaged for each sample replicate.

Double quantum filtered (DQF) sequence experiments were used to evaluate sodium binding by selectively characterizing the behavior of sodium ions in restricted mobility states. A phase cycled pulse sequence was used to eliminate SQ coherences:

$$(\pi/2)_{\varphi} - \frac{\tau}{2} - (\pi)_{\varphi+90} - \left(\frac{\pi}{2}\right)_{\varphi} - \delta - \left(\frac{\pi}{2}\right)_{\varphi} - \mathrm{Acq}(t)_{\varphi} \quad (9)$$

where τ is the creation time and δ is the DQ evolution time. DQ coherences were isolated using a four-step phase cycle of $\varphi = 0°, 90°, 180°, 270°$; $\varphi' = 2(0°, 180°)$. For each sample, DQF spectra were acquired for 25 τ values (from 100 μs to 48.1 ms) at δ = 10 μs, and the spectrum with the largest peak area ($\tau = \tau^{opt}$) was used for relative binding calculations. To calculate the value of τ^{opt}, MestReNova software (Version 8.1, Mestrelab Research, S.L., Santiago de Compostela, Spain) was used to determine the DQF spectrum peak intensity (I_{DQ}) at each τ value. I_{DQ} data can be modeled as a function of τ:

$$I_{DQ} = k * \left[\exp\left(-\frac{\tau}{T_{2s}^{DQ}}\right) - \exp\left(-\frac{\tau}{T_{2f}^{DQ}}\right)\right] \quad (10)$$

where k is a constant and T_{2s}^{DQ} and T_{2f}^{DQ} are the DQF relaxation times for the 'slow' (-1/2 → 1/2) and 'fast' (-3/2 → -1/2, 1/2 → 3/2) transitions, respectively. τ^{opt} can then be calculated from T_{2s}^{DQ} and T_{2f}^{DQ}:

$$\tau^{opt} = \frac{\ln\left(T_{2s}^{DQ}/T_{2f}^{DQ}\right)}{\left(1/T_{2f}^{DQ} - 1/T_{2s}^{DQ}\right)} \quad (11)$$

The Solver function in Microsoft Excel 2010 (Microsoft Corporation, Redmond, WA) was used to fit the I_{DQ} data to Equation 10, calculate the R^2 value of the model fittings, and calculate τ^{opt} using Equation 11. Figure 3.1 shows a representative DQF spectra array for 25 τ values, and a plot with the experimental maximum peak intensity for each spectrum and data fitted to Equation 10.

SQ and DQF spectra were acquired in triplicate and the areas of the spectra (A_{SQ}, A_{DQ} respectively) were averaged for each sample batch replicate. A_{DQ} was calculated by baselining

the DQF spectra such that $I = 0$ at the zero derivative points and determining the peak area between the zero derivative points (Figure 3.2) (Allis et al. 1991; Mouaddab et al. 2007). A_{SQ} and A_{DQ} were calculated using Microsoft Excel 2010 using a trapezoidal approximation calculation:

$$\int_a^b f(x)dx \approx (b-a)\left[\frac{f(a)+f(b)}{2}\right] \tag{12}$$

and the relative amount of 'bound' sodium ions was calculated from the ratio of the averaged areas from the DQF and SQ spectra (A_{DQ}/A_{SQ}) (Gobet et al. 2010). For each sample, SQ and DQF experiments were recorded with an identical number of scans (1024), repetition times (200 ms), and receiver gains (optimized by sample).

Statistical analysis

Analysis of variance (ANOVA) and Fisher's Least Significant Difference (LSD) were used to analyze for significant differences between all formulations for particle size and ^{23}Na NMR data. To analyze for significant differences due to systematic treatment effects, dependent t-tests were used to analyze applicable formulations due to changes in treatments with two levels (% Protein, % NaCl, homogenization pressure) and analysis of variance (ANOVA) with Fisher's Least Significant Difference (LSD) were used to analyze applicable formulations due to changes in the treatment with three levels (% Fat). To analyze significant differences between sample subsets differing by only one treatment factor, independent t-tests (2-level treatments) and ANOVA (3-level treatments) were used. Statistical analysis was performed using OriginPro 2016 (OriginLab Corporation, Northampton, MA) with a type I error significance level (α) of 0.05.

3.4 Results and Discussion

Particle size analysis

The average dispersed particle size, d_{43}, of the emulsion in the fat containing samples is included in Appendix B. The samples treated with higher homogenization pressures had significantly smaller fat particles. This was due to increased shear and degree of homogenization with the higher applied homogenization pressure, and the trends were consistent with results found in previous studies (Lee et al. 2009; Kuhn and Cunha 2012; Kuo and Lee 2014). Increasing protein content in a sample also resulted in a significant decrease in particle size. This could be due to more protein being available to adsorb to and stabilize the emulsion interface, reducing coalescence and resulting in a smaller mean particle size (Innocente et al. 2009; Lee et al. 2009). Also supporting this hypothesis is that the samples with increased protein content prepared at higher homogenization pressure had the smallest d_{43} values, indicating the additional protein stabilized the increased surface area resulting from the higher shear forces.

Relaxation times T_1 and T_2

SQ T_1 and T_2 relaxation times were measured for all sample formulations (Table 3.2). Figures 3.3-3.10 display graphs and analysis comparing T_1 and T_2 relaxation times across the different treatments (8 and 16% w/w protein; 0, 11, and 22% w/w fat; 1.5 and 3.5% w/w NaCl; 14 and 55 MPa homogenization pressure).

Increasing protein content from 8 to 16% resulted in a significant decrease in total sodium mobility ($p < 0.001$ for T_1, $p < 0.001$ for T_2) as a systematic effect as well as within each sample pair where protein content was the only formulation change (Figures 3.3 and 3.4). This reduction in mobility can be attributed to increased protein-sodium ion interactions with

increased protein content. Mobility is also affected by viscosity and the freedom of nuclei to move through a medium, so a denser protein network with more interprotein interactions could also impede sodium mobility.

Increasing fat content (from 0 to 11 to 22%) in samples with 8% protein also resulted in significantly lower mobility of the total sodium ion population ($p < 0.001$ for T_1, $p < 0.001$ for T_2, Figures 3.5 and 3.6). Gels formulated with constant protein content but higher fat content have higher protein concentration in the continuous phase and a denser protein network. These gels also have less water available to act as transportation medium for aqueous sodium. Similar trends were observed by Andriot and others (2011) and Boisard and others (2013) in model cheeses, however in their studies dry matter/water ratios were held constant and the effects of increasing protein content and decreasing fat content could not be decoupled. This study was able to successfully explore the separate effects of varying protein and fat content on overall sodium mobility.

Varying the salt content between 1.5 and 3.5% did not significantly affect overall sodium mobility (Figures 3.7 and 3.8). This was attributed to the system possibly being beyond 'binding' saturation, in which case most of the sodium ions in the system were in the highly mobile state and further increasing the amount of sodium would not significantly affect overall mobility. This could also explain why varying homogenization pressure between 14 and 55 MPa did not affect overall mobility (Figures 3.9 and 3.10). If the system was sufficiently beyond 'binding' saturation, then varying homogenization pressure in the experimental range may not have altered the microstructure enough to influence overall mobility. To determine if the 'binding' sites were saturated with sodium ions, a sample with lower NaCl content (0.5% w/w, coded 8-11-0.5-55) was formulated and compared to samples with 1.5 and 3.5% NaCl. Samples without added NaCl

were also made (containing only 0.035% w/w salt that was endogenous to the WPI and AMF starting materials) but the sodium content was too low to obtain a ^{23}Na NMR signal. The SQ and DQF ^{23}Na NMR data for this subset of samples is shown in Table 3.3. Both relaxation times (T_1 and T_2) were significantly lower in samples with 0.5% NaCl than in the higher sodium content samples. The lower overall sodium mobility in the 0.5% samples supports the hypothesis that samples reach 'binding' saturation at NaCl content below 1.5%. Future studies could explore a more inclusive range of NaCl contents to explore saturation trends in this model system.

DQF creation time

DQF experimental data was fit to Equation (10) to determine T_{2s}^{DQ} and T_{2f}^{DQ} ($R^2 > 0.947$ for all model fittings), and DQ creation time, τ^{opt}, was calculated from T_{2s}^{DQ} and T_{2f}^{DQ} using Equation (11) for all sample formulations (Table 3.2). Figures 3.11-3.14 display graphs and analysis comparing τ^{opt} values across the different treatments (8 and 16% w/w protein; 0, 11, and 22% w/w fat; 1.5 and 3.5% w/w NaCl; 14 and 55 MPa homogenization pressure).

τ^{opt} values significantly decreased when protein ($p < 0.001$) or fat ($p = 0.002$) content increased over the explored ranges (Figures 3.11 and 3.12). This decrease in τ^{opt} corresponds to a more ordered environment around the 'bound' sodium in formulations with increasing protein or fat content, which is consistent with the overall mobility trends found from the SQ experiments and past literature results (Boisard et al. 2013). Increasing salt content resulted in a weaker system around the 'bound' sodium ($p = 0.034$, Figure 3.13), which can be attributed to the protein network weakening due to protein aggregation. The strength of heat-set whey protein gels increases with increasing salt concentration until a critical salt concentration (dependent on the matrix and salt species) is reached and the structure becomes coarser and weakens (Kinekawa

et al. 1998). The weakening of the structure between 1.5 and 3.5% NaCl suggests that the critical concentration of salt may be less than 3.5%. τ^{opt} also significantly decreased with increased homogenization pressure ($p = 0.005$ across all samples, $p' = 0.004$ across only fat-containing samples, Figure 3.14). Increasing homogenization pressure decreases lipid particle size and improves emulsion droplet homogeneity resulting in a firmer gel (Jost et al. 1989). Although homogenization pressure did have an effect on matrix structure and τ^{opt}, the protein and fat content had more significant effects on τ^{opt} and were the dominant determining factors.

Relative 'bound' sodium fraction

The relative amount of 'bound' sodium, A_{DQ}/A_{SQ}, was calculated for all sample formulations (Table 3.2). Figures 3.15, 3.16, 3.18, and 3.19 display graphs and analysis comparing A_{DQ}/A_{SQ} across the different treatments (8 and 16% w/w protein; 0, 11, and 22% w/w fat; 1.5 and 3.5% w/w NaCl; 14 and 55 MPa homogenization pressure).

The relative 'bound' sodium fraction significantly increased with increased protein ($p < 0.001$) or fat ($p < 0.001$) content (Figures 3.15 and 3.16). Samples with increased dry matter (protein + fat) content had less water and therefore higher aqueous protein concentration and more opportunities for sodium ions to interact with protein. Figure 3.17 compares A_{DQ}/A_{SQ} values averaged for samples with the same dry matter content, and there is a trend of increasing A_{DQ}/A_{SQ} with increasing dry matter. The emulsion gels with 27% dry matter (16% protein, 11% fat) had higher relative 'bound' sodium than samples with 30% dry matter (8% protein, 22% fat) which indicates that type of dry matter matters in addition to quantity. In this experiment, sodium ions are more likely to interact with protein than fat which may explain the higher relative 'bound' fraction in emulsion samples with higher protein content but comparable total dry

matter. Although increasing the salt content did not have a statistically significant effect on 'bound' sodium fraction, there was a trend of 'bound' sodium decreasing when salt content was increased (Figure 3.18). This supports the hypothesis that the system is saturated with sodium below 1.5% NaCl, as sodium added beyond the saturation point would contribute less to the 'bound' sodium signal (A_{DQ}) than the overall sodium signal (A_{SQ}). Finally, the relative 'bound' fraction was not significantly affected by homogenization pressure across all samples ($p = 0.136$, Figure 3.19), but did significantly increase when considering only the fat-containing samples ($p' = 0.038$). Although homogenization pressure can affect protein interactions in the non-fat samples, the homogenization pressure was shown to have a significant effect on lipid particle size in the emulsions (influencing both protein and lipid interactions). The increase in 'bound' fraction in the fat-containing samples could have resulted from the increased interfacial surface area (and increased inter-protein interactions) when homogenization pressure was increased (Lee et al. 2009).

3.5 Conclusions

For this study, the effects of changing formulation and processing parameters on sodium mobility and binding behavior were characterized by ^{23}Na NMR spectroscopy. The particle size measurements by laser diffraction show that altering formulation and homogenization conditions influenced emulsion particle size. SQ ^{23}Na NMR experiments found that overall sodium mobility decreased with increasing protein and fat levels. Overall sodium mobility did not significantly change between 1.5 and 3.5% NaCl and 14 and 55 MPa homogenization pressure, which was attributed to sodium ions in the system being beyond 'binding' saturation concentration. From DQF ^{23}Na NMR experiments, it was found that increasing protein content, fat content, or

homogenization pressure resulted in a more ordered environment coordinated to the 'bound' sodium and a higher relative 'bound' sodium fraction. In conclusion, sodium mobility and availability in a lipid/protein-based emulsion gel can be altered by modulating the composition and microstructure which has implications for future efforts in sodium reduction.

3.6 Literature Cited

Allis JL, Seymour AML, Radda GK. 1991. Absolute quantification of intracellular Na+ using triple-quantum-filtered sodium-23 NMR. J. Magn. Reson. 93(1):71–76.

Andriot I, Boisard L, Vergoignan C, Salles C, Guichard E. 2011. Sodium Ions in Model Cheeses at Molecular and Macroscopic Levels. In: Renou J-P, Belton PS, Webb GA, editors. Magnetic Resonance in Food Science: An Exciting Future. Vol. 53. p. 67–70.

Boisard L, Andriot I, Arnould C, Achilleos C, Salles C, Guichard E. 2013. Structure and composition of model cheeses influence sodium NMR mobility, kinetics of sodium release and sodium partition coefficients. Food Chem. 136(2):1070–1077.

Boisard L, Andriot I, Martin C, Septier C, Boissard V, Salles C, Guichard E. 2014. The salt and lipid composition of model cheeses modifies in-mouth flavour release and perception related to the free sodium ion content. Food Chem. 145:437–444.

Busch JLHC, Yong FYS, Goh SM. 2013. Sodium reduction: Optimizing product composition and structure towards increasing saltiness perception. Trends Food Sci. Technol. 29(1):21–34.

de Wardener H, MacGregor G. 2002. Harmful effects of dietary salt in addition to hypertension. J. Hum. Hypertens. 16(4):213–223.

Defnet E. 2015. Investigation of sodium binding through implementation and application of single- and double-quantum filtered 23Na NMR spectroscopy. Master's thesis. University of Illinois at Urbana-Champaign.

Defnet E, Zhu L, Schmidt SJ. 2016. Characterization of sodium mobility, binding, and apparent viscosity in full-fat and reduced-fat model emulsion systems. J. Food Meas. Charact.:1–9.

Dietary Guidelines Advisory Committee. 2010. Report of the Dietary Guidelines Advisory Committee on the Dietary Guidelines for Americans, 2010. Washington, DC: United States Department of Agriculture.

Gobet M, Mouaddab M, Cayot N, Bonny J-M, Guichard E, Le Quéré J-L, Moreau C, Foucat L. 2009. The effect of salt content on the structure of iota-carrageenan systems: 23 Na DQF NMR and rheological studies. Magn. Reson. Chem. 47(4):307–12.

Gobet M, Rondeau-Mouro C, Buchin S, Le Quéré JL, Guichard E, Foucat L, Moreau C. 2010. Distribution and mobility of phosphates and sodium ions in cheese by solid-state 31P and double-quantum filtered 23Na NMR spectroscopy. Magn. Reson. Chem. 48(4):297–303.

Innocente N, Biasutti M, Venir E, Spaziani M, Marchesini G. 2009. Effect of high-pressure homogenization on droplet size distribution and rheological properties of ice cream mixes. J. Dairy Sci. 92(5):1864–1875.

Jost R, Dannenberg F, Rosset J. 1989. Heat-set gels based on oil/water emulsions: an application of whey protein functionality. Food Microstruct. 8(1):23–28.

Kinekawa Y-I, Fuyuki T, Kitabatake N. 1998. Effects of Salts on the Properties of Sols and Gels Prepared from Whey Protein Isolate and Process Whey Protein. J. Dairy Sci. 81(6):1532–1544.

Kuhn KR, Cunha RL. 2012. Flaxseed oil – Whey protein isolate emulsions: Effect of high pressure homogenization. J.Food Eng. 111(2):449–457.

Kuo W-Y, Lee Y. 2014. Temporal Sodium Release Related to Gel Microstructural Properties — Implications for Sodium Reduction. J.Food Sci. 79(11):2245–2252.

Lee S-H, Lefèvre T, Subirade M, Paquin P. 2009. Effects of ultra-high pressure homogenization on the properties and structure of interfacial protein layer in whey protein-stabilized emulsion. Food Chem. 113(1):191–195.

Michalski M-C, Briard V, Michel F. 2001. Optical parameters of milk fat globules for laser light scattering measurements. Lait 81(6):787–796.

Mouaddab M, Foucat L, Donnat JP, Renou JP, Bonny JM. 2007. Absolute quantification of Na+ bound fraction by double-quantum filtered 23Na NMR spectroscopy. J. Magn. Reson. 189(1):151–5.

National Cancer Institute. 2016. Sources of Sodium among the U.S. Population, 2005-06. http://epi.grants.cancer.gov/diet/foodsources/sodium/. Accessed 2016 May 9.

Picouet P a., Sala X, Garcia-Gil N, Nolis P, Colleo M, Parella T, Arnau J. 2012. High pressure processing of dry-cured ham: Ultrastructural and molecular changes affecting sodium and water dynamics. Innov. Food Sci. Emerg. Technol. 16:335–340.

Rosett TR, Shirley L, Schmidt SJ, Klein BP. 1994. Na+ binding as measured by 23Na nuclear magnetic resonance spectroscopy influences the perception of saltiness in gum solutions. J.Food Sci. 59(1):206–210.

3.7 Tables and Figures

Table 3.1 Formulation and homogenization pressure sample matrix for ^{23}Na NMR experiments.

Protein (% w/w)	Fat (% w/w)	NaCl (% w/w)	Pressure (MPa)	Sample Code
8	0	1.5	14	8-0-1.5-14
			55	8-0-1.5-55
		3.5	14	8-0-3.5-14
			55	8-0-3.5-55
	11	0.5	55	8-0-0.5-55
		1.5	14	8-11-1.5-14
			55	8-11-1.5-55
		3.5	14	8-11-3.5-14
			55	8-11-3.5-55
	22	1.5	14	8-22-1.5-14
			55	8-22-1.5-55
		3.5	14	8-22-3.5-14
			55	8-22-3.5-55
16	0	1.5	14	16-0-1.5-14
			55	16-0-1.5-55
		3.5	14	16-0-3.5-14
			55	16-0-3.5-55
	11	1.5	14	16-11-1.5-14
			55	16-11-1.5-55
		3.5	14	16-11-3.5-14
			55	16-11-3.5-55

Table 3.2 Summary of results from SQ and DQF ^{23}Na NMR experiments.

Sample	T_1 (ms)	T_2 (ms)	τ_{opt} (ms)	A_{DQ}/A_{SQ}
8-0-1.5-14	39.14 ± 0.77 ab	22.58 ± 0.90 a	10.81 ± 0.59 bc	0.0046 ± 0.0005 j
8-0-1.5-55	38.32 ± 0.85 b	22.64 ± 0.44 a	10.68 ± 0.19 c	0.0046 ± 0.0006 j
8-0-3.5-14	39.72 ± 0.85 a	22.23 ± 0.43 a	13.39 ± 2.68 a	0.0046 ± 0.0002 j
8-0-3.5-55	39.51 ± 0.63 a	22.22 ± 0.35 a	11.81 ± 0.73 b	0.0043 ± 0.0003 j
8-11-1.5-14	33.79 ± 0.21 c	11.52 ± 0.69 a	10.22 ± 0.24 cd	0.0233 ± 0.0006 fg
8-11-1.5-55	34.49 ± 1.41 c	11.19 ± 0.42 e	10.01 ± 0.15 cde	0.0248 ± 0.0006 ef
8-11-3.5-14	34.37 ± 0.69 c	11.82 ± 0.28 ef	10.82 ± 0.06 bc	0.0215 ± 0.0003 g
8-11-3.5-55	34.21 ± 0.57 c	11.45 ± 0.08 de	10.50 ± 0.09 c	0.0232 ± 0.0002 fg
8-22-1.5-14	32.15 ± 0.70 d	10.40 ± 0.16 g	8.99 ± 0.02 ef	0.0261 ± 0.0001 de
8-22-1.5-55	32.71 ± 0.79 d	10.29 ± 0.44 g	8.66 ± 0.23 f	0.0279 ± 0.0008 cd
8-22-3.5-14	32.67 ± 0.51 d	10.55 ± 0.02 fg	9.31 ± 0.40 def	0.0252 ± 0.0010 ef
8-22-3.5-55	32.16 ± 0.50 d	10.05 ± 0.23 g	8.71 ± 0.24 f	0.0279 ± 0.0016 cd
16-0-1.5-14	26.87 ± 0.12 e	12.60 ± 0.30 bc	8.92 ± 0.12 ef	0.0105 ± 0.0001 hi
16-0-1.5-55	27.37 ± 0.21 e	13.19 ± 0.68 b	8.68 ± 0.36 f	0.0098 ± 0.0003 i
16-0-3.5-14	26.72 ± 0.16 e	11.57 ± 0.06 e	9.31 ± 0.04 def	0.0126 ± 0.0001 h
16-0-3.5-55	27.08 ± 0.17 e	12.31 ± 0.14 cd	8.95 ± 0.02 ef	0.0101 ± 0.0023 i
16-11-1.5-14	23.17 ± 0.47 f	7.64 ± 0.06 h	5.90 ± 0.18 g	0.0337 ± 0.0024 b
16-11-1.5-55	23.25 ± 0.38 f	7.73 ± 0.56 h	5.45 ± 0.10 g	0.0368 ± 0.0045 a
16-11-3.5-14	23.71 ± 0.26 f	7.93 ± 0.03 h	6.17 ± 0.19 g	0.0300 ± 0.0017 c
16-11-3.5-55	23.16 ± 0.20 f	7.66 ± 0.20 h	5.38 ± 0.06 g	0.0390 ± 0.0006 a

Sample code represents [Protein (% w/w)]-[Fat (% w/w)]-[NaCl (% w/w)]-[Homogenization pressure (MPa)]. T_1, single quantum (SQ) longitudinal relaxation time; T_2, SQ transverse relaxation time; τ_{opt}, double quantum (DQ) creation time; A_{DQ}/A_{SQ}, relative 'bound' sodium fraction. Results are expressed as mean ± standard deviation (n = 3). Values in the same column with different letters were significantly different ($\alpha = 0.05$).

Table 3.3 Summary of results from SQ and DQF ^{23}Na NMR experiments for 8-11-xx-55 samples.

Sample	T_1 (ms)	T_2 (ms)	τ_{opt} (ms)	A_{DQ}/A_{SQ}
8-11-0.5-55	31.05 ± 0.23 b	10.05 ± 0.31 b	8.28 ± 0.05 c	0.0306 ± 0.0001 a
8-11-1.5-55	34.49 ± 1.41 a	11.19 ± 0.42 a	10.01 ± 0.15 b	0.0248 ± 0.0006 b
8-11-3.5-55	34.21 ± 0.57 a	11.45 ± 0.08 a	10.50 ± 0.09 a	0.0232 ± 0.0002 c

Sample code represents [Protein (% w/w)]-[Fat (% w/w)]-[NaCl (% w/w)]-[Homogenization pressure (MPa)]. T_1, single quantum (SQ) longitudinal relaxation time; T_2, SQ transverse relaxation time; τ_{opt}, double quantum (DQ) creation time; A_{DQ}/A_{SQ}, relative 'bound' sodium fraction. Results are expressed as mean ± standard deviation (n = 3). Values in the same column with different letters were significantly different ($\alpha = 0.05$).

Figure 3.1 Representative DQF spectra array and fitted data.

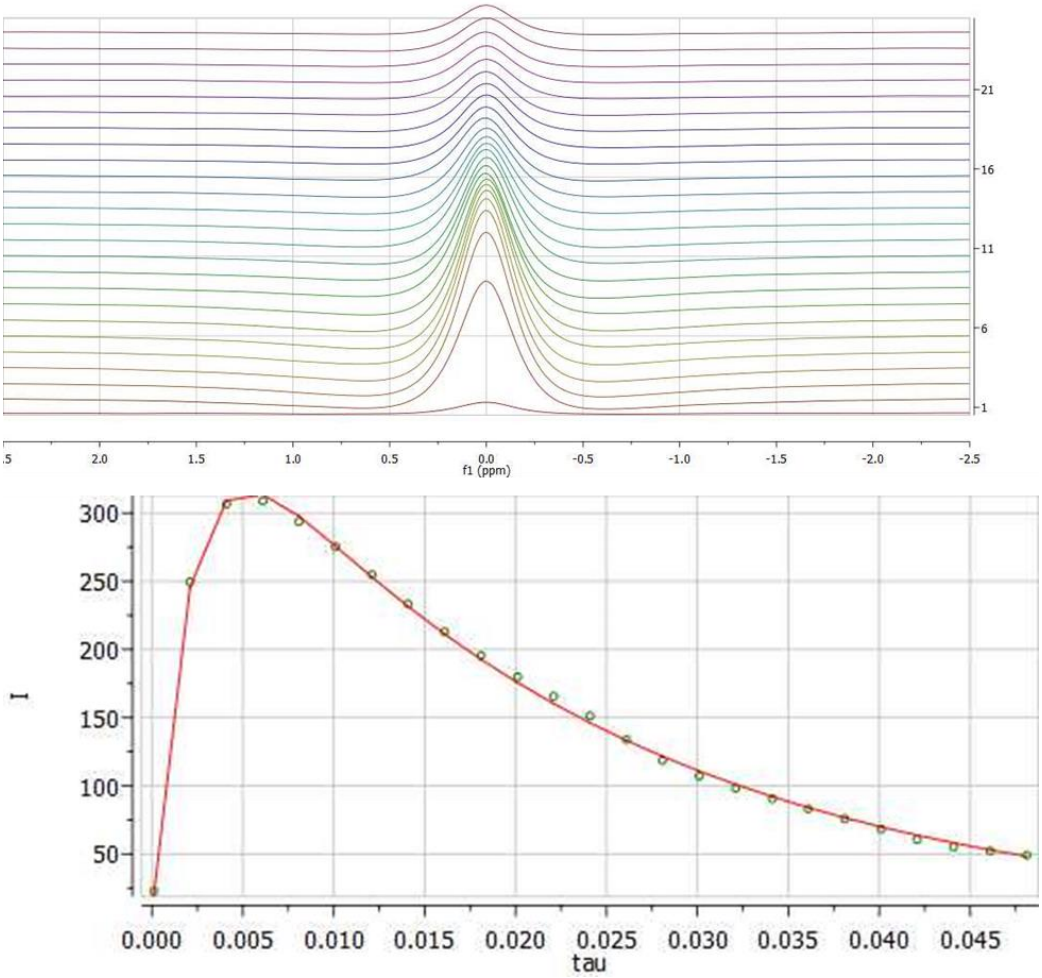

DQF spectra arrayed by τ (top) and plot of experimental max peak intensity (I_{DQ}) as a function of τ with fitted curve (bottom) for a 16-11-3.5-55 sample (sample code represents [Protein (% w/w)]-[Fat (% w/w)]-[NaCl (% w/w)]-[Homogenization pressure (MPa)]). Circles are experimentally acquired I_{DQ} values, line is the fitted data.

Figure 3.2 SQ and DQF curve areas used for area calculations.

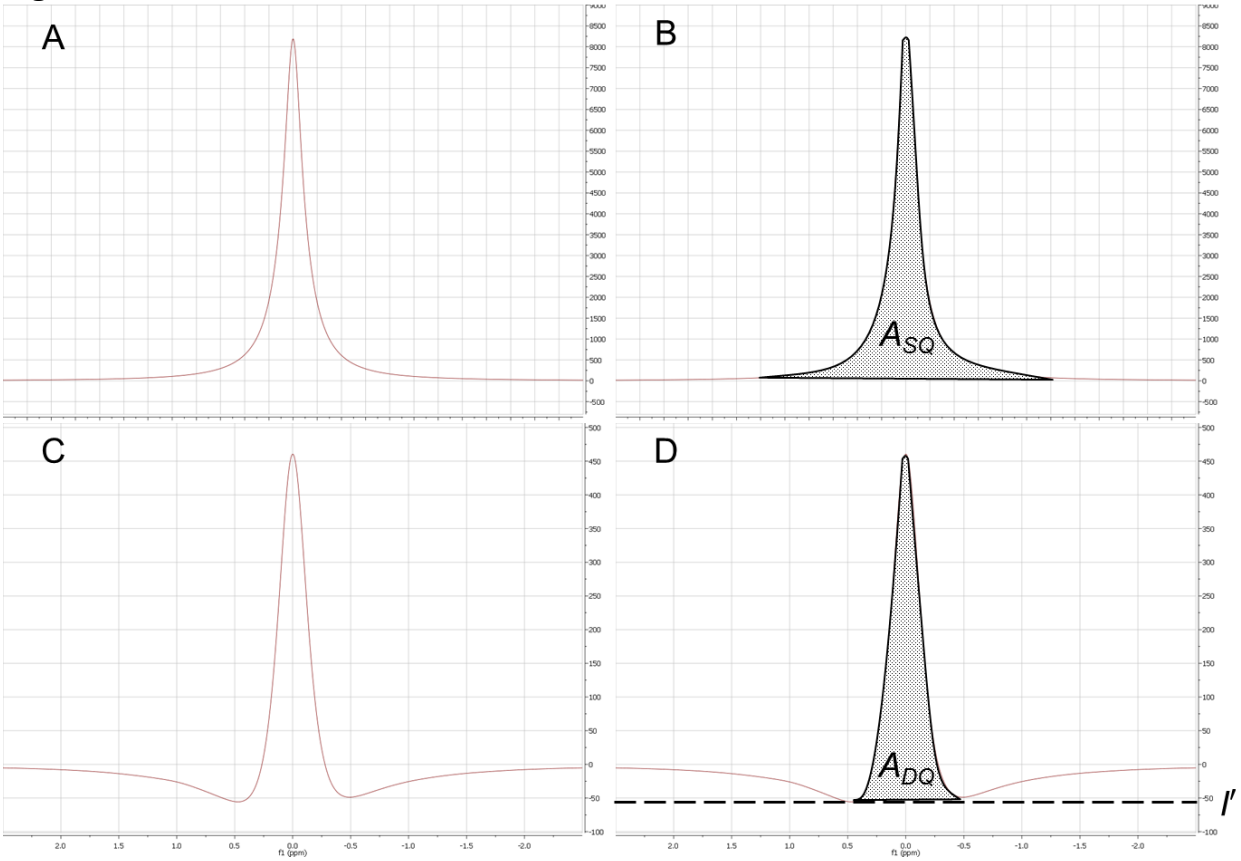

Representative SQ and DQF curves and the areas used to calculate A_{SQ} and A_{DQ}. (A) SQ spectrum, (B) A_{SQ}, (C) DQF spectrum, (D) A_{DQ}. Dashed line in (D) indicates the initial intensity value of DQF signal zero derivative points (I') which was established as the new baseline ($I' = 0$) for A_{DQ} calculations.

Figure 3.3 ^{23}Na NMR SQ longitudinal relaxation time (T_1) by protein content (8 and 16% w/w).

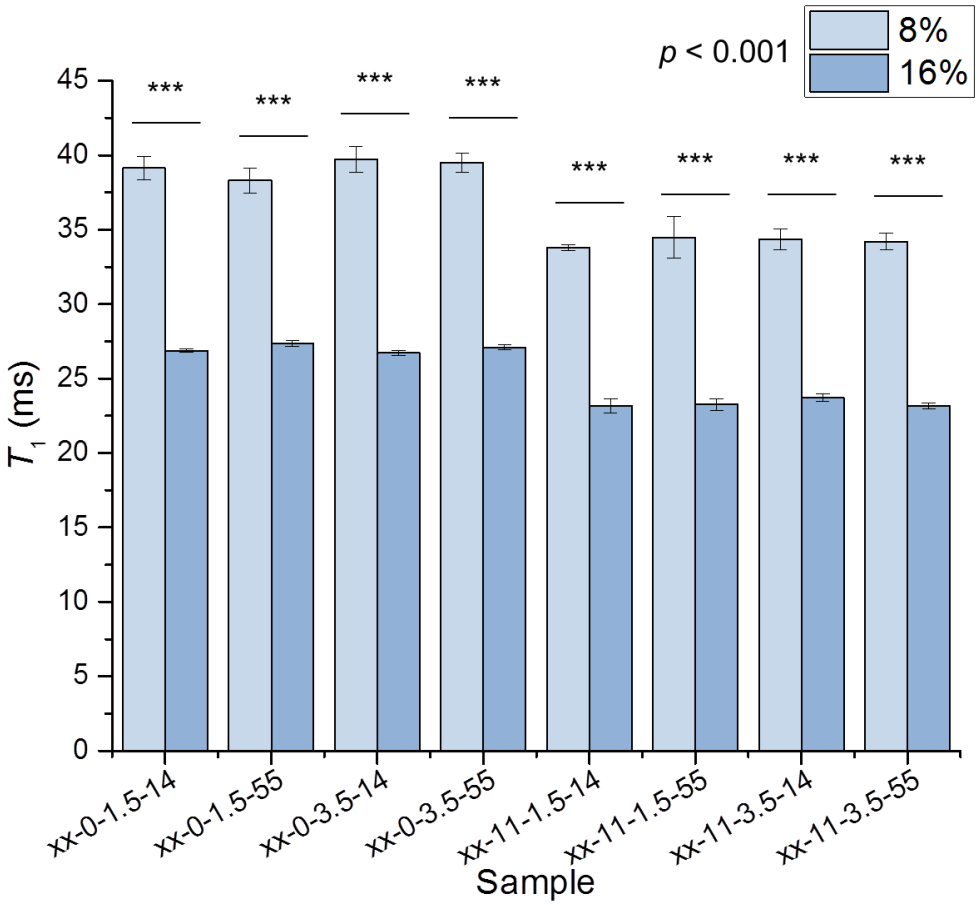

Sample code represents [Protein (% w/w)]-[Fat (% w/w)]-[NaCl (% w/w)]-[Homogenization pressure (MPa)], with protein content (xx) indicated by bar shading. Results are expressed as mean ± standard deviation (n = 3). */**/*** indicates a significant difference ($\alpha = 0.05/0.01/0.001$, respectively) within sample pairs by independent t-test. p is the p-value for systematic treatment effect obtained by a dependent t-test comparing means for all sample pairs.

Figure 3.4 ^{23}Na NMR SQ transverse relaxation time (T_2) by protein content (8 and 16% w/w).

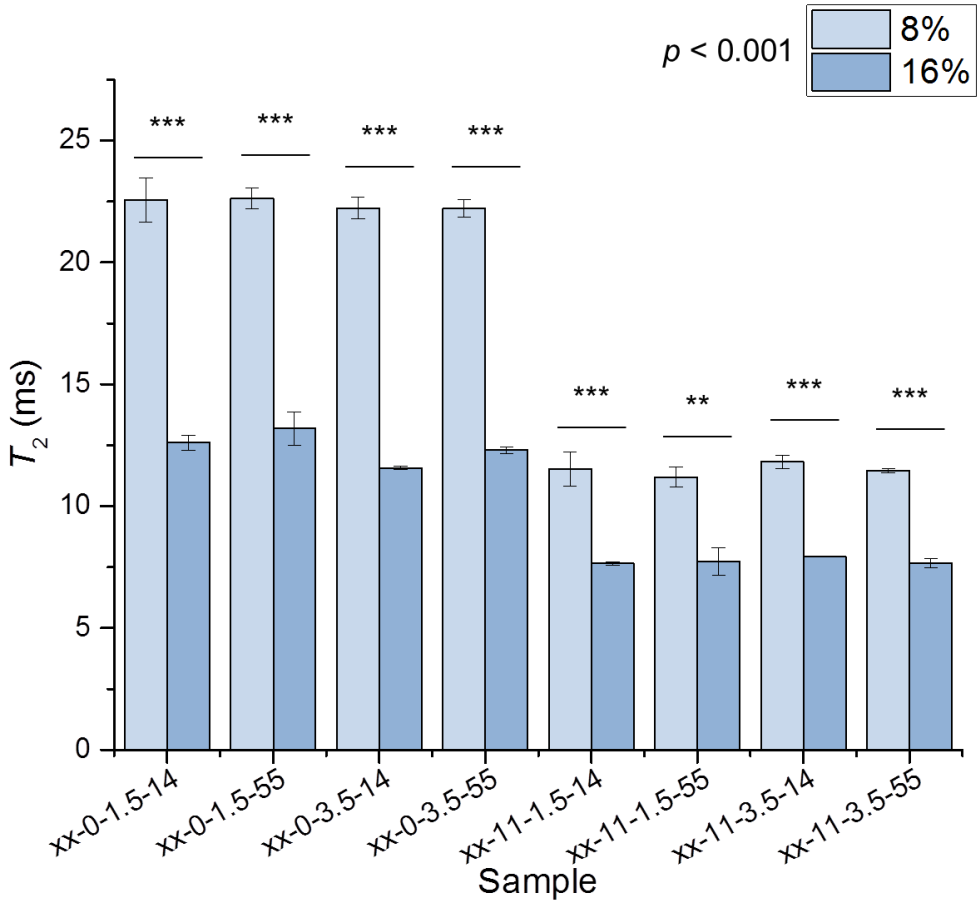

Sample code represents [Protein (% w/w)]-[Fat (% w/w)]-[NaCl (% w/w)]-[Homogenization pressure (MPa)], with protein content (xx) indicated by bar shading. Results are expressed as mean ± standard deviation (n = 3). */**/*** indicates a significant difference ($\alpha = 0.05/0.01/0.001$, respectively) within sample pairs by independent t-test. p is the p-value for systematic treatment effect obtained by a dependent t-test comparing means for all sample pairs.

Figure 3.5 ^{23}Na NMR SQ longitudinal relaxation time (T_1) by fat content (0, 11, and 22% w/w).

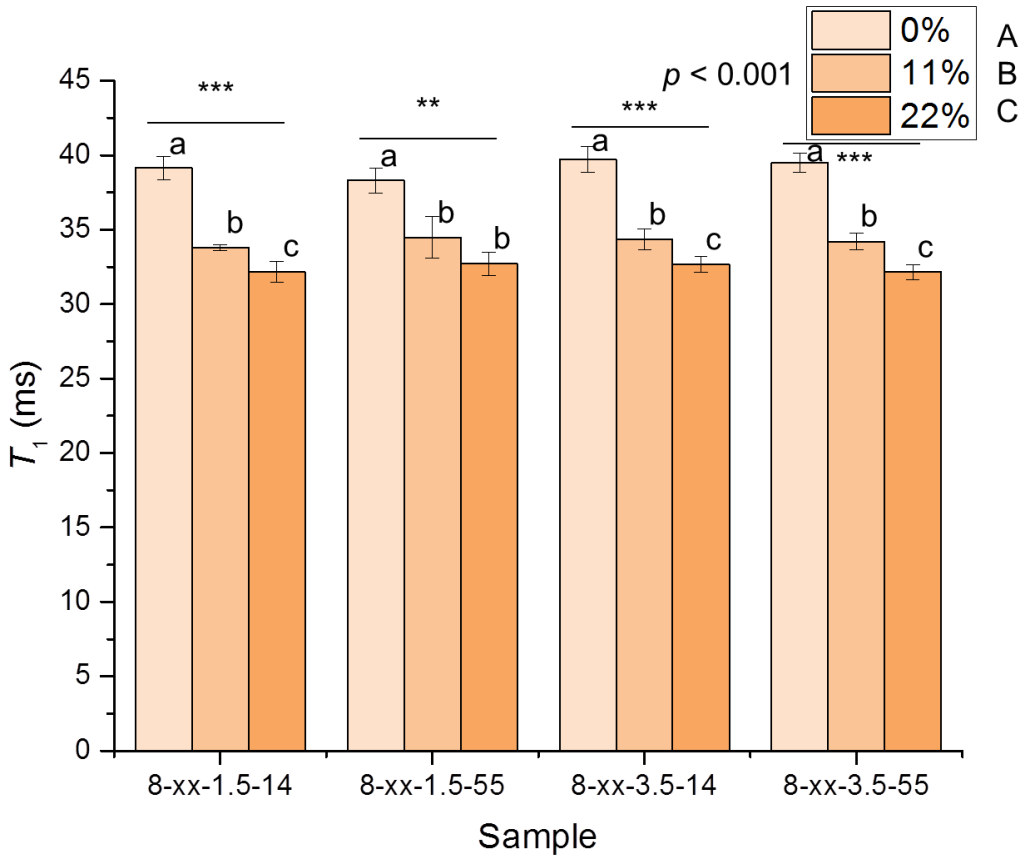

Sample code represents [Protein (% w/w)]-[Fat (% w/w)]-[NaCl (% w/w)]-[Homogenization pressure (MPa)], with fat content (xx) indicated by bar shading. Results are expressed as mean ± standard deviation (n = 3). */**/*** indicates a significant difference ($\alpha = 0.05/0.01/0.001$, respectively) within sample trios by ANOVA. Values in the same column with different letters were significantly different ($\alpha = 0.05$). p is the p-value for systematic treatment effect obtained by ANOVA comparing means for all samples. Treatments with different letters were significantly different ($\alpha = 0.05$).

Figure 3.6 ^{23}Na NMR SQ transverse relaxation time (T_2) by fat content (0, 11, and 22% w/w).

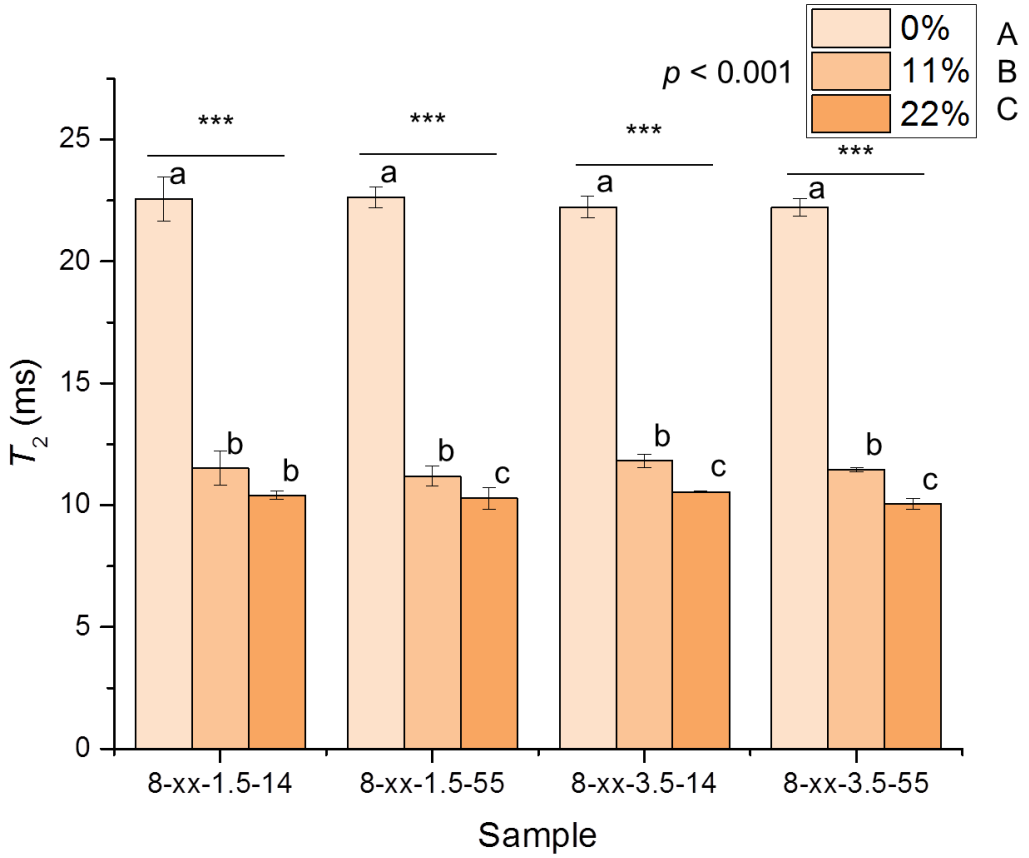

Sample code represents [Protein (% w/w)]-[Fat (% w/w)]-[NaCl (% w/w)]-[Homogenization pressure (MPa)], with fat content (xx) indicated by bar shading. Results are expressed as mean ± standard deviation (n = 3). */**/*** indicates a significant difference ($\alpha = 0.05/0.01/0.001$, respectively) within sample trios by ANOVA. Values in the same column with different letters were significantly different ($\alpha = 0.05$). p is the p-value for systematic treatment effect obtained by ANOVA comparing means for all samples. Treatments with different letters were significantly different ($\alpha = 0.05$).

Figure 3.7 ^{23}Na NMR SQ longitudinal relaxation time (T_1) by NaCl content (1.5 and 3.5% w/w).

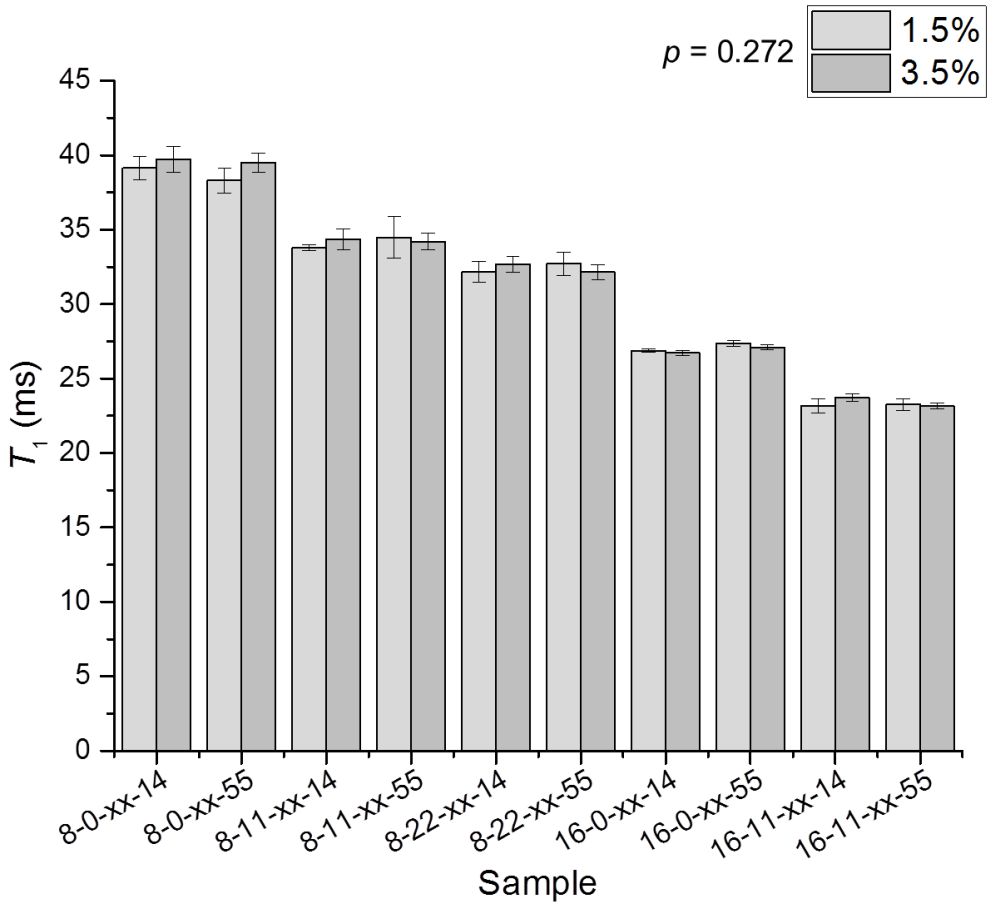

Sample code represents [Protein (% w/w)]-[Fat (% w/w)]-[NaCl (% w/w)]-[Homogenization pressure (MPa)], with NaCl content (xx) indicated by bar shading. Results are expressed as mean ± standard deviation (n = 3). */**/*** indicates a significant difference ($\alpha = 0.05/0.01/0.001$, respectively) within sample pairs by independent t-test. p is the p-value for systematic treatment effect obtained by a dependent t-test comparing means for all sample pairs.

Figure 3.8 ^{23}Na NMR SQ transverse relaxation time (T_2) by NaCl content (1.5 and 3.5% w/w).

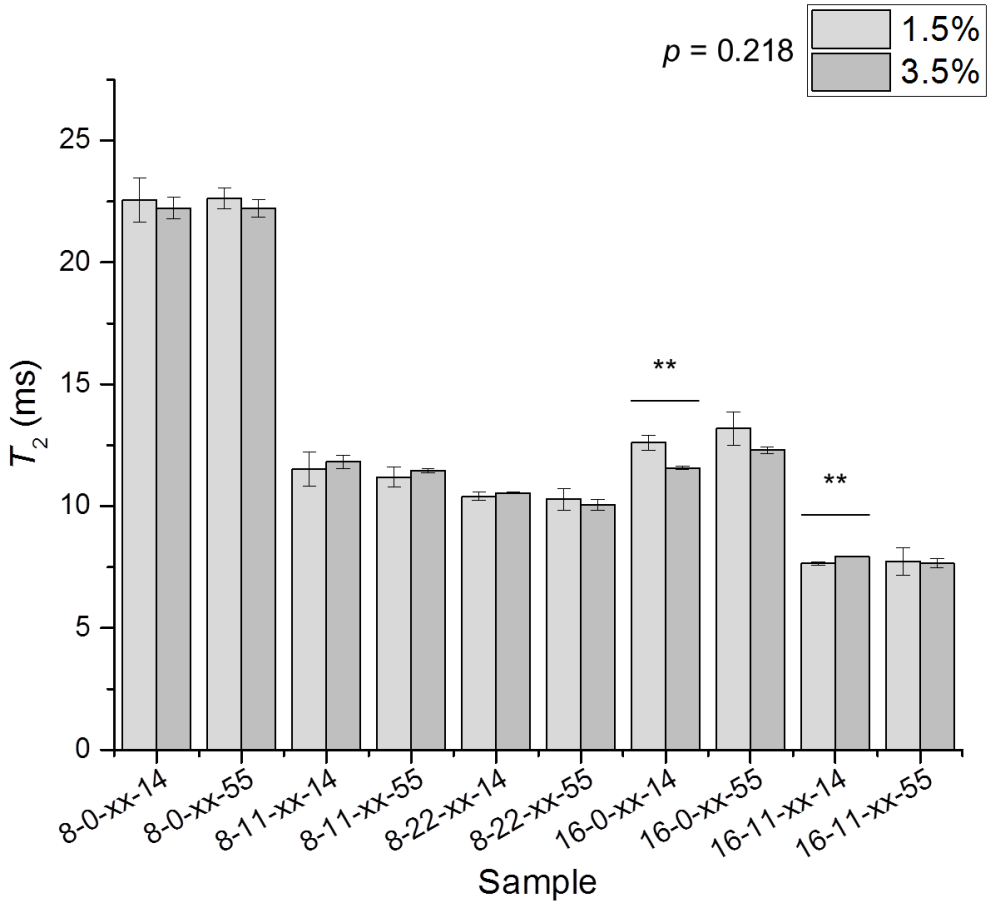

Sample code represents [Protein (% w/w)]-[Fat (% w/w)]-[NaCl (% w/w)]-[Homogenization pressure (MPa)], with NaCl content (xx) indicated by bar shading. Results are expressed as mean ± standard deviation (n = 3). */**/*** indicates a significant difference ($\alpha = 0.05/0.01/0.001$, respectively) within sample pairs by independent t-test. p is the p-value for systematic treatment effect obtained by a dependent t-test comparing means for all sample pairs.

Figure 3.9 ^{23}Na NMR SQ longitudinal relaxation time (T_1) by homogenization pressure (14 and 55 MPa).

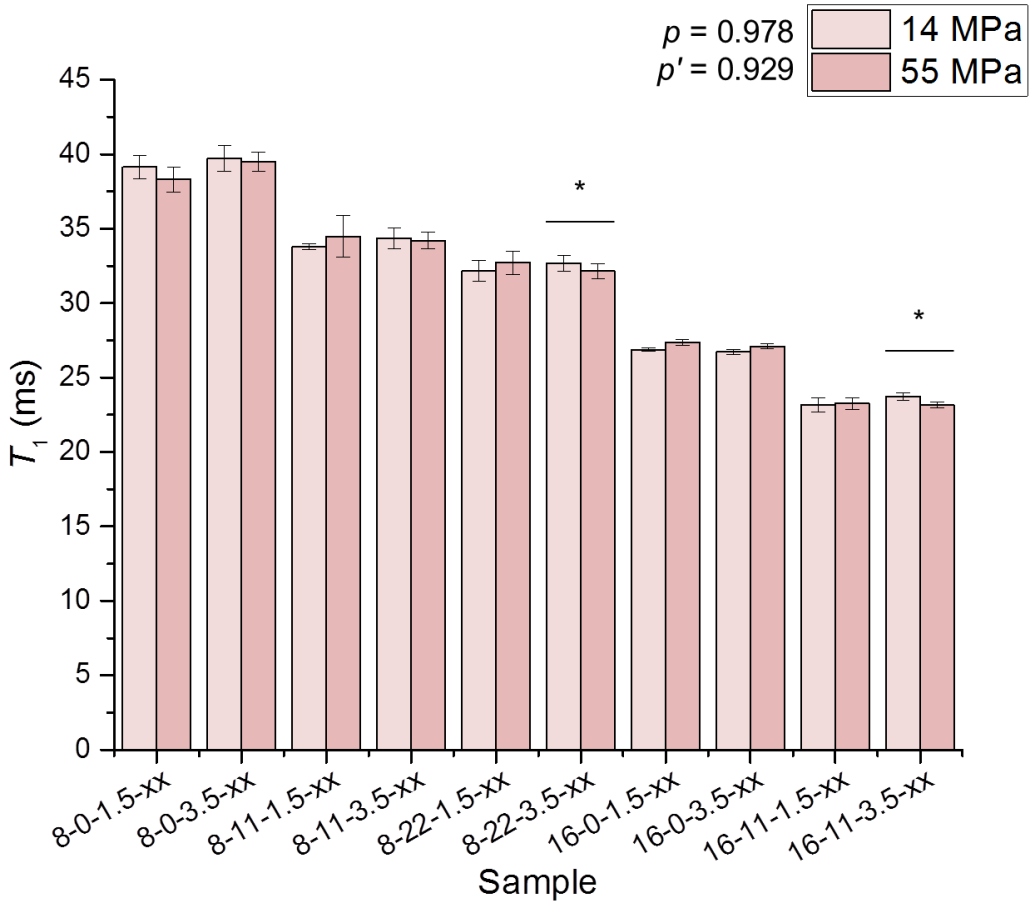

Sample code represents [Protein (% w/w)]-[Fat (% w/w)]-[NaCl (% w/w)]-[Homogenization pressure (MPa)], with homogenization pressure (xx) indicated by bar shading. Results are expressed as mean ± standard deviation (n = 3). */**/*** indicates a significant difference ($\alpha = 0.05/0.01/0.001$, respectively) within sample pairs by independent t-test. p is the p-value for systematic treatment effect obtained by a dependent t-test comparing means for all sample pairs. p' is the p-value for systematic treatment effect obtained by a dependent t-test comparing means for only sample pairs containing fat.

Figure 3.10 ^{23}Na NMR SQ transverse relaxation time (T_2) by homogenization pressure (14 and 55 MPa).

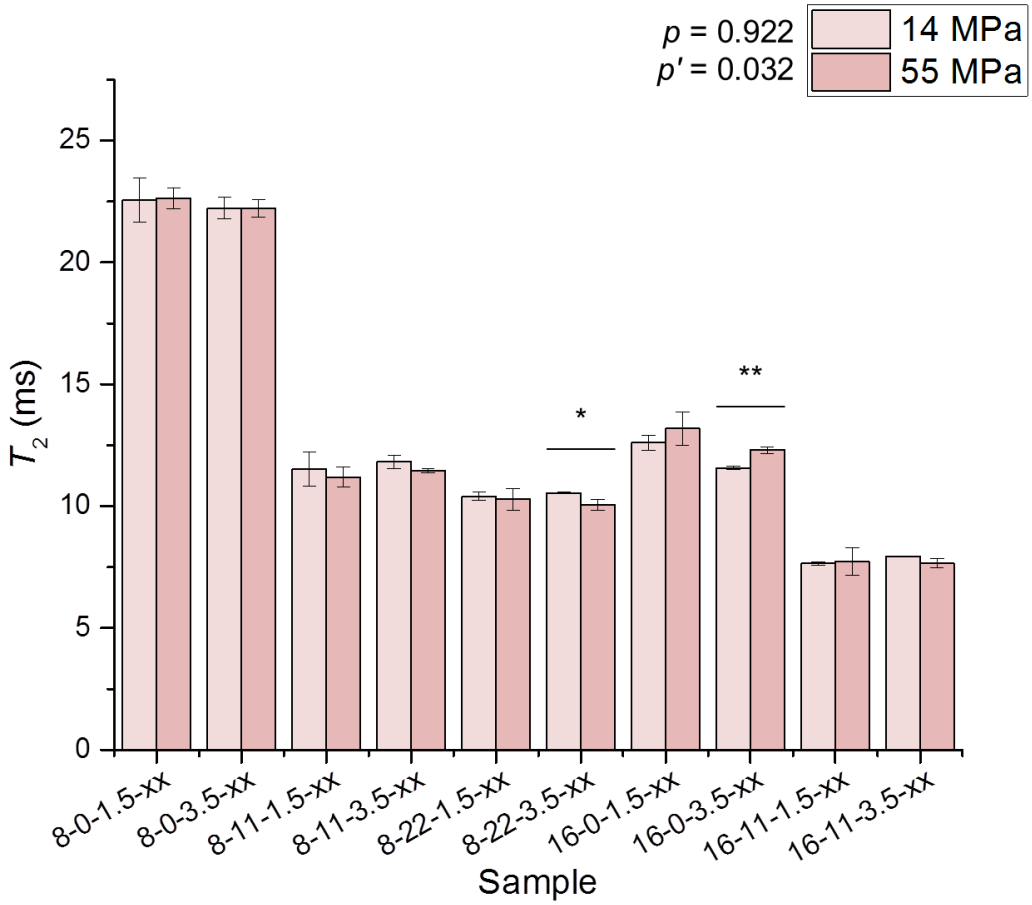

Sample code represents [Protein (% w/w)]-[Fat (% w/w)]-[NaCl (% w/w)]-[Homogenization pressure (MPa)], with homogenization pressure (xx) indicated by bar shading. Results are expressed as mean ± standard deviation (n = 3). */**/*** indicates a significant difference ($\alpha = 0.05/0.01/0.001$, respectively) within sample pairs by independent t-test. p is the p-value for systematic treatment effect obtained by a dependent t-test comparing means for all sample pairs. p' is the p-value for systematic treatment effect obtained by a dependent t-test comparing means for only sample pairs containing fat.

Figure 3.11 ^{23}Na NMR DQ creation time (τ^{opt}) by protein content (8 and 16% w/w).

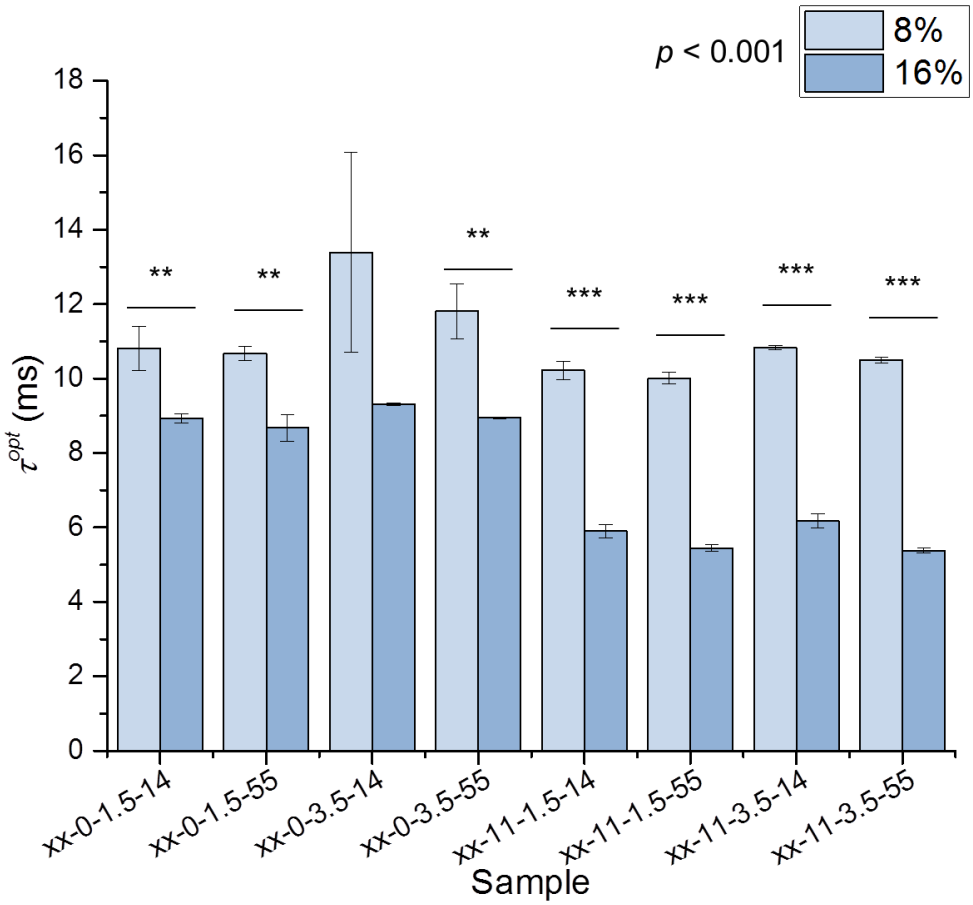

Sample code represents [Protein (% w/w)]-[Fat (% w/w)]-[NaCl (% w/w)]-[Homogenization pressure (MPa)], with protein content (xx) indicated by bar shading. Results are expressed as mean ± standard deviation (n = 3). */**/*** indicates a significant difference ($\alpha = 0.05/0.01/0.001$, respectively) within sample pairs by independent t-test. p is the p-value for systematic treatment effect obtained by a dependent t-test comparing means for all sample pairs.

Figure 3.12 ^{23}Na NMR DQ creation time (τ^{opt}) by fat content (0, 11, and 22% w/w).

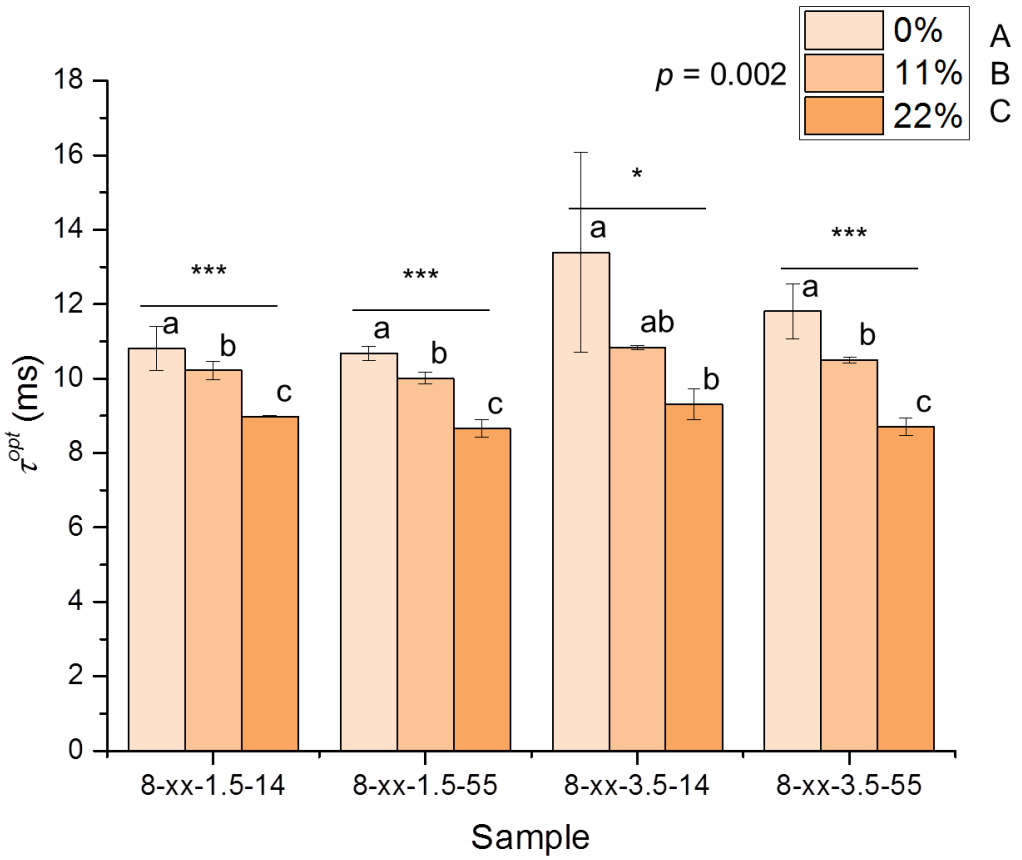

Sample code represents [Protein (% w/w)]-[Fat (% w/w)]-[NaCl (% w/w)]-[Homogenization pressure (MPa)], with fat content (xx) indicated by bar shading. Results are expressed as mean ± standard deviation (n = 3). */**/*** indicates a significant difference ($\alpha = 0.05/0.01/0.001$, respectively) within sample trios by ANOVA. Values in the same column with different letters were significantly different ($\alpha = 0.05$). p is the p-value for systematic treatment effect obtained by ANOVA comparing means for all samples. Treatments with different letters were significantly different ($\alpha = 0.05$).

Figure 3.13 ^{23}Na NMR DQ creation time (τ^{opt}) by NaCl content (1.5 and 3.5% w/w).

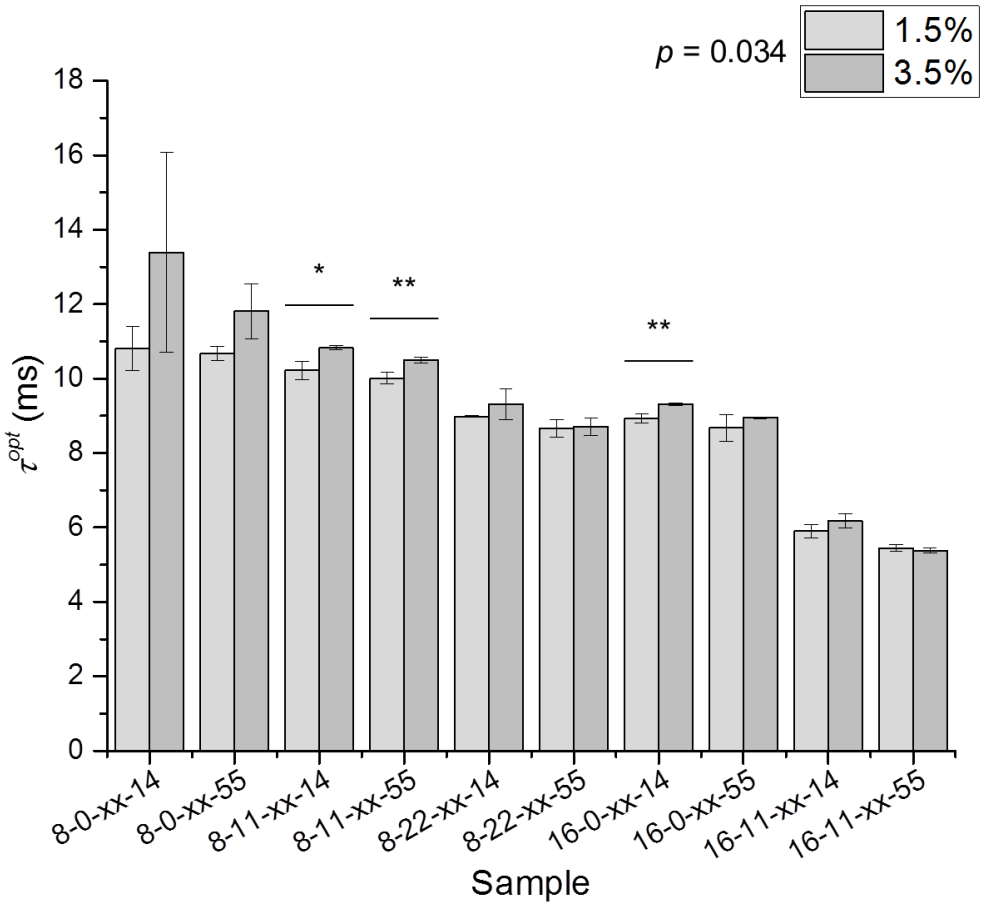

Sample code represents [Protein (% w/w)]-[Fat (% w/w)]-[NaCl (% w/w)]-[Homogenization pressure (MPa)], with NaCl content (xx) indicated by bar shading. Results are expressed as mean ± standard deviation (n = 3). */**/*** indicates a significant difference ($\alpha = 0.05/0.01/0.001$, respectively) within sample pairs by independent t-test. p is the p-value for systematic treatment effect obtained by a dependent t-test comparing means for all sample pairs.

Figure 3.14 ^{23}Na NMR DQ creation time (τ^{opt}) by homogenization pressure (14 and 55 MPa).

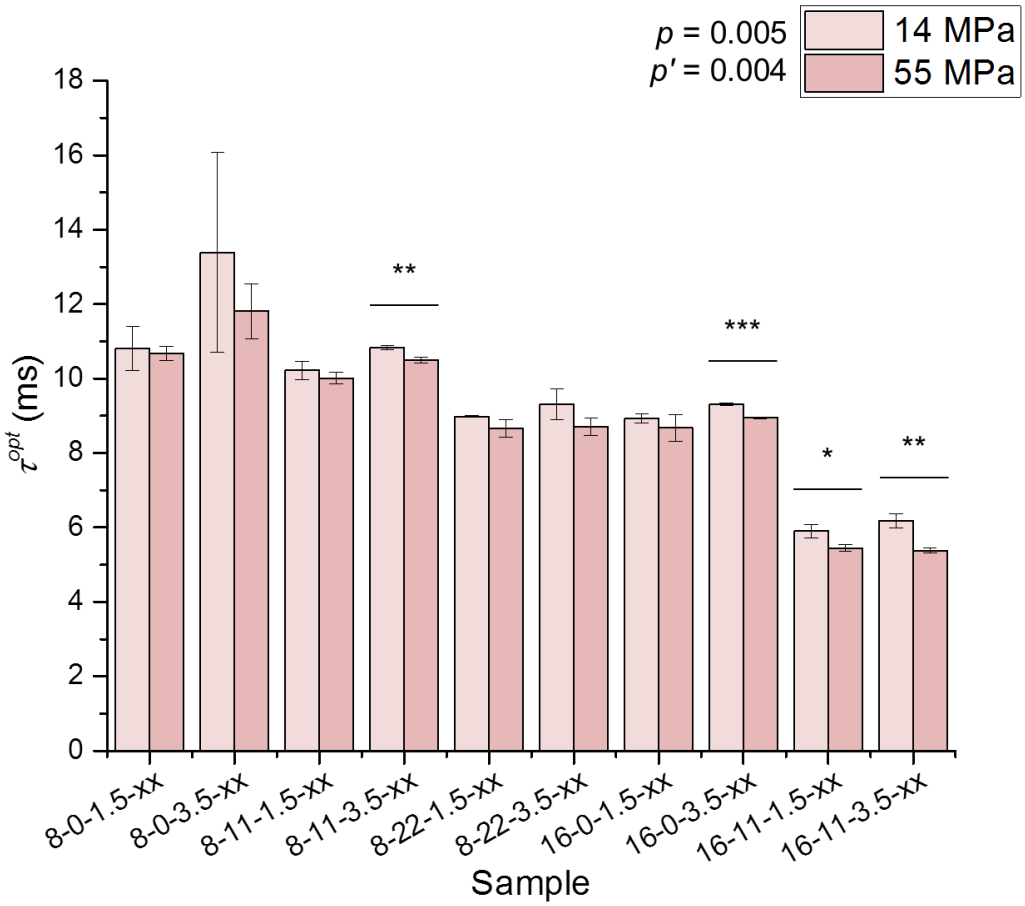

Sample code represents [Protein (% w/w)]-[Fat (% w/w)]-[NaCl (% w/w)]-[Homogenization pressure (MPa)], with homogenization pressure (xx) indicated by bar shading. Results are expressed as mean ± standard deviation (n = 3). */**/*** indicates a significant difference ($\alpha = 0.05/0.01/0.001$, respectively) within sample pairs by independent t-test. p is the p-value for systematic treatment effect obtained by a dependent t-test comparing means for all sample pairs. p' is the p-value for systematic treatment effect obtained by a dependent t-test comparing means for only sample pairs containing fat.

Figure 3.15 Relative 'bound' sodium (A_{DQ}/A_{SQ}) by protein content (8 and 16% w/w).

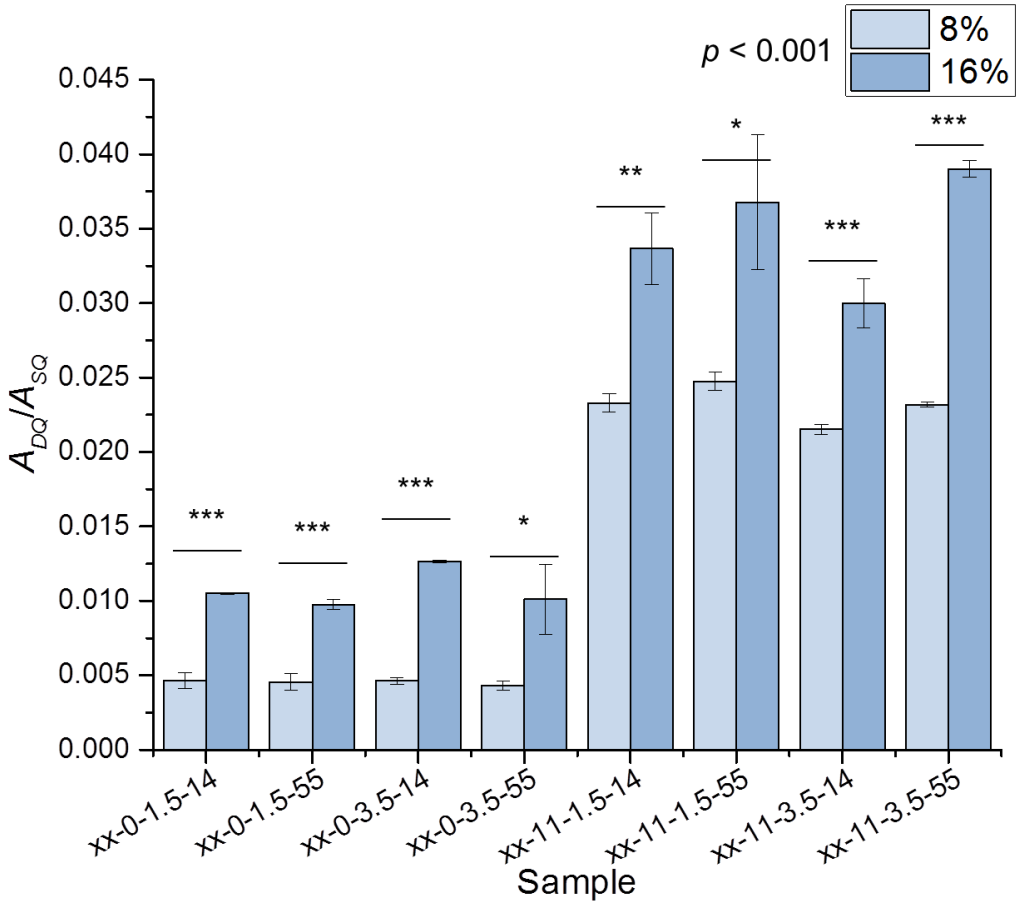

Sample code represents [Protein (% w/w)]-[Fat (% w/w)]-[NaCl (% w/w)]-[Homogenization pressure (MPa)], with protein content (xx) indicated by bar shading. Results are expressed as mean ± standard deviation (n = 3). */**/*** indicates a significant difference ($\alpha = 0.05/0.01/0.001$, respectively) within sample pairs by independent t-test. p is the p-value for systematic treatment effect obtained by a dependent t-test comparing means for all sample pairs.

Figure 3.16 Relative 'bound' sodium (A_{DQ}/A_{SQ}) by fat content (0, 11, and 22% w/w).

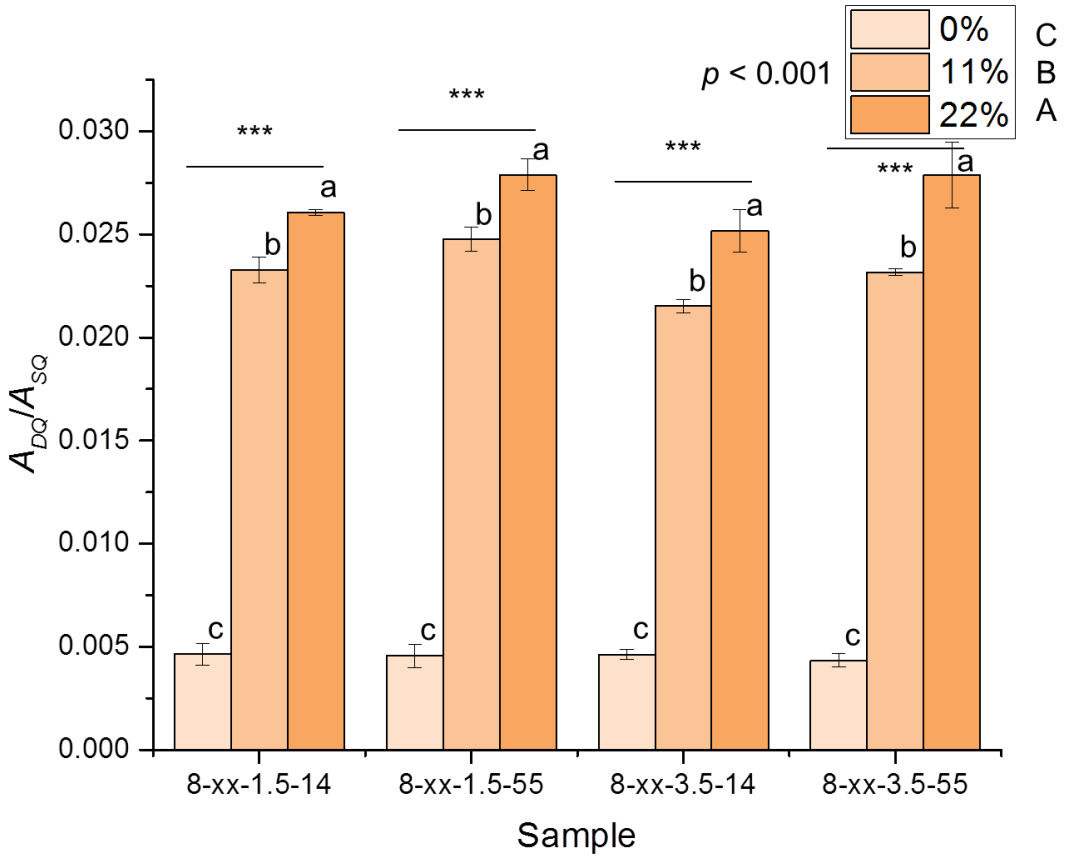

Sample code represents [Protein (% w/w)]-[Fat (% w/w)]-[NaCl (% w/w)]-[Homogenization pressure (MPa)], with fat content (xx) indicated by bar shading. Results are expressed as mean ± standard deviation (n = 3). */**/*** indicates a significant difference ($\alpha = 0.05/0.01/0.001$, respectively) within sample trios by ANOVA. Values in the same column with different letters were significantly different ($\alpha = 0.05$). p is the p-value for systematic treatment effect obtained by ANOVA comparing means for all samples. Treatments with different letters were significantly different ($\alpha = 0.05$).

Figure 3.17 Relative 'bound' sodium (A_{DQ}/A_{SQ}) by dry matter (protein + fat) content.

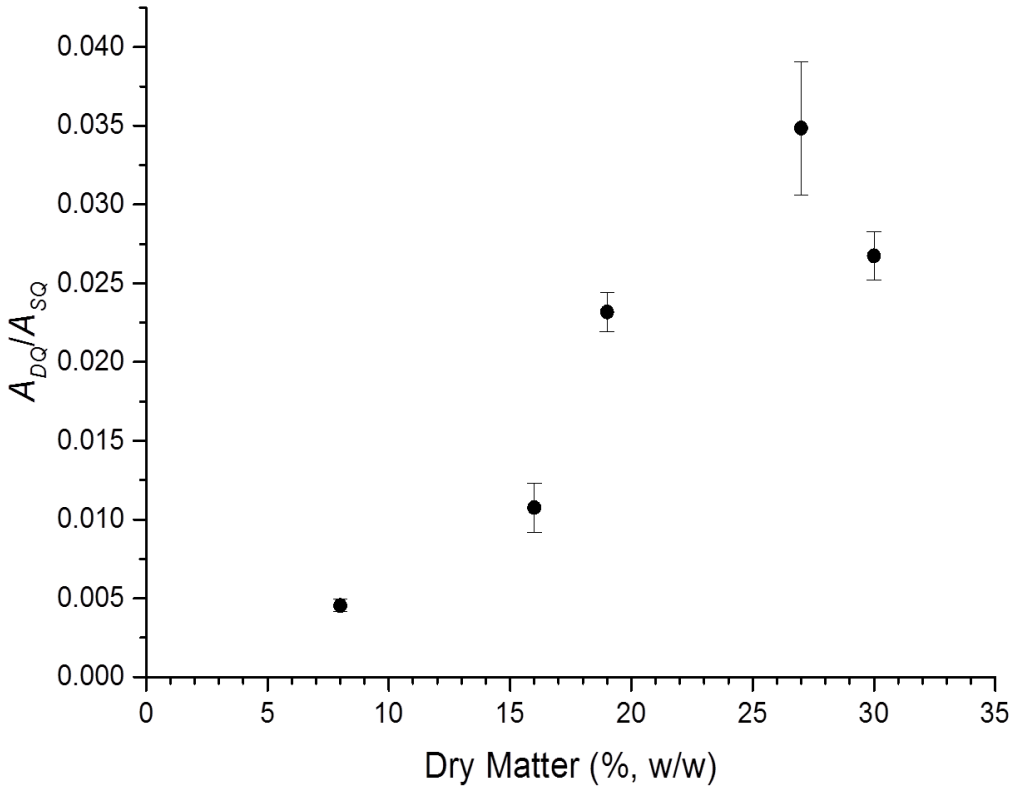

Results are expressed as mean ± standard deviation (n = 12).

Figure 3.18 Relative 'bound' sodium (A_{DQ}/A_{SQ}) by NaCl content (1.5 and 3.5% w/w).

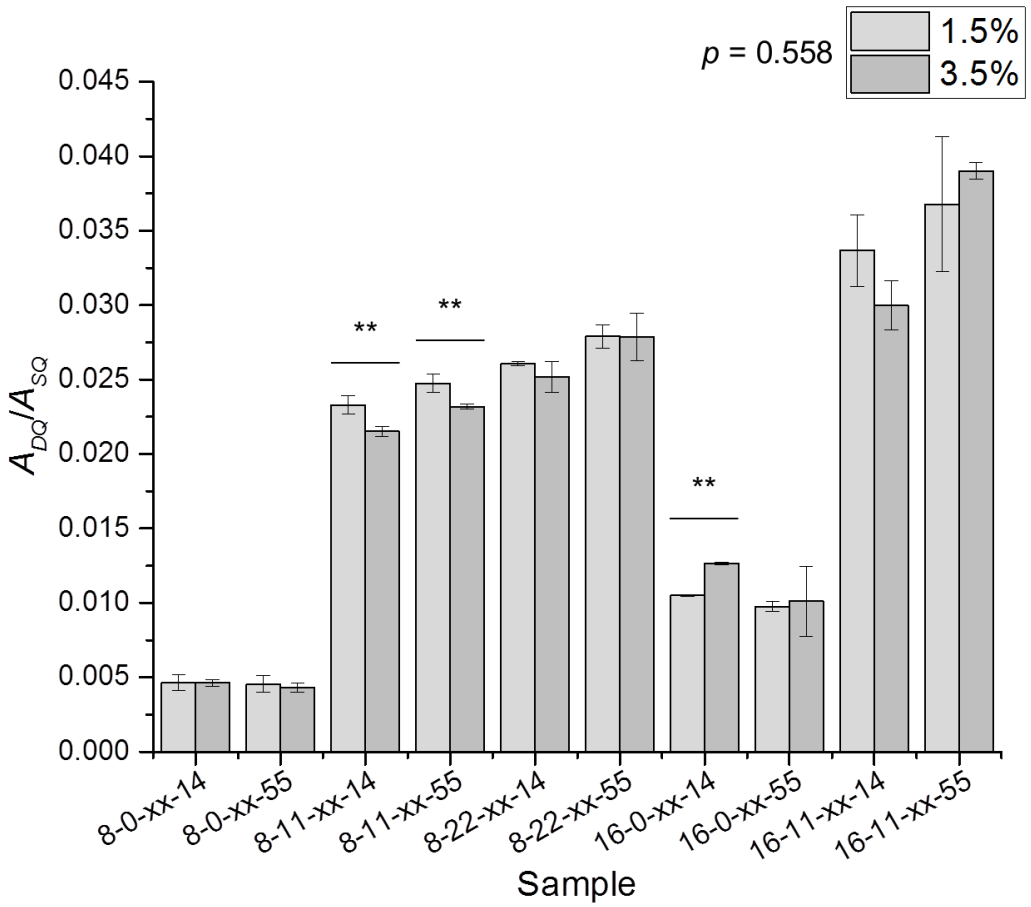

Sample code represents [Protein (% w/w)]-[Fat (% w/w)]-[NaCl (% w/w)]-[Homogenization pressure (MPa)], with NaCl content (xx) indicated by bar shading. Results are expressed as mean ± standard deviation (n = 3). */**/*** indicates a significant difference ($\alpha = 0.05/0.01/0.001$, respectively) within sample pairs by independent t-test. p is the p-value for systematic treatment effect obtained by a dependent t-test comparing means for all sample pairs.

Figure 3.19 Relative 'bound' sodium (A_{DQ}/A_{SQ}) by homogenization pressure (14 and 55 MPa).

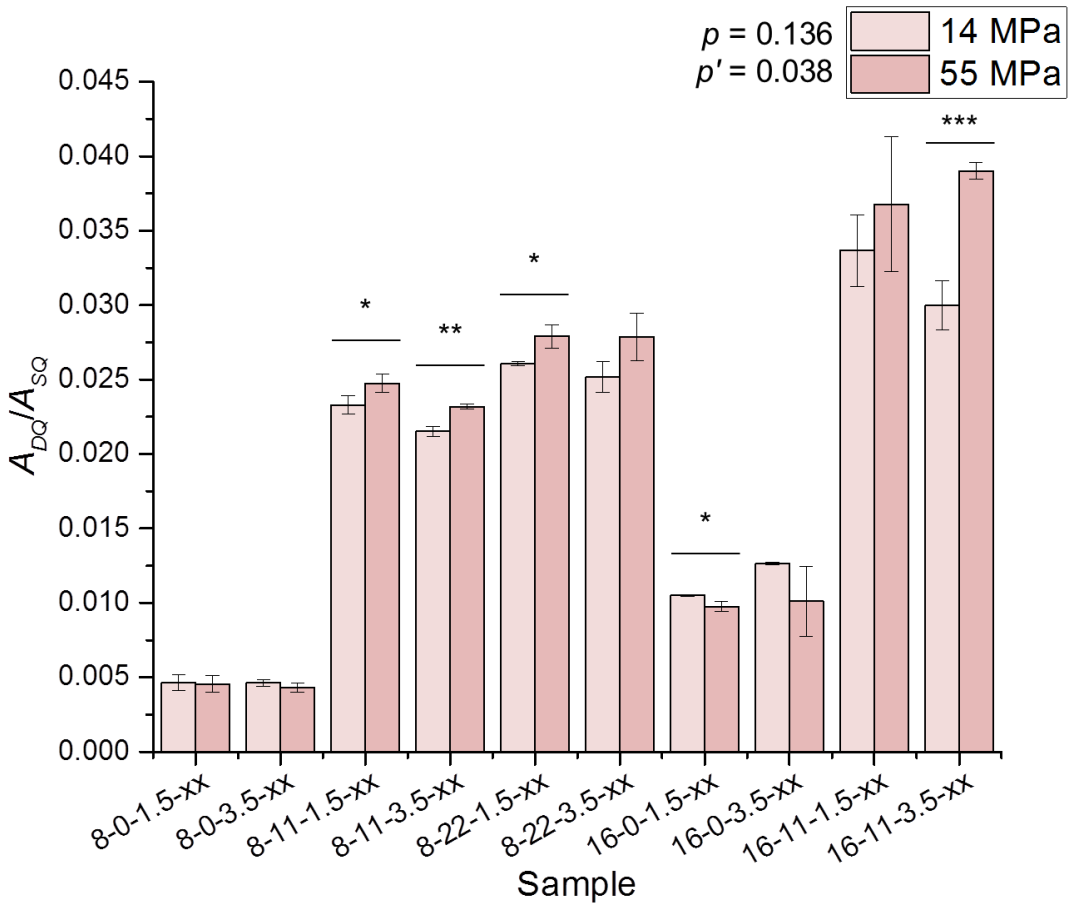

Sample code represents [Protein (% w/w)]-[Fat (% w/w)]-[NaCl (% w/w)]-[Homogenization pressure (MPa)], with homogenization pressure (xx) indicated by bar shading. Results are expressed as mean ± standard deviation (n = 3). */**/*** indicates a significant difference ($\alpha = 0.05/0.01/0.001$, respectively) within sample pairs by independent t-test. p is the p-value for systematic treatment effect obtained by a dependent t-test comparing means for all sample pairs. p' is the p-value for systematic treatment effect obtained by a dependent t-test comparing means for only sample pairs containing fat.

Chapter 4. Characterization of Intrinsic Material Properties of a Model Lipoproteic Emulsion Gel by Oscillatory and Creep Compliance Rheometry

4.1 Abstract

The effects of varying formulation and processing parameters on rheological properties in a model lipid/protein-based (lipoproteic) emulsion gel were studied. Heat-set model lipoproteic emulsion gels were prepared with varying levels of protein (whey protein isolate, 8 and 11 % w/w), lipid (anhydrous milk fat, 0, 11, and 22 % w/w), and NaCl (1.5 and 3.5 % w/w), homogenized under different levels of high pressure homogenization (14 and 55 MPa). Small deformation oscillatory rheometry and creep compliance/recovery experiments were used to characterize intrinsic structural properties and matrix interactions. Creep compliance behavior of the gel system was successfully modeled by a four-component Burgers model. Shear storage (G') and loss (G'') moduli and Newtonian viscosity (η_N) increased while instantaneous compliance (J_0) and retarded compliance (J_1) decreased with increasing protein, fat, or salt content or increasing homogenization pressure. Increasing G' and decreasing J_0 and J_1 reflect the formation of firmer, more solid gels with improved three-dimensional structure. The larger η_N values reflect more resistance to flow and less protein network breakdown over long time. This study highlighted how the intrinsic mechanical and rheological properties of the model emulsion gel are affected by formulation and processing parameters. The data obtained in this study provide information on factors affecting protein network structure and strength, properties which may affect sensory saltiness perception and are important considerations for sodium reduction in lipid/protein-based foods.

4.2 Introduction

Excessive dietary sodium intake presents a major health concern in the United States and throughout other parts of the world (de Wardener and MacGregor 2002), leading to many efforts to reduce sodium content in processed foods. Foods with a lipoproteic emulsion matrix (i.e. processed cheeses and meats) are of particular interest due to prevalence in the diet and their relative contribution to dietary sodium (Dietary Guidelines Advisory Committee 2010; National Cancer Institute 2016). However, sodium plays a role in desired sensory and textural properties via matrix interactions (Kuo and Lee 2014a), so a deeper understanding of these interactions is crucial to sodium reduction efforts.

Strategies to reduce sodium content include changing sodium behavior and perception by altering structural design or chemical mechanisms (Busch et al. 2013). These strategies alter intermolecular interactions which can affect sodium concentration, release, and availability. Incorporating active filler particles (i.e. emulsified fat particles) into heat-set protein-based gels can alter protein interactions and gel rheological profile (Liu and Tang 2011). Past studies have found that increasing homogenization pressure applied to lipid/protein-based emulsions decreased particle size, increased interfacial protein interactions, and in some cases reduced protein-lipid interactions (Chen and Dickinson 1999; Lee et al. 2009). It has also been found that altering formulation and processing parameters affected emulsion gel microstructure and sodium release during large deformation, which has implications for sensory saltiness perception (Kuo and Lee 2014b).

For viscoelastic food systems such as cheeses, small amplitude oscillatory rheometry is useful for characterizing viscoelastic properties because it does not induce irreversible structural changes (Ma et al. 1996). Rheological behavior can also be conceptualized by mechanical

models comprised of various arrangements of springs and dashpots (in parallel and/or in series). Modeling can mathematically relate deformation to mechanical properties such as solid character, elasticity, and viscosity (Ma et al. 1996; Steffe 1996). In cheeses and emulsion gel matrices, modeling creep compliance and recovery can provide insight into molecular interactions and network structure which have implications for molecular mobility and sensory perception.

The objective of this study was to determine how formulation and processing parameters affect intrinsic protein network structure and mechanical properties in a model lipoproteic emulsion gel. Model emulsion gels were prepared with varying formulation (% Protein, % Fat, % NaCl) and processing conditions (homogenization pressure), and intrinsic rheological properties were characterized by small deformation oscillatory rheometry and creep compliance/recovery rheometry. It was hypothesized that increasing interfacial protein interactions (by increasing protein, fat, or salt content or homogenization pressure) would increase the three-dimensional order of the protein network and gel rigidity. The food matrix impacts sensory perception via interactions with sodium ions and textural properties (Mosca et al. 2015), therefore sodium reduction efforts require a deeper understanding of the factors influencing matrix properties.

4.3 Materials and Methods

Emulsion gel preparation

The model gel formulation and preparation procedures were adapted from the method developed by Kuo and Lee (2014). Whey protein isolate (WPI, Hilmar 9000) was donated by Hilmar Ingredients (Hilmar, CA), anhydrous milkfat (AMF) was purchased from Danish Maid

Butter Company (Chicago, IL), and sodium chloride (NaCl, Crystalline/Certified ACS) was purchased from Fisher Scientific (Fair Lawn, NJ). Table 4.1 lists the formulation and homogenization pressures used for each emulsion gel, which were selected for overlap with prior research by Kuo and Lee (focusing on microstructure, sodium release, mass deformation texture analysis, and sensory analysis) for potential data correlation. Samples were coded by their formulation and homogenization pressures in the format of: [Protein (% w/w)]-[Fat (% w/w)]-[NaCl (% w/w)]-[Homogenization pressure (MPa)]. For example, a sample containing 8% protein, 11% fat, and 3.5% NaCl homogenized at 55 MPa would have the code 8-11-3.5-55. An incomplete factorial structure resulted due to samples with simultaneous higher protein and fat levels (16% Protein and 22% Fat) forming viscous, aerated gels unsuitable for sample gel preparation following high pressure homogenization.

The procedure for preparing and homogenizing the lipoproteic emulsion solutions is described in Chapter 3, and the same methods and process variables (14 and 55 MPa homogenization pressure) were used in this study up to the gelation step. Three batch replicates were prepared for each sample. Particle size of the emulsion solutions was analyzed by laser diffraction, and the particle size analysis methodology is described in Chapter 3.

Rheological analysis samples were gelled in Teflon tubes. Samples were loaded by gently pipetting emulsion solutions into Teflon tubes (76.2 mm length, 25.4 mm inner diameter) lined with Teflon tape (for easier gel removal). Teflon tubes were heated in a 90 °C water bath for 30 minutes to induce gelation, then were removed and stored overnight at 4 °C. One sample tube was prepared from each batch replicate.

Rheological analysis

Following overnight storage, a stainless steel cheese slicer was used to cut gels perpendicular to the length of the tube (slice diameter of ~25 mm and thickness of ~4 mm) and the end slices from each gel were discarded. Gel disks were stored in sealed plastic containers between slicing and analysis to prevent sample desiccation. An ARES-G2 oscillatory rheometer equipped with an Advanced Peltier System was used for rheological measurements, and TRIOS® software was used to collect and analyze data (TA Instruments, New Castle, DE). Strain sweep and creep compliance/recovery tests were conducted with a serrated parallel top plate (25 mm diameter) and 4 mm gap at 25 °C.

The detailed protocol for rheological measurements can be found in Appendix C. The gel disks were centered on the lower plate, the top plate was lowered to the experimental gap distance, and excess sample was trimmed away. Samples were left in this position for 3 minutes for temperature equilibration and loading stress relaxation. Oscillatory strain sweeps were conducted from 0.01 to 10.0% strain at 1.0 Hz to identify the linear viscoelastic region. Small deformation rheological properties were characterized within the linear viscoelastic region (0.1% strain, 1.0 Hz), and for each sample formulation stress and strain values were selected from within the linear viscoelastic region for creep compliance tests. Following an additional 3 minutes of sample equilibration and 5 minutes of instrument equilibration, creep compliance/recovery tests were conducted. A constant shear stress (determined from amplitude sweep, $\tau_0 = 2$, 10, 20, or 50 Pa depending on formulation) was applied for 180 seconds with the strain (γ) measured as a function of time, which was then expressed as creep compliance, $J(t)$:

$$J(t) = \frac{\gamma(t)}{\tau_0} \tag{13}$$

The stress was removed and sample recovery was measured for 300 seconds. Two gel disks were measured and the calculated results were averaged for each sample tube replicate.

Statistical analysis

Analysis of variance (ANOVA) and Fisher's Least Significant Difference (LSD) were used to analyze for significant differences between all formulations for particle size and collected rheometry data. To analyze for significant differences due to systematic treatment effects, dependent t-tests were used to analyze applicable formulations due to changes in treatments with two levels (% Protein, % NaCl, homogenization pressure) and analysis of variance (ANOVA) with Fisher's Least Significant Difference (LSD) were used to analyze applicable formulations due to changes in the treatment with three levels (% Fat). To analyze significant differences between sample subsets differing by only one treatment factor, independent t-tests (2-level treatments) and ANOVA (3-level treatments) were used. Statistical analysis was performed using OriginPro 2016 (OriginLab Corporation, Northampton, MA) with a type I error significance level (α) of 0.05.

4.4 Results and Discussion

Oscillatory rheometry

Oscillatory strain sweeps were conducted from 0.01 to 10.0% strain at 1.0 Hz to characterize small deformation rheological properties and identify the linear viscoelastic region for further analysis and creep compliance/recovery experiments. Shear storage (elastic, G') and loss (viscous, G'') moduli were determined in the linear viscoelastic region (0.1% strain, 1.0 Hz) and can be found in Table 4.2. Increasing protein, fat, or salt content or increasing

homogenization pressure increased G' and G''. The increase in modulus value is indicative of increased intermolecular interactions (Chen and Dickinson 1998). The moduli values were averaged for samples with the same dry matter content (protein + fat, % w/w) and are shown in Figure 4.1. The moduli values and the ratio of G' to G'' increase with increasing dry matter content, though samples with 16% protein had higher values than 8% protein samples with similar total dry matter. It has been concluded that an increase in G' relative to G'' is due to an increased three-dimensional structure (Ma et al. 1996), which in this study is due to a denser, more ordered protein network.

Modeling creep compliance data

Stress and strain values were selected from the amplitude sweep data to ensure creep tests were conducted in the linear viscoelastic region. Creep compliance data were fitted using TRIOS® software to a four-component Burgers model (Figure 4.2):

$$J(t) = J_0 + J_1\left(1 - e^{-\frac{t}{\tau}}\right) + \frac{\tau}{\eta_N} \tag{14}$$

where J_0 is the instantaneous elastic compliance (Pa^{-1}) of the Maxwell spring component, J_1 and τ are the retarded elastic compliance (Pa^{-1}) and the retardation time (s), respectively, associated with the Kelvin-Voigt element, and η_N is the Newtonian viscosity (Pa·s) of the Maxwell dashpot component (Steffe 1996). Microsoft Excel was used to calculate the fitting error (mean absolute percentage error, MAPE) between the experimental and modeled data as follows:

$$\text{MAPE} = \frac{1}{n}\sum_{i=1}^{n}\left|\frac{E_i - M_i}{E_i}\right| \tag{15}$$

where n is the number of fitted points, E_i is the experimental value, and M_i is the modeled value. Figure 4.3 displays a representative plot of experimental modeled data. For each sample, the data was fit for 180 data points and the fitting error was less than 0.83%. The use of the Burgers model to describe mechanical behavior is consistent with past studies on heat-set whey protein emulsion gels (Chen et al. 2000) and cheese systems (Ma et al. 1996; Olivares et al. 2009), though a six-component Burgers model was used in some cases. A four-component Burgers model comprised of one Maxwell and one Kelvin-Voigt element was determined to be adequate to describe the behavior of the model gel system in this study.

Creep compliance parameters

The instantaneous elastic compliance values (J_0), retarded compliance (J_1), retardation time (τ), and Newtonian viscosity (η_N) were determined from a four-component Burgers model for all sample formulations and are shown in Table 4.3. Figures 4.4-4.19 display graphs and analysis comparing the creep compliance parameters across the different treatments (8 and 16% w/w protein; 0, 11, and 22% w/w fat; 1.5 and 3.5% w/w NaCl; 14 and 55 MPa homogenization pressure).

J_0 may be associated with intrinsic protein network structure, with higher J_0 values indicating more elastic deformation and freedom for polypeptide strands to rearrange (Lynch and Mulvihill 1994; Ma et al. 1996). Increasing protein content from 8 to 16% resulted in a significant decrease in J_0, ($p = 0.012$, Figure 4.4) as a systematic effect as well as within each sample pair where protein content was the only formulation change. The gels formulated with 16% protein had relatively lower J_0 values than analogous 8% protein samples, indicating the higher protein gels were more rigid. This agrees with the oscillatory rheometry results which

found the higher shear moduli values for the higher protein content gels. The increased rigidity is likely due to increased inter-protein interactions and a denser protein network (more relative protein and less relative water). Similarly, increasing fat content (from 0 to 11 or 22% in samples with 8% protein also resulted in significantly lower J_0 values ($p < 0.001$, Figure 4.5) and more rigid gels. Chen and Dickinson (1999) also found that dispersed oil droplets increased gel strength in heat-set whey protein emulsion gels. When whey protein is the sole emulsifier in the system (as it was in this study), the emulsifying proteins at the oil-water interface interact with protein in the aqueous phase and the dispersed oil acts as an active filler which strengthens the gel. The formulations with added fat also had a higher aqueous protein concentration which could contribute to gel rigidity. Firmer gels were also obtained when NaCl content was increased from 1.5 to 3.5% ($p = 0.038$, Figure 4.6). This is consistent with past literature results which found that increasing ionic strength below a critical concentration increases interprotein interactions and gel strength (Kinekawa et al. 1998). Increasing homogenization pressure did not have a significant effect across all samples ($p = 0.440$, Figure 4.7), but there was a trend across fat-containing samples of lower J_0values with increasing homogenization pressure ($p' = 0.058$). The effect in fat-containing gels may be due to increasing homogenization pressure resulting in reduced particle size and increased interfacial surface area (Appendix B), which allows for more interactions between the interfacial and aqueous proteins.

J_1 has been found to represent principal viscoelastic character, with higher J_1 values reflecting less solid and more viscoelastic character (Subramanian et al. 2003; Olivares et al. 2009). J_1 values followed similar trends as J_0 values for the applied treatments. There was a statistically significant decrease in J_1 when increasing protein from 8 to 16% ($p = 0.012$, Figure 4.8) or fat content from 0 to 11 or 22% ($p < 0.001$, Figure 4.9). The increased protein fraction

and interactions between the protein molecules resulted in a gel with more solid and less viscoelastic character. Increasing salt content from 1.5 to 3.5% did not significantly affect J_1 ($p = 0.259$, Figure 4.10). Increasing homogenization pressure did not have a significant effect on retarded compliance across all samples ($p = 0.194$, Figure 4.11), but there was a trend of decreased J_1 with increased pressure in fat-containing samples ($p' = 0.051$). The increased solid character can be explained by the increased pressure resulting in smaller dispersed filler particles with more opportunities for interfacial surface interactions.

For the formulation effects, τ was not significantly affected by changing protein ($p = 0.184$, Figure 4.12) or fat content ($p = 0.068$, Figure 4.13), but was significantly increased with increased NaCl content ($p = 0.043$, Figure 4.14). A higher value τ indicates a longer time to reach maximal deformation under applied stress, which can be interpreted as τ being inversely related to elastic character (Ojijo et al. 2004). The increased ionic character may have reduced repulsion between protein groups and increased intermolecular interactions, thus reducing network elasticity (Kinekawa et al. 1998). There was a trend of lower τ values with increased homogenization pressure in fat-containing samples ($p' = 0.051$, Figure 4.15). The reduction of filler particle size may have resulted in a more continuous and uniform protein network which could contribute to improved elasticity.

η_N reflects mechanical behavior of the fluid element of the system and resistance to flow over longer times (Lynch and Mulvihill 1994; Olivares et al. 2009). η_N significantly increased with increasing protein ($p < 0.001$, Figure 4.16), fat ($p = 0.004$, Figure 4.17), and NaCl ($p = 0.004$, Figure 4.18) content and increasing homogenization pressure ($p = 0.013$, Figure 4.19). The experiments were conducted at room temperature below the melting temperature of the dispersed AMF, so η_N explains the fluid behavior resulting of the protein network structure

breaking down (Lynch and Mulvihill 1994; Ma et al. 1996; Subramanian et al. 2003). Treatments that increased intermolecular interactions resulted in a stronger protein network that was more resistant to breakdown over long periods of applied stress.

4.5 Conclusions

For this study, the effects of changing formulation and processing parameters on intrinsic rheological properties were characterized by oscillatory rheometry and creep/recovery tests. The particle size measurements by laser diffraction show that altering formulation and homogenization conditions influenced emulsion particle size. Increasing protein, fat, or NaCl content or homogenization pressure increased shear storage and loss moduli because of increased intermolecular interactions and three-dimensional structure. The mechanical behavior of the model gel system was successfully modeled using the Burgers model with four components (one Maxwell element and one Kelvin-Voigt element in series). Gels with more rigid, solid character were obtained with increasing protein, fat, or NaCl content or homogenization pressure due to a denser protein network and increased protein interactions. In conclusion, selected treatments were found to alter molecular interactions and affect compliance which may have implications for sodium behavior in the matrix and sensory perception.

4.6 Literature Cited

Busch JLHC, Yong FYS, Goh SM. 2013. Sodium reduction: Optimizing product composition and structure towards increasing saltiness perception. Trends Food Sci. Technol. 29(1):21–34.

Chen J, Dickinson E. 1998. Viscoelastic Properties of Heat-Set Whey Protein Emulsion Gels. J. Texture Stud. 29(3):285–304.

Chen J, Dickinson E. 1999. Effect of surface character of filler particles on rheology of heat-set whey protein emulsion gels. Colloids Surfaces B Biointerfaces 12(3-6):373–381.

Chen J, Dickinson E, Langton M, Hermansson A-M. 2000. Mechanical properties and microstructure of heat-set whey protein emulsion gels: effect of emulsifiers. LWT-Food Sci. Technol. 307:299–307.

de Wardener H, MacGregor G. 2002. Harmful effects of dietary salt in addition to hypertension. J. Hum. Hypertens. 16(4):213–223.

Dietary Guidelines Advisory Committee. 2010. Report of the Dietary Guidelines Advisory Committee on the Dietary Guidelines for Americans, 2010. Washington, DC: United States Department of Agriculture.

Kinekawa Y-I, Fuyuki T, Kitabatake N. 1998. Effects of Salts on the Properties of Sols and Gels Prepared from Whey Protein Isolate and Process Whey Protein. J. Dairy Sci. 81(6):1532–1544.

Kuhn KR, Cunha RL. 2012. Flaxseed oil – Whey protein isolate emulsions: Effect of high pressure homogenization. J.Food Eng. 111(2):449–457.

Kuo W-Y, Lee Y. 2014a. Effect of Food Matrix on Saltiness Perception-Implications for Sodium Reduction. Compr. Rev. Food Sci. Food Saf. 13(5):906–923.

Kuo W-Y, Lee Y. 2014b. Temporal Sodium Release Related to Gel Microstructural Properties — Implications for Sodium Reduction. J.Food Sci. 79(11):2245–2252.

Lee S-H, Lefèvre T, Subirade M, Paquin P. 2009. Effects of ultra-high pressure homogenization on the properties and structure of interfacial protein layer in whey protein-stabilized emulsion. Food Chem. 113(1):191–195.

Liu F, Tang C. 2011. Cold , gel-like whey protein emulsions by microfluidisation emulsification : Rheological properties and microstructures. Food Chem. 127(4):1641–1647.

Lynch MG, Mulvihill DM. 1994. The influence of caseins on the rheology of i-carrageenan gels. Food Hydrocoll. 8(3-4):317–329.

Ma L, Drake MA, Barbosa-Canovas G V, Swanson BG. 1996. Viscoelastic Properties of Reduced-fat and Full-fat Cheddar Cheeses. J.Food Sci. 61(4):821–823.

Mosca AC, Andriot I, Guichard E, Salles C. 2015. Binding of Na^+ ions to proteins: Effect on taste perception. Food Hydrocoll. 51:33–40.

National Cancer Institute. 2016. Sources of Sodium among the U.S. Population, 2005-06. http://epi.grants.cancer.gov/diet/foodsources/sodium/. Accessed 2016 May 9.

Ojijo NKO, Kesselman E, Shuster V, Eichler S, Eger S, Neeman I, Shimoni E. 2004. Changes in microstructural, thermal, and rheological properties of olive oil/monoglyceride networks during storage. Food Res. Int. 37(4):385–393.

Olivares ML, Zorrilla SE, Rubiolo AC. 2009. Rheological properties of mozzarella cheese determined by creep/recovery tests: Effect of sampling direction,test temperature and ripening

time. J. Texture Stud. 40(3):300–318.

Steffe JF. 1996. Rheological Methods in Food Process Engineering. 2nd ed. East Lansing, MI: Freeman Press.

Subramanian R, Muthukumarappan K, Gunasekaran S. 2003. Effect of methocel as a water binder on the linear viscoelastic properties of Mozzarella cheese during early stages of maturation. J. Texture Stud. 34(4):361–380.

4.7 Tables and Figures

Table 4.1 Formulation and homogenization pressure sample matrix for rheometry experiments.

Protein (% w/w)	Fat (% w/w)	NaCl (% w/w)	Pressure (MPa)	Sample Code
8	0	1.5	14	8-0-1.5-14
			55	8-0-1.5-55
		3.5	14	8-0-3.5-14
			55	8-0-3.5-55
	11	1.5	14	8-11-1.5-14
			55	8-11-1.5-55
		3.5	14	8-11-3.5-14
			55	8-11-3.5-55
	22	1.5	14	8-22-1.5-14
			55	8-22-1.5-55
		3.5	14	8-22-3.5-14
			55	8-22-3.5-55
16	0	1.5	14	16-0-1.5-14
			55	16-0-1.5-55
		3.5	14	16-0-3.5-14
			55	16-0-3.5-55
	11	1.5	14	16-11-1.5-14
			55	16-11-1.5-55
		3.5	14	16-11-3.5-14
			55	16-11-3.5-55

Table 4.2 Summary of small deformation rheological properties.

Sample	G' (Pa)	G'' (Pa)
8-0-1.5-14	2.26×10^3 j	3.86×10^2 j
8-0-1.5-55	3.64×10^3 j	6.32×10^2 j
8-0-3.5-14	3.07×10^3 j	5.31×10^2 j
8-0-3.5-55	2.76×10^3 j	4.98×10^2 j
8-11-1.5-14	8.54×10^3 ij	1.41×10^3 ij
8-11-1.5-55	2.32×10^4 h	3.95×10^3 h
8-11-3.5-14	1.46×10^4 hi	2.49×10^3 hi
8-11-3.5-55	3.69×10^4 g	6.32×10^3 fg
8-22-1.5-14	3.68×10^4 g	5.92×10^3 g
8-22-1.5-55	8.37×10^4 c	1.34×10^4 c
8-22-3.5-14	5.01×10^4 de	8.23×10^3 e
8-22-3.5-55	1.05×10^5 a	1.70×10^4 a
16-0-1.5-14	2.37×10^4 h	4.03×10^3 h
16-0-1.5-55	1.81×10^4 hi	3.07×10^3 hi
16-0-3.5-14	3.62×10^4 g	6.09×10^3 fg
16-0-3.5-55	4.75×10^4 ef	8.09×10^3 e
16-11-1.5-14	4.57×10^4 efg	7.67×10^3 ef
16-11-1.5-55	8.66×10^4 bc	1.46×10^4 bc
16-11-3.5-14	6.01×10^4 d	9.96×10^3 d
16-11-3.5-55	9.58×10^4 ab	1.60×10^4 ab

Sample code represents [Protein (% w/w)]-[Fat (% w/w)]-[NaCl (% w/w)]-[Homogenization pressure (MPa)], G' is the shear storage modulus, and G'' is the shear loss modulus measured at 0.1 % strain and 1 Hz. Results are expressed as mean (n = 3). Values in the same column with different letters were significantly different ($\alpha = 0.05$).

Table 4.3 Summary of results from creep compliance experiments.

Sample	J_0 (10^{-5}/Pa)	J_1 (10^{-5}/Pa)	τ (s)	η_N (10^5 Pa·s)
8-0-1.5-14	57.56 ± 17.85 a	29.53 ± 7.27 a	18.05 ± 1.08 abc	5.83 ± 1.76 l
8-0-1.5-55	55.80 ± 25.41 a	20.44 ± 8.14 b	17.76 ± 0.21 abc	9.49 ± 3.56 kl
8-0-3.5-14	41.24 ± 7.12 b	20.75 ± 0.99 b	17.45 ± 0.76 c	8.54 ± 1.39 kl
8-0-3.5-55	50.86 ± 5.37 ab	24.32 ± 3.18 b	17.86 ± 0.28 abc	6.53 ± 0.63 l
8-11-1.5-14	15.06 ± 0.97 c	6.84 ± 0.36 c	18.06 ± 0.29 abc	21.66 ± 1.62 jkl
8-11-1.5-55	5.38 ± 0.15 cd	2.60 ± 0.11 d	17.99 ± 0.29 abc	54.39 ± 0.94 hi
8-11-3.5-14	8.94 ± 0.89 cd	4.38 ± 0.46 cd	18.38 ± 0.39 ab	34.41 ± 3.74 ijk
8-11-3.5-55	3.35 ± 0.39 cd	1.68 ± 0.22 d	18.41 ± 0.78 ab	90.35 ± 11.41 fg
8-22-1.5-14	3.45 ± 0.18 cd	1.57 ± 0.05 d	18.38 ± 0.31 ab	95.08 ± 2.37 ef
8-22-1.5-55	1.48 ± 0.06 d	0.65 ± 0.03 d	17.77 ± 0.29 bc	250.92 ± 19.65 ab
8-22-3.5-14	2.60 ± 0.52 d	1.25 ± 0.20 d	18.54 ± 0.13 a	114.81 ± 18.60 def
8-22-3.5-55	1.14 ± 0.13 d	0.51 ± 0.05 d	18.36 ± 0.41 ab	278.27 ± 19.97 a
16-0-1.5-14	5.50 ± 1.09 cd	2.59 ± 0.51 d	17.50 ± 0.10 c	64.28 ± 14.88 gh
16-0-1.5-55	7.03 ± 1.30 cd	3.32 ± 0.65 cd	17.47 ± 0.20 c	48.81 ± 10.79 hij
16-0-3.5-14	3.63 ± 0.52 cd	1.72 ± 0.25 d	17.83 ± 0.19 abc	96.51 ± 11.45 ef
16-0-3.5-55	2.61 ± 0.04 d	1.25 ± 0.02 d	18.01 ± 0.28 abc	125.02 ± 2.84 d
16-11-1.5-14	2.75 ± 0.24 d	1.26 ± 0.11 d	17.90 ± 0.51 abc	121.40 ± 12.94 de
16-11-1.5-55	1.43 ± 0.24 d	0.98 ± 0.25 d	17.72 ± 0.18 abc	246.40 ± 41.68 b
16-11-3.5-14	2.15 ± 0.46 d	0.57 ± 0.03 d	18.28 ± 0.37 ab	162.24 ± 39.22 c
16-11-3.5-55	1.26 ± 0.10 d	0.57 ± 0.03 d	17.99 ± 0.17 abc	274.23 ± 19.12 a

Sample code represents [Protein (% w/w)]-[Fat (% w/w)]-[NaCl (% w/w)]-[Homogenization pressure (MPa)], J_0 is the instantaneous compliance, J_1 is the retarded compliance, τ is the retardation time, and η_N is the Newtonian viscosity. Results are expressed as mean ± standard deviation (n = 3). Values in the same column with different letters were significantly different ($\alpha = 0.05$).

Figure 4.1 Storage (G') and loss (G'') moduli by dry matter (protein + fat) content.

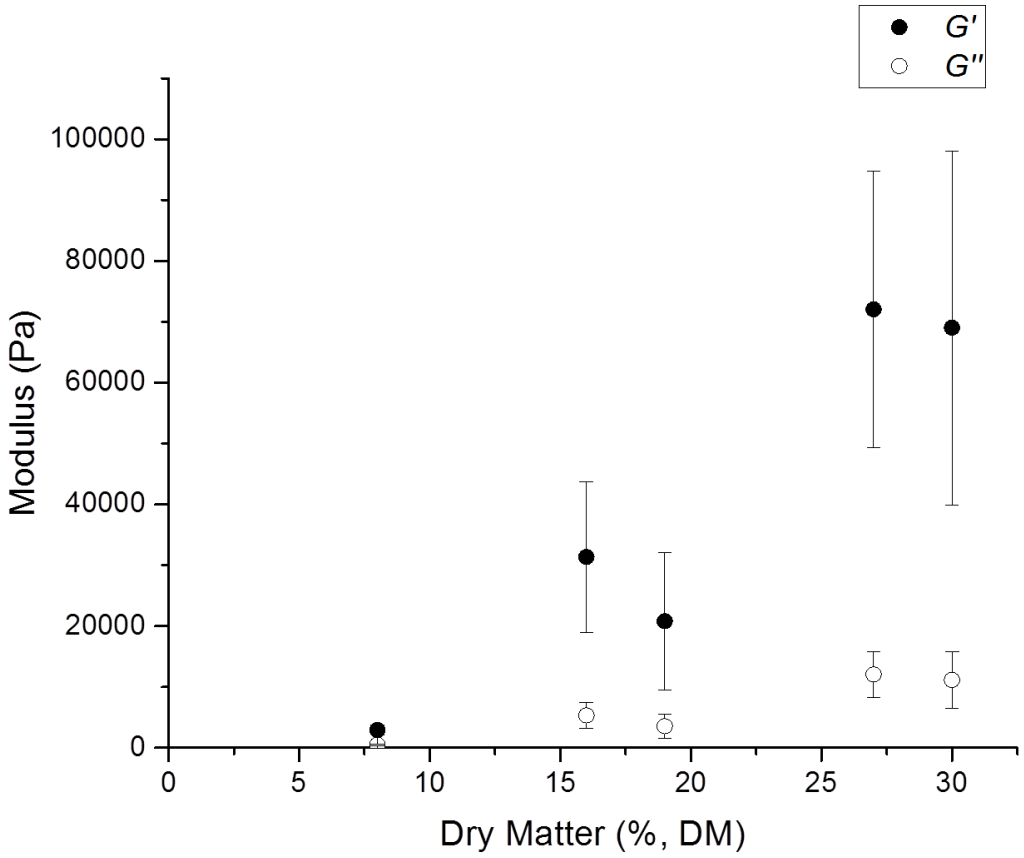

Results are expressed as mean ± standard deviation (n = 12).

Figure 4.2 Mechanical model of a four-element Burger body.

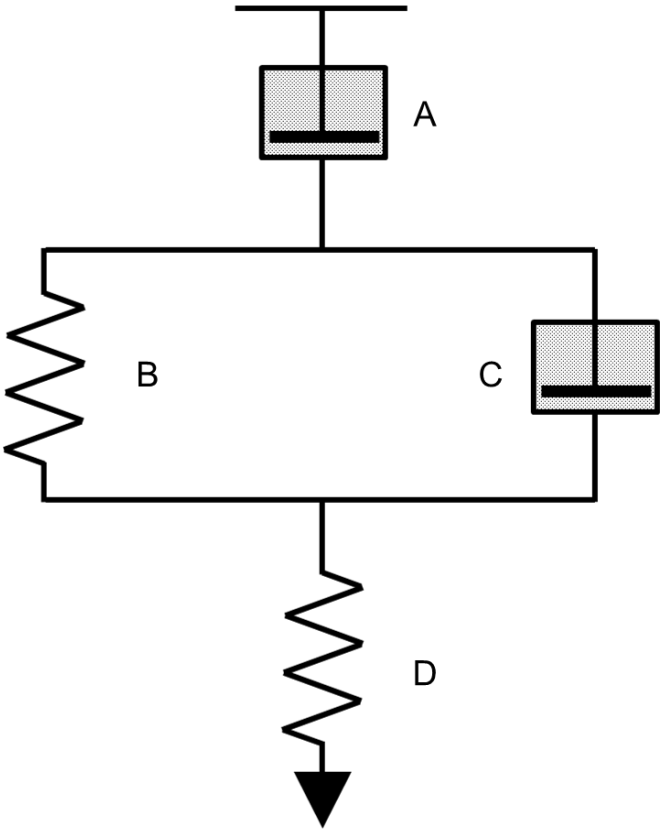

Four-element Burger body consisting of a (A) Maxwell dashpot, (B) Kelvin-Voigt spring and (C) dashpot, and (D) Maxwell spring in series.

Figure 4.3 Representative plot of experimental and modeled creep compliance data for an 8-11-15-55 sample.

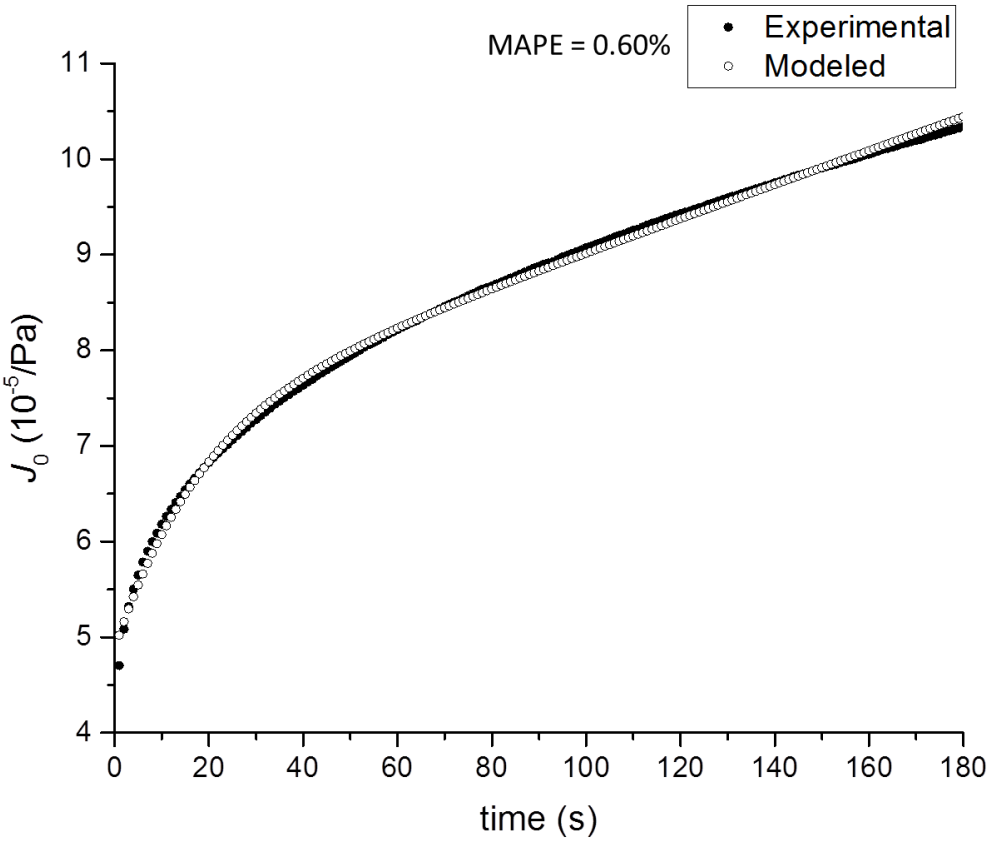

Sample code represents [Protein (% w/w)]-[Fat (% w/w)]-[NaCl (% w/w)]-[Homogenization pressure (MPa)]. Fitting error was calculated as Mean Absolute Percentage Error (MAPE) by Equation 15 with $n = 180$.

Figure 4.4 Instantaneous compliance (J_0) by protein content (8 and 16% w/w).

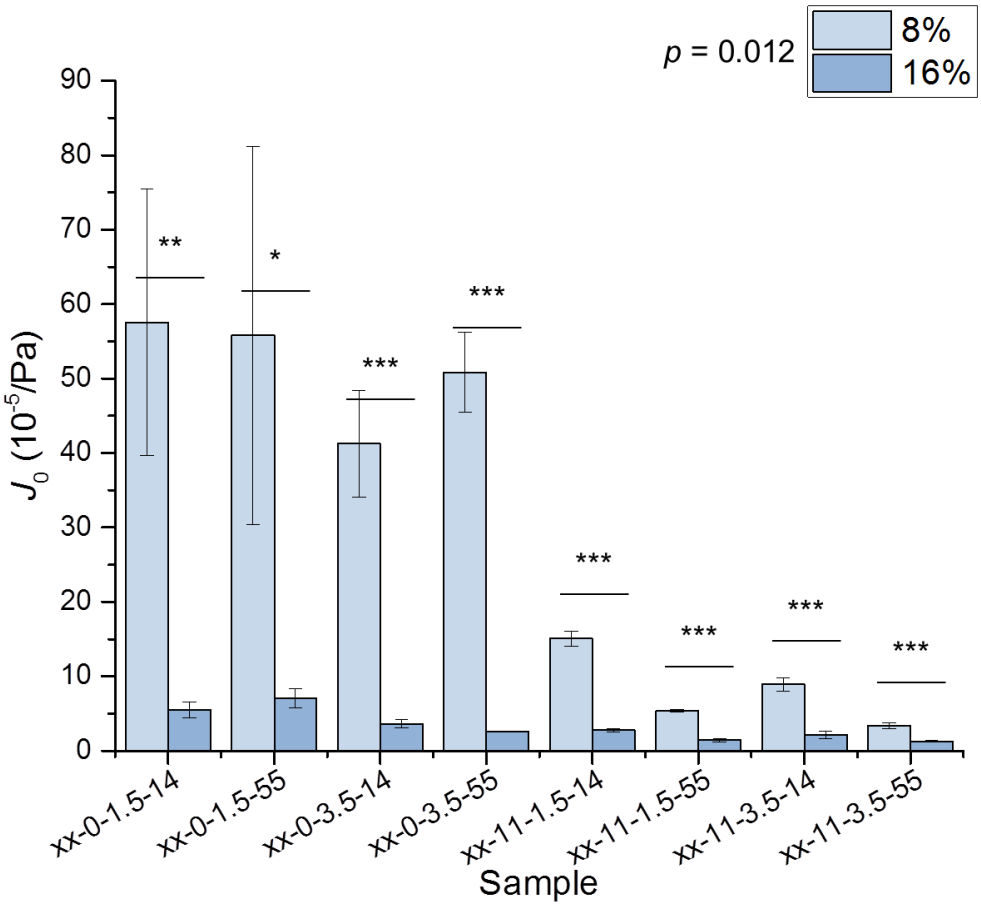

Sample code represents [Protein (% w/w)]-[Fat (% w/w)]-[NaCl (% w/w)]-[Homogenization pressure (MPa)], with protein content (xx) indicated by bar shading. Results are expressed as mean ± standard deviation (n = 3). */**/*** indicates a significant difference ($\alpha = 0.05/0.01/0.001$, respectively) within sample pairs by independent t-test. p is the p-value for systematic treatment effect obtained by a dependent t-test comparing means for all sample pairs.

Figure 4.5 Instantaneous compliance (J_0) by fat content (0, 11, and 22% w/w).

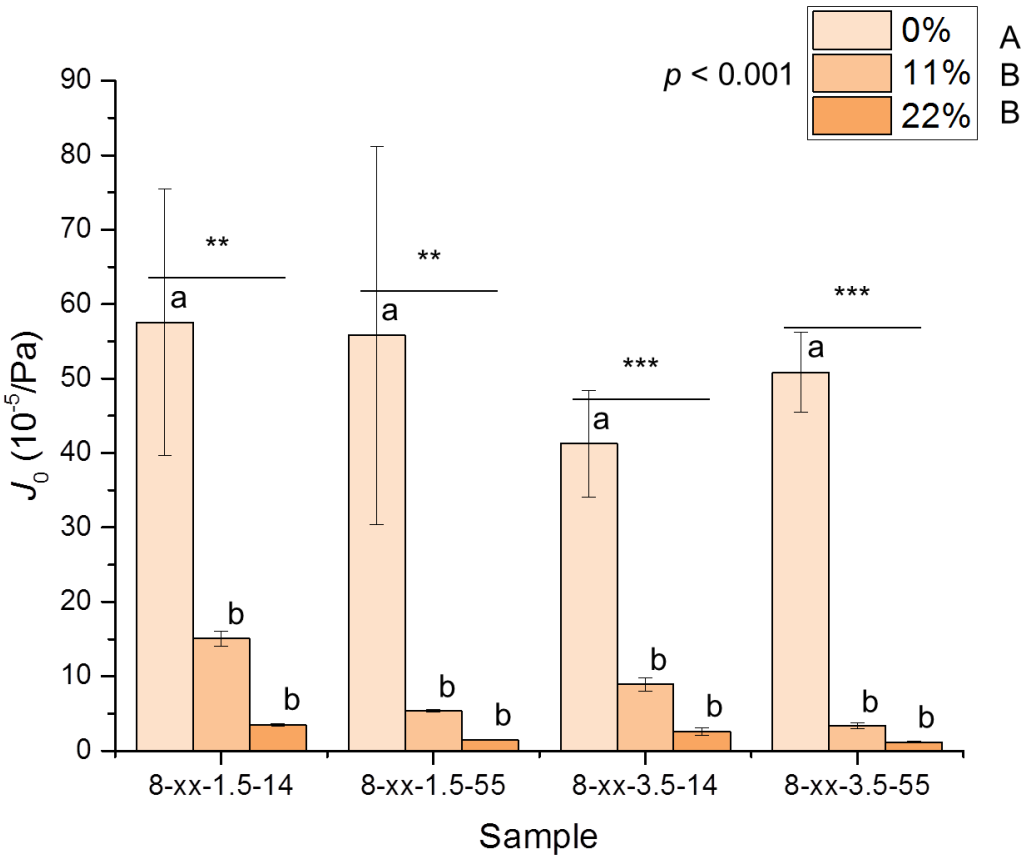

Sample code represents [Protein (% w/w)]-[Fat (% w/w)]-[NaCl (% w/w)]-[Homogenization pressure (MPa)], with fat content (xx) indicated by bar shading. Results are expressed as mean ± standard deviation (n = 3). */**/*** indicates a significant difference ($\alpha = 0.05/0.01/0.001$, respectively) within sample trios by ANOVA. Values in the same column with different letters were significantly different ($\alpha = 0.05$). p is the p-value for systematic treatment effect obtained by ANOVA comparing means for all samples. Treatments with different letters were significantly different ($\alpha = 0.05$).

Figure 4.6 Instantaneous compliance (J_0) by NaCl content (1.5 and 3.5% w/w).

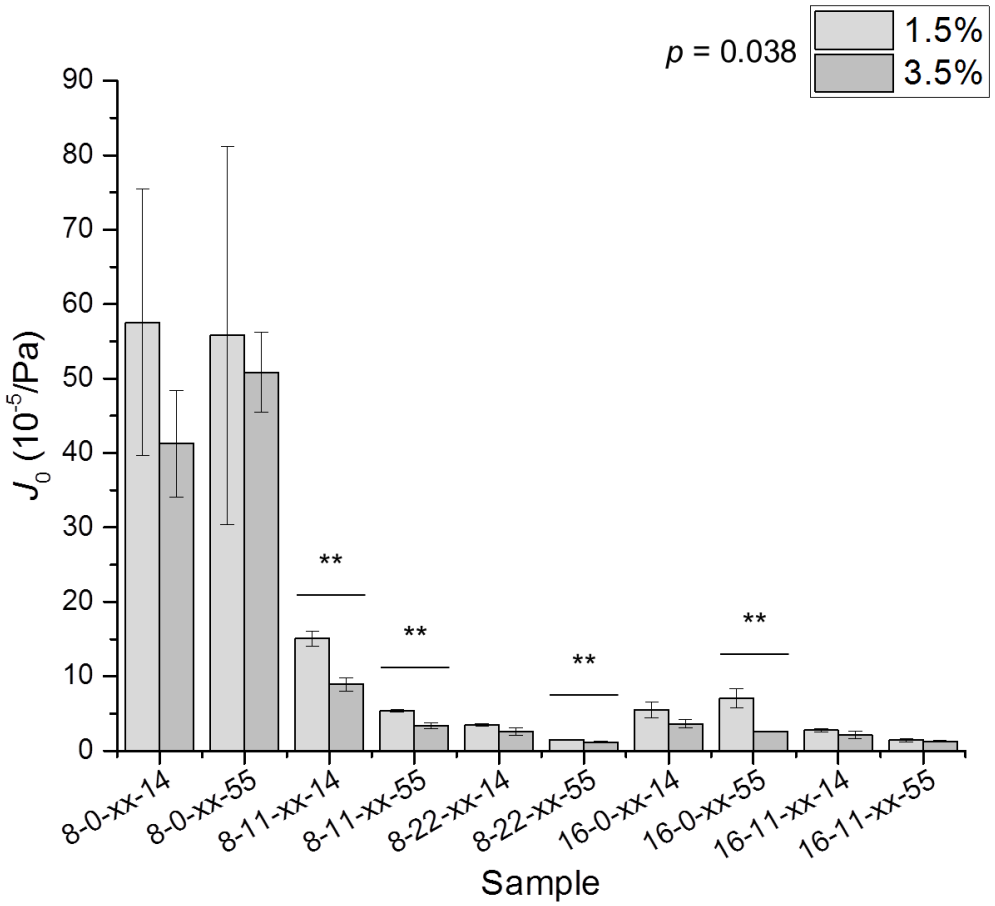

Sample code represents [Protein (% w/w)]-[Fat (% w/w)]-[NaCl (% w/w)]-[Homogenization pressure (MPa)], with NaCl content (xx) indicated by bar shading. Results are expressed as mean ± standard deviation (n = 3). */**/*** indicates a significant difference ($\alpha = 0.05/0.01/0.001$, respectively) within sample pairs by independent t-test. p is the p-value for systematic treatment effect obtained by a dependent t-test comparing means for all sample pairs.

Figure 4.7 Instantaneous compliance (J_0) by homogenization pressure (14 and 55 MPa).

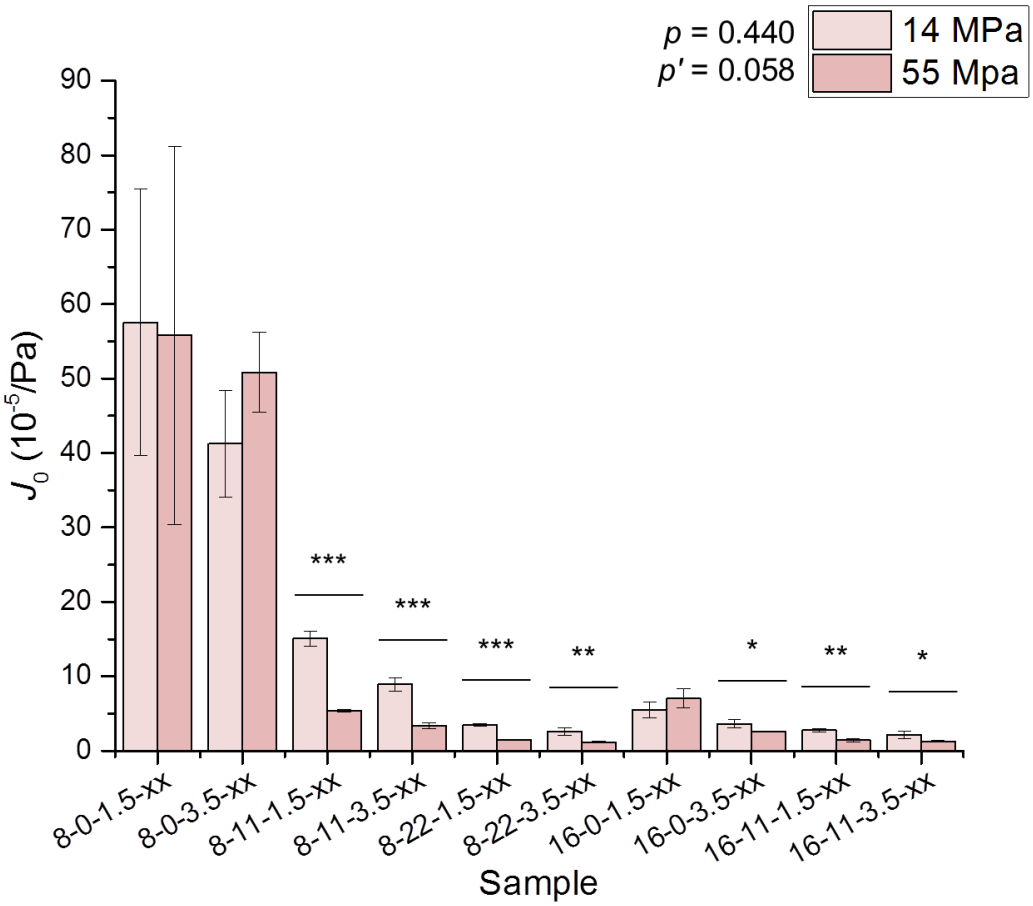

Sample code represents [Protein (% w/w)]-[Fat (% w/w)]-[NaCl (% w/w)]-[Homogenization pressure (MPa)], with homogenization pressure (xx) indicated by bar shading. Results are expressed as mean ± standard deviation (n = 3). */**/*** indicates a significant difference ($\alpha = 0.05/0.01/0.001$, respectively) within sample pairs by independent t-test. p is the p-value for systematic treatment effect obtained by a dependent t-test comparing means for all sample pairs. p' is the p-value for systematic treatment effect obtained by a dependent t-test comparing means for only sample pairs containing fat.

Figure 4.8 Retarded compliance (J_1) by protein content (8 and 16% w/w).

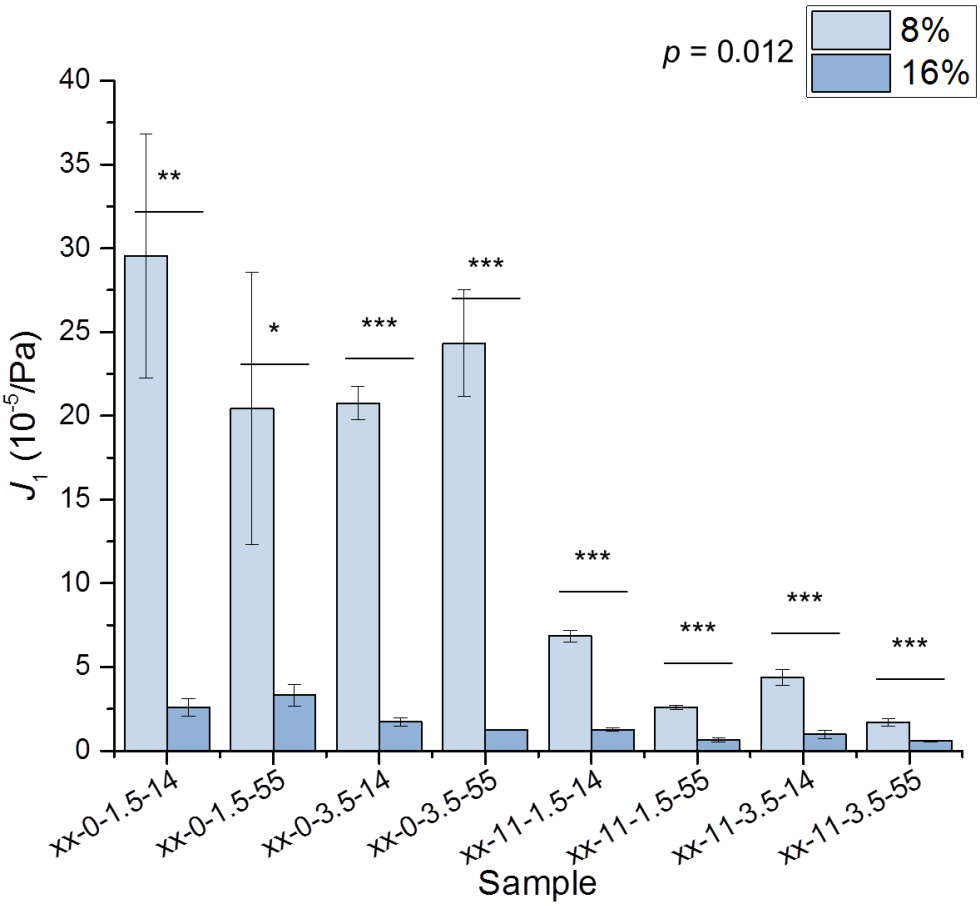

Sample code represents [Protein (% w/w)]-[Fat (% w/w)]-[NaCl (% w/w)]-[Homogenization pressure (MPa)], with protein content (xx) indicated by bar shading. Results are expressed as mean ± standard deviation (n = 3). */**/*** indicates a significant difference ($\alpha = 0.05/0.01/0.001$, respectively) within sample pairs by independent t-test. p is the p-value for systematic treatment effect obtained by a dependent t-test comparing means for all sample pairs.

Figure 4.9 Retarded compliance (J_1) by fat content (0, 11, and 22% w/w).

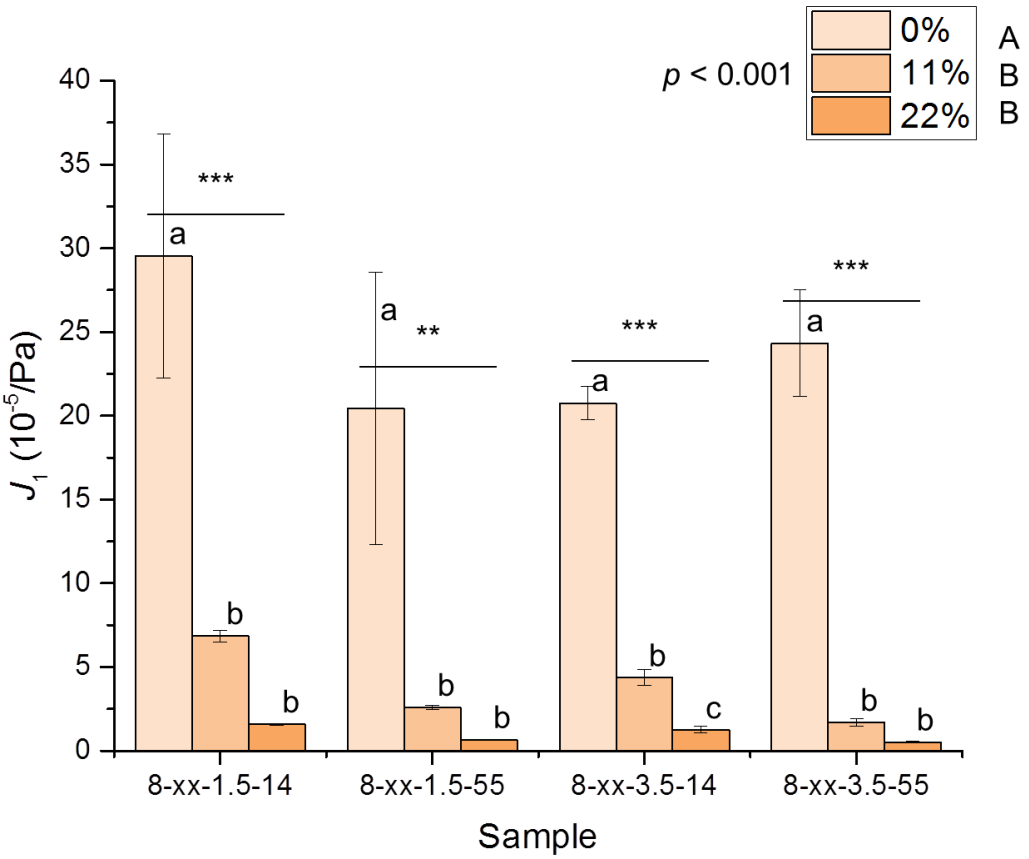

Sample code represents [Protein (% w/w)]-[Fat (% w/w)]-[NaCl (% w/w)]-[Homogenization pressure (MPa)], with fat content (xx) indicated by bar shading. Results are expressed as mean ± standard deviation (n = 3). */**/*** indicates a significant difference ($\alpha = 0.05/0.01/0.001$, respectively) within sample trios by ANOVA. Values in the same column with different letters were significantly different ($\alpha = 0.05$). p is the p-value for systematic treatment effect obtained by ANOVA comparing means for all samples. Treatments with different letters were significantly different ($\alpha = 0.05$).

Figure 4.10 Retarded compliance (J_1) by NaCl content (1.5 and 3.5% w/w).

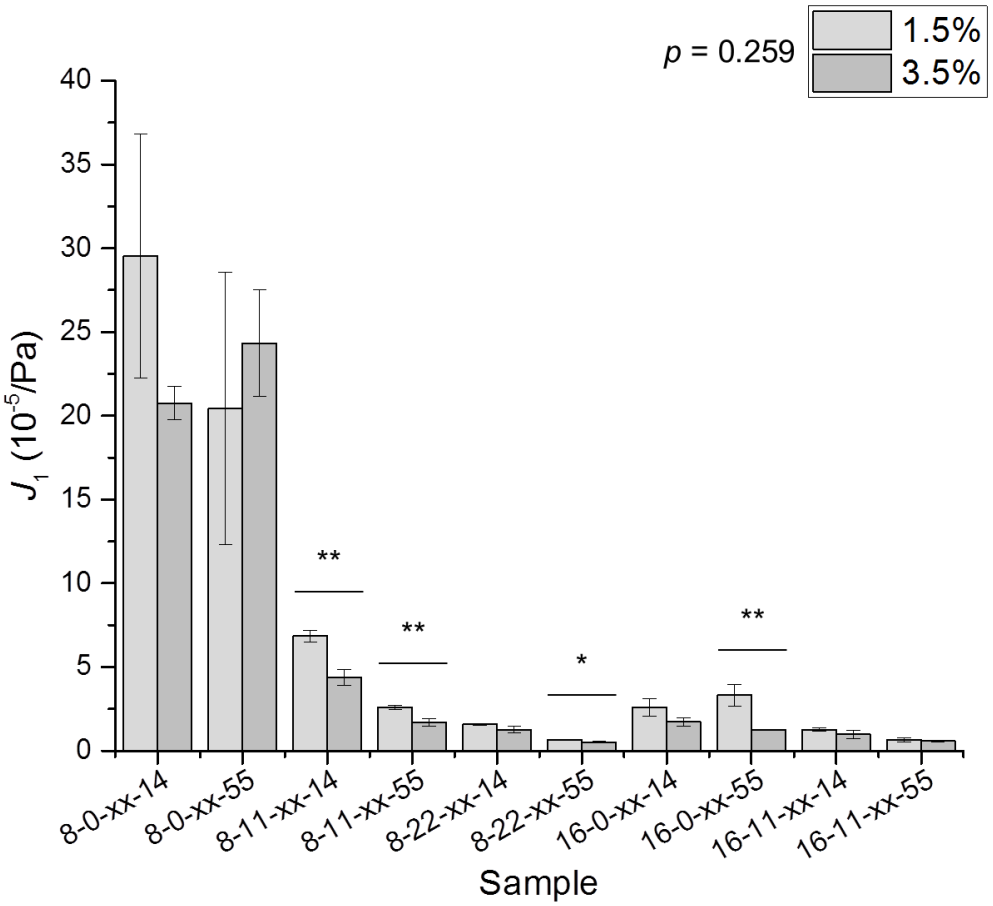

Sample code represents [Protein (% w/w)]-[Fat (% w/w)]-[NaCl (% w/w)]-[Homogenization pressure (MPa)], with NaCl content (xx) indicated by bar shading. Results are expressed as mean ± standard deviation (n = 3). */**/*** indicates a significant difference ($\alpha = 0.05/0.01/0.001$, respectively) within sample pairs by independent t-test. p is the p-value for systematic treatment effect obtained by a dependent t-test comparing means for all sample pairs.

Figure 4.11 Retarded compliance (J_1) by homogenization pressure (14 and 55 MPa).

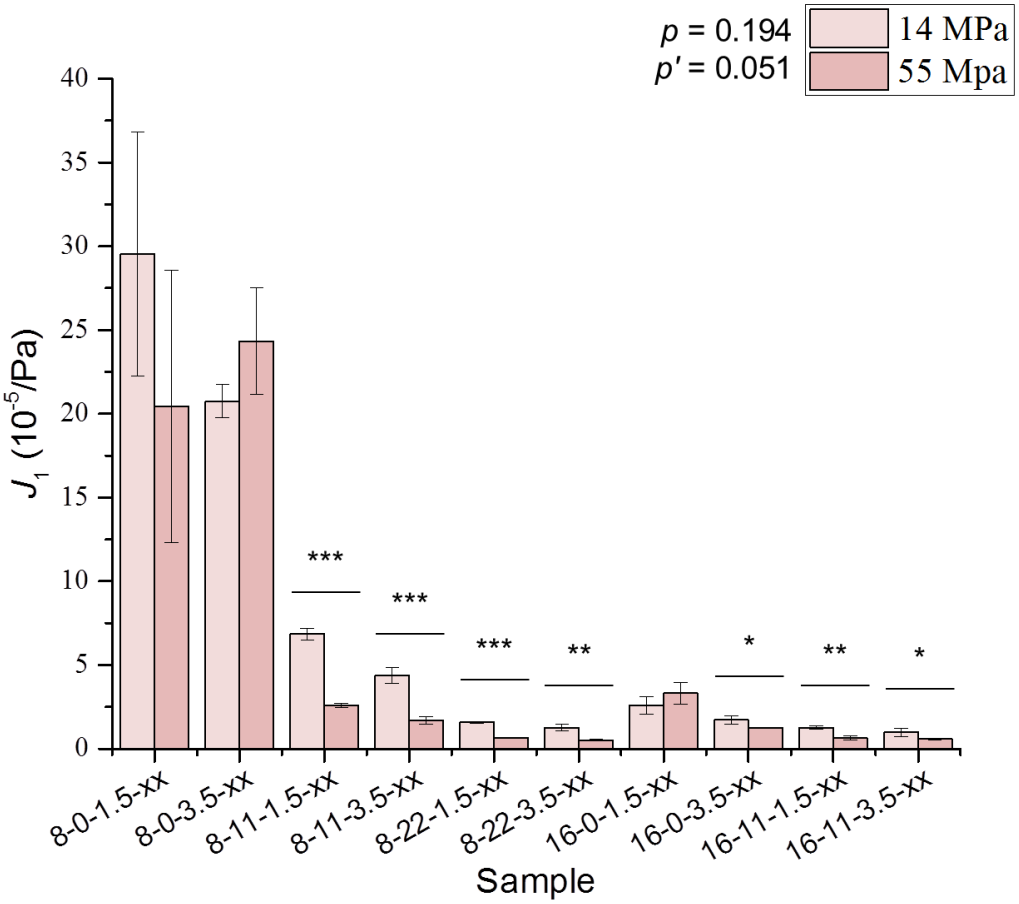

Sample code represents [Protein (% w/w)]-[Fat (% w/w)]-[NaCl (% w/w)]-[Homogenization pressure (MPa)], with homogenization pressure (xx) indicated by bar shading. Results are expressed as mean ± standard deviation (n = 3). */**/*** indicates a significant difference ($\alpha = 0.05/0.01/0.001$, respectively) within sample pairs by independent t-test. p is the p-value for systematic treatment effect obtained by a dependent t-test comparing means for all sample pairs. p' is the p-value for systematic treatment effect obtained by a dependent t-test comparing means for only sample pairs containing fat.

Figure 4.12 Retardation time (τ) by protein content (8 and 16% w/w).

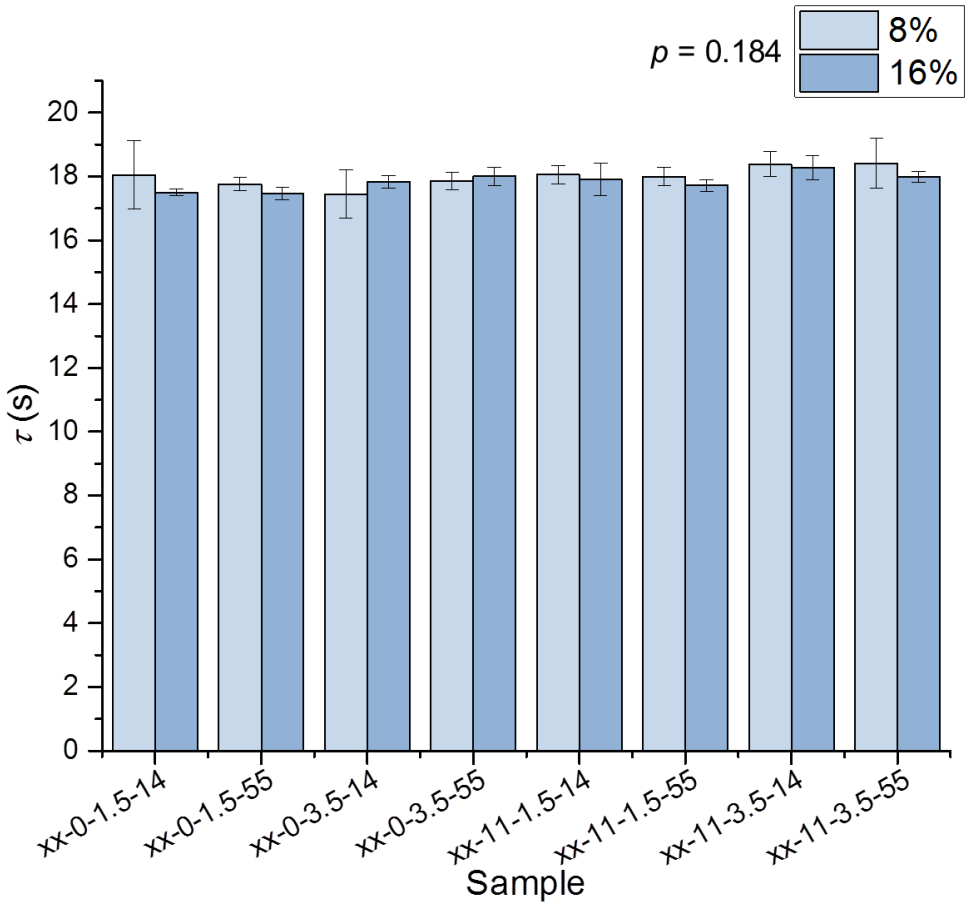

Sample code represents [Protein (% w/w)]-[Fat (% w/w)]-[NaCl (% w/w)]-[Homogenization pressure (MPa)], with protein content (xx) indicated by bar shading. Results are expressed as mean ± standard deviation (n = 3). */**/*** indicates a significant difference ($\alpha = 0.05/0.01/0.001$, respectively) within sample pairs by independent t-test. p is the p-value for systematic treatment effect obtained by a dependent t-test comparing means for all sample pairs.

Figure 4.13 Retardation time (τ) by fat content (0, 11, and 22% w/w).

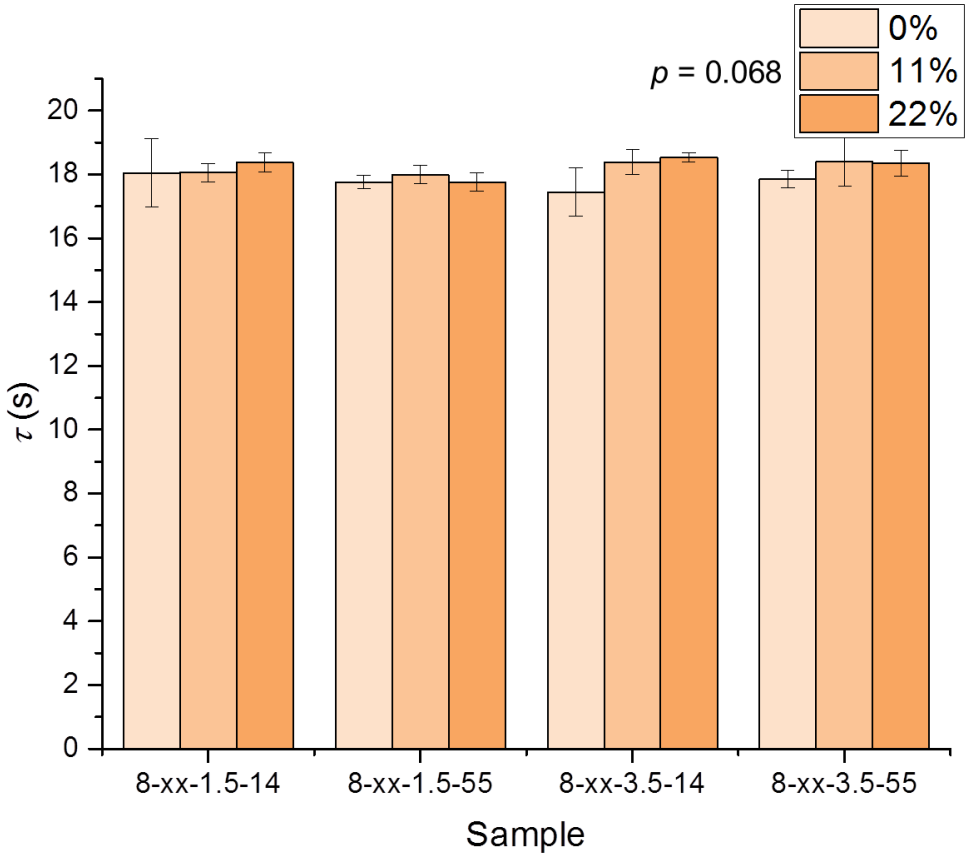

Sample code represents [Protein (% w/w)]-[Fat (% w/w)]-[NaCl (% w/w)]-[Homogenization pressure (MPa)], with fat content (xx) indicated by bar shading. Results are expressed as mean ± standard deviation (n = 3). */**/*** indicates a significant difference ($\alpha = 0.05/0.01/0.001$, respectively) within sample trios by ANOVA. Values in the same column with different letters were significantly different ($\alpha = 0.05$). p is the p-value for systematic treatment effect obtained by ANOVA comparing means for all samples. Treatments with different letters were significantly different ($\alpha = 0.05$).

Figure 4.14 Retardation time (τ) by NaCl content (1.5 and 3.5% w/w).

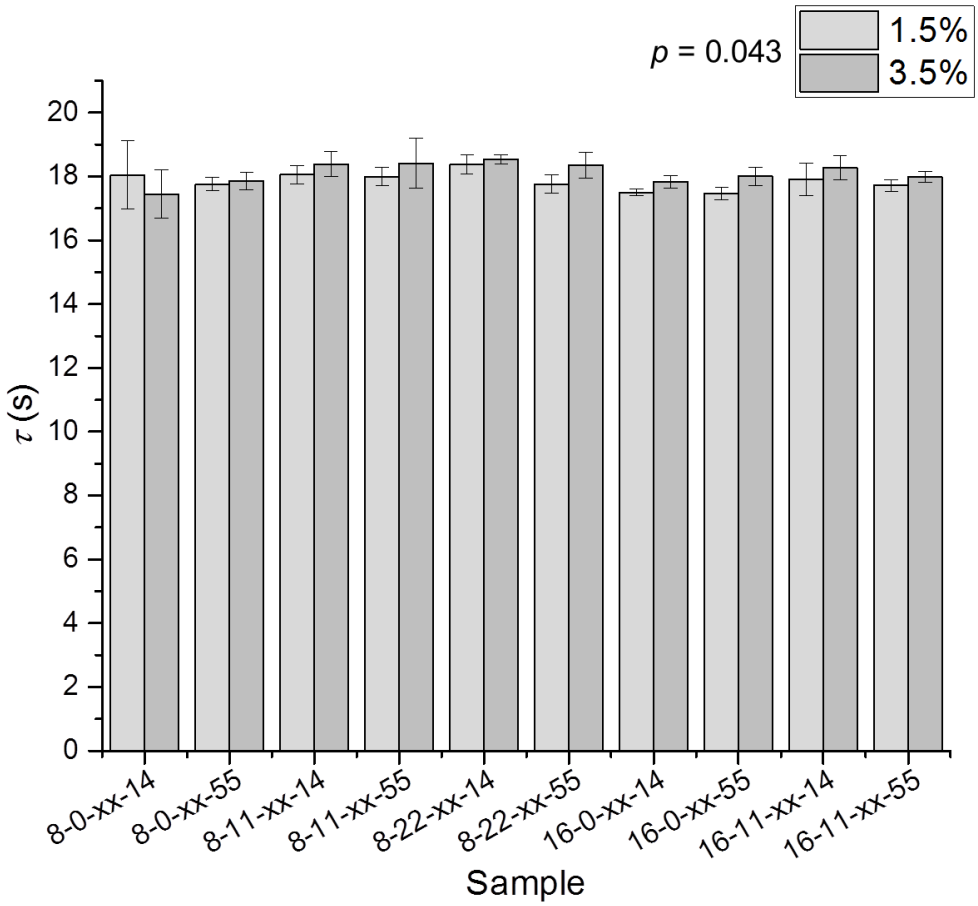

Sample code represents [Protein (% w/w)]-[Fat (% w/w)]-[NaCl (% w/w)]-[Homogenization pressure (MPa)], with NaCl content (xx) indicated by bar shading. Results are expressed as mean ± standard deviation (n = 3). */**/*** indicates a significant difference ($\alpha = 0.05/0.01/0.001$, respectively) within sample pairs by independent t-test. p is the p-value for systematic treatment effect obtained by a dependent t-test comparing means for all sample pairs.

Figure 4.15 Retardation time (τ) by homogenization pressure (14 and 55 MPa).

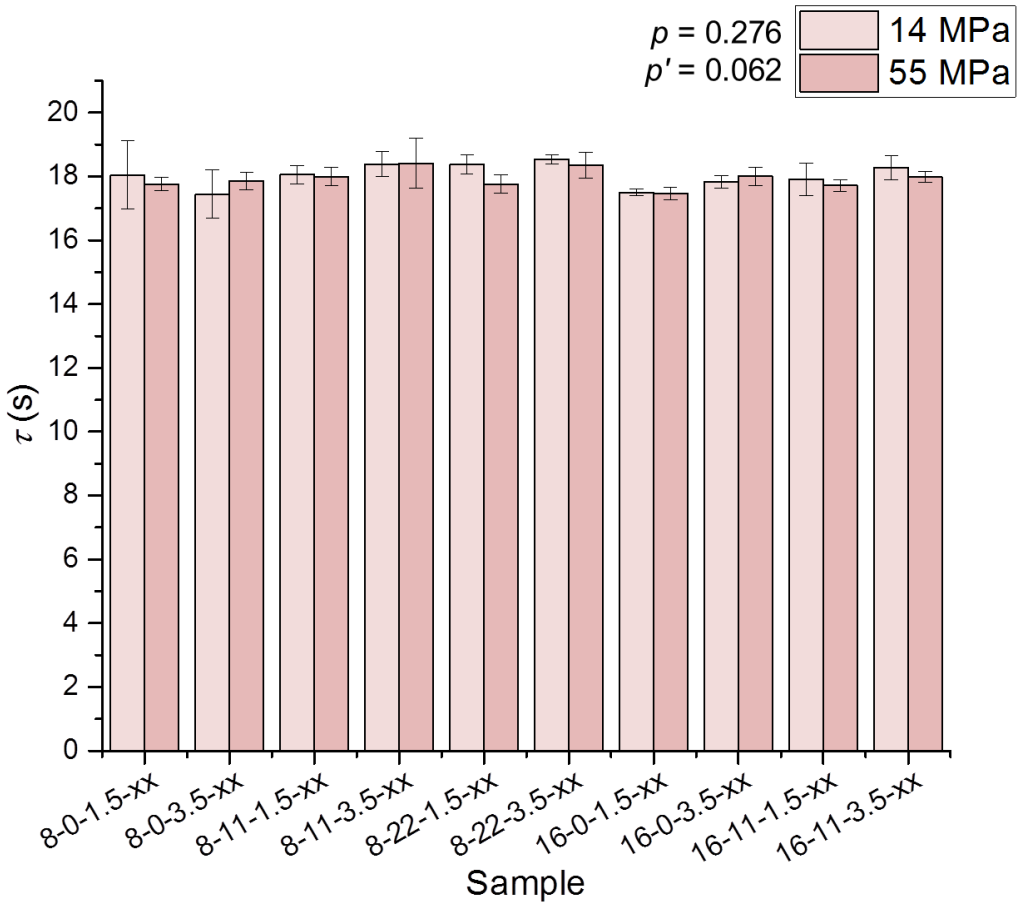

Sample code represents [Protein (% w/w)]-[Fat (% w/w)]-[NaCl (% w/w)]-[Homogenization pressure (MPa)], with homogenization pressure (xx) indicated by bar shading. Results are expressed as mean ± standard deviation (n = 3). */**/*** indicates a significant difference ($\alpha = 0.05/0.01/0.001$, respectively) within sample pairs by independent t-test. p is the p-value for systematic treatment effect obtained by a dependent t-test comparing means for all sample pairs. p' is the p-value for systematic treatment effect obtained by a dependent t-test comparing means for only sample pairs containing fat.

Figure 4.16 Newtonian viscosity (η_N) by protein content (8 and 16% w/w).

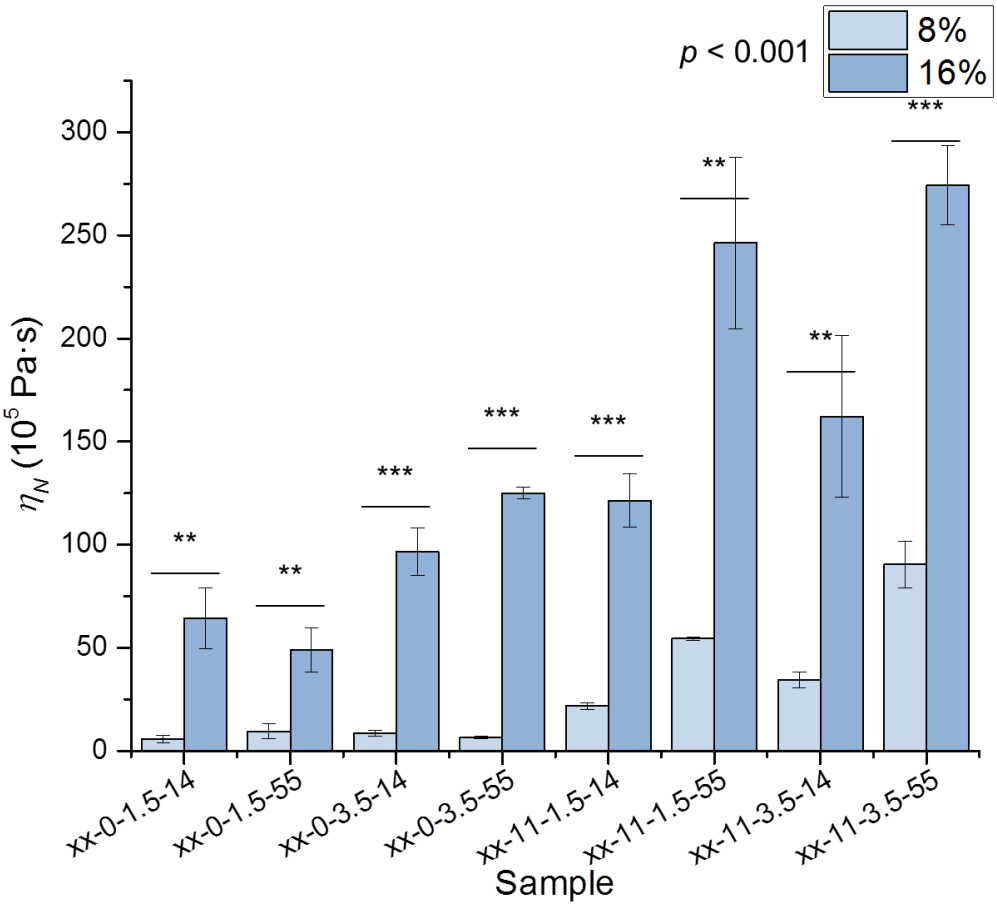

Sample code represents [Protein (% w/w)]-[Fat (% w/w)]-[NaCl (% w/w)]-[Homogenization pressure (MPa)], with protein content (xx) indicated by bar shading. Results are expressed as mean ± standard deviation (n = 3). */**/*** indicates a significant difference ($\alpha = 0.05/0.01/0.001$, respectively) within sample pairs by independent t-test. p is the p-value for systematic treatment effect obtained by a dependent t-test comparing means for all sample pairs.

Figure 4.17 Newtonian viscosity (η_N) by fat content (0, 11, and 22% w/w).

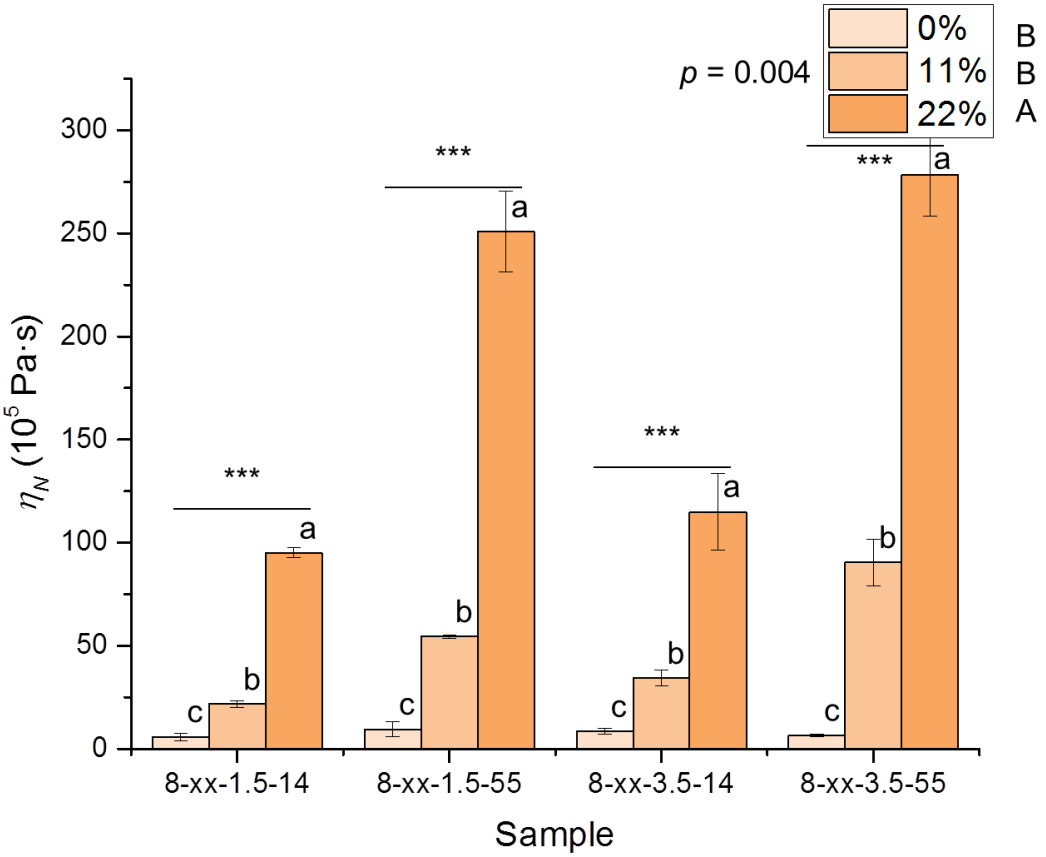

Sample code represents [Protein (% w/w)]-[Fat (% w/w)]-[NaCl (% w/w)]-[Homogenization pressure (MPa)], with fat content (xx) indicated by bar shading. Results are expressed as mean ± standard deviation (n = 3). */**/*** indicates a significant difference ($\alpha = 0.05/0.01/0.001$, respectively) within sample trios by ANOVA. Values in the same column with different letters were significantly different ($\alpha = 0.05$). p is the p-value for systematic treatment effect obtained by ANOVA comparing means for all samples. Treatments with different letters were significantly different ($\alpha = 0.05$).

Figure 4.18 Newtonian viscosity (η_N) by NaCl content (1.5 and 3.5% w/w).

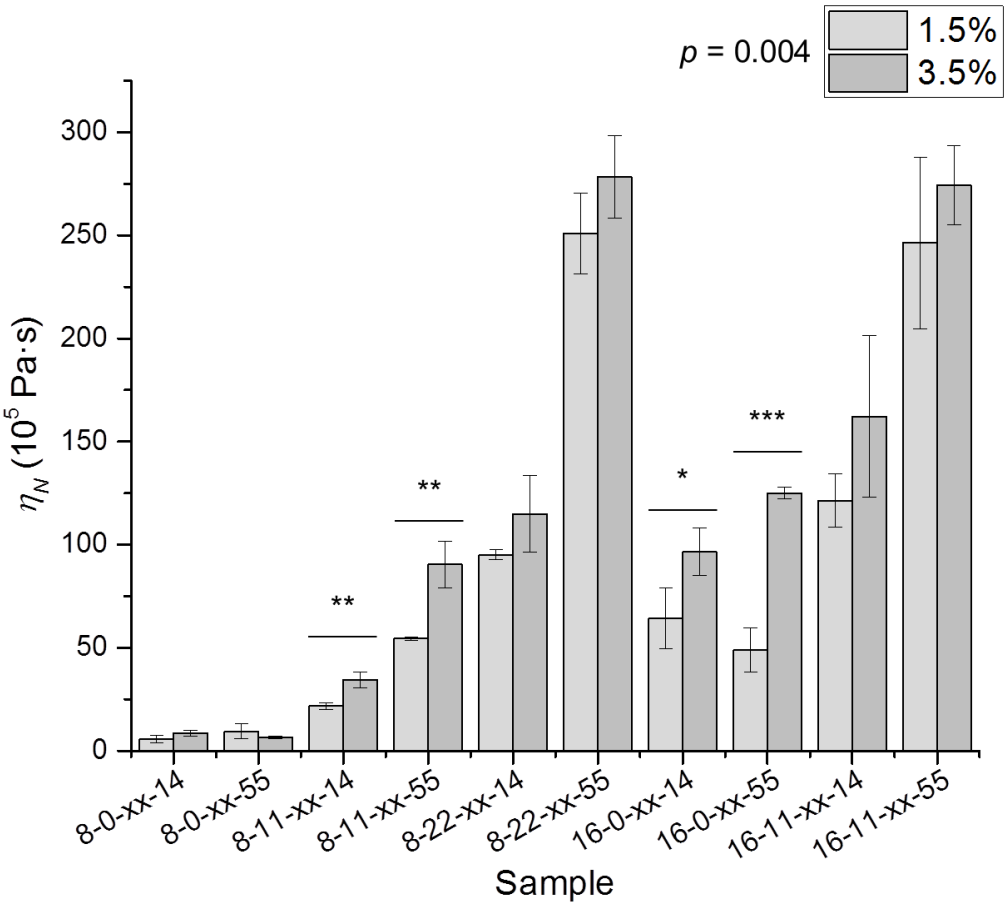

Sample code represents [Protein (% w/w)]-[Fat (% w/w)]-[NaCl (% w/w)]-[Homogenization pressure (MPa)], with NaCl content (xx) indicated by bar shading. Results are expressed as mean ± standard deviation (n = 3). */**/*** indicates a significant difference ($\alpha = 0.05/0.01/0.001$, respectively) within sample pairs by independent t-test. p is the p-value for systematic treatment effect obtained by a dependent t-test comparing means for all sample pairs.

Figure 4.19 Newtonian viscosity (η_N) by homogenization pressure (14 and 55 MPa).

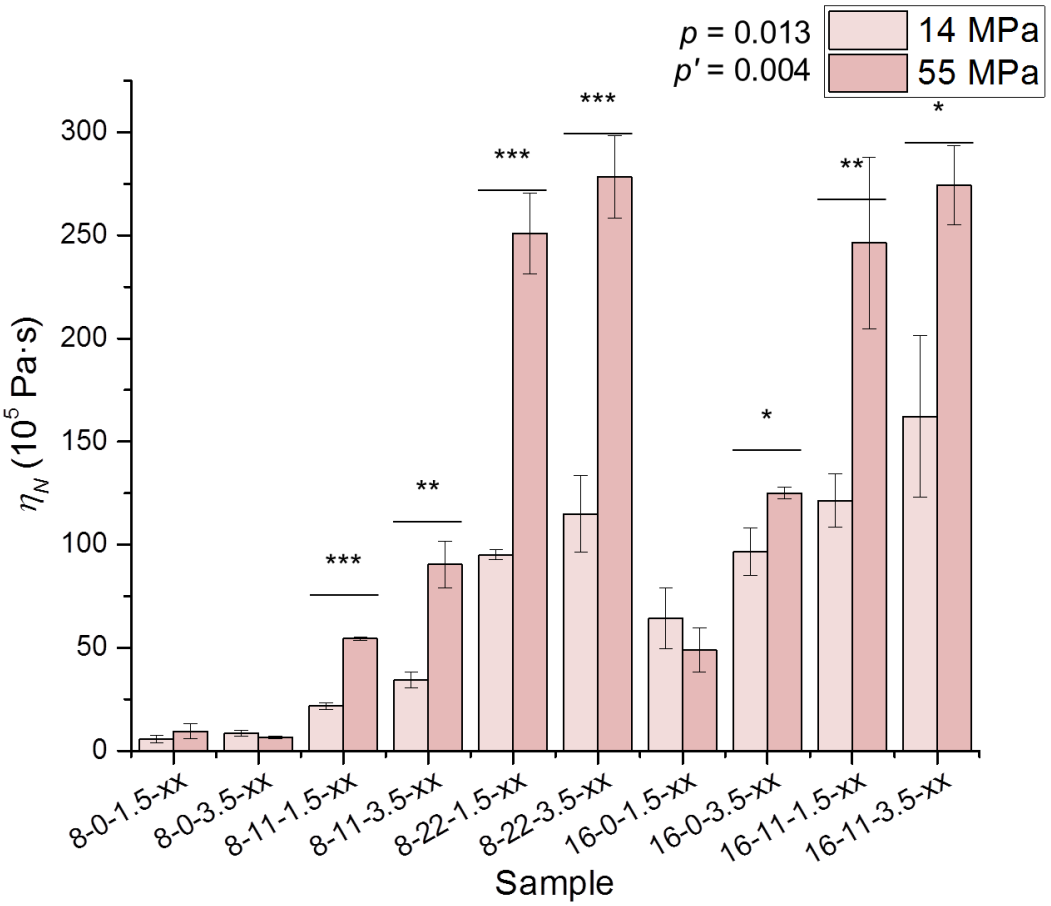

Sample code represents [Protein (% w/w)]-[Fat (% w/w)]-[NaCl (% w/w)]-[Homogenization pressure (MPa)], with homogenization pressure (xx) indicated by bar shading. Results are expressed as mean ± standard deviation (n = 3). */**/*** indicates a significant difference ($\alpha = 0.05/0.01/0.001$, respectively) within sample pairs by independent t-test. p is the p-value for systematic treatment effect obtained by a dependent t-test comparing means for all sample pairs. p' is the p-value for systematic treatment effect obtained by a dependent t-test comparing means for only sample pairs containing fat.

Chapter 5. Correlation of Sodium Mobility and Binding, Rheology, and Sensory Properties in a Model Lipoproteic Emulsion Gel

5.1 Abstract

Foods with a lipid/protein-based (lipoproteic) emulsion structure (such as processed cheeses and meats) are prime targets for sodium reduction due to their significant contributions to dietary sodium and the negative health risks associated with excessive sodium consumption. However, sodium also contributes to sensory texture and taste, therefore it is important to understand how sodium reduction strategies may affect desired properties. Sodium mobility/binding and rheological properties were correlated with sensory taste and texture data for heat-set model lipoproteic emulsion gels prepared with varying levels of whey protein isolate and anhydrous milkfat under different levels of high pressure homogenization. Sodium mobility and binding were characterized by ^{23}Na nuclear magnetic resonance (NMR) spectroscopy, rheological properties were characterized by small deformation oscillatory rheometry and creep compliance rheometry, and sensory properties were profiled by quantitative descriptive analysis (QDA). Sensory salty taste correlated negatively with dry matter (protein and fat) content, relative 'bound' (exhibiting restricted mobility) sodium fraction (A_{DQ}/A_{SQ}), viscosity (η_N), and shear moduli (G'; G''), and correlated positively with sodium mobility (single quantum relaxation time, T_2) and elastic compliance (J_0; J_1). A_{DQ}/A_{SQ} had the strongest correlation with salty taste, indicating that factors influencing relative amounts of 'bound' sodium may significantly impact saltiness perception. Syneresis texture (defined as the expulsion of liquid with chewing) also correlated positively with salty taste and T_2, and negatively with dry matter content and A_{DQ}/A_{SQ}, suggesting that sodium mobility and saltiness perception may be related by serum release during mastication. The correlation between saltiness perception and syneresis

with rheological properties also suggests that factors increasing intermolecular interactions and gel firmness may affect mastication behavior and saltiness perception.

5.2 Introduction

Excessive dietary sodium intake presents a major concern due to associated negative health risks, including high blood pressure, stroke, cardiovascular damage, and renal failure (de Wardener and MacGregor 2002). Foods with a lipoproteic emulsion matrix, such as processed cheeses and meats, are of great interest in sodium reduction research due to their dietary sodium contribution and the role of sodium in desired sensory properties (Dietary Guidelines Advisory Committee 2010; National Cancer Institute 2016). However, efforts to reduce sodium content in these food products must also account for potential detrimental impacts on desired properties, such as sensory saltiness perception, texture, and shelf-stability.

Saltiness perception is a multi-faceted phenomena, and is affected by physicochemical processes, mechanical properties, and mastication behavior (Panouillé et al. 2011). Strategies to reduce sodium content include changing sodium availability or modulating textural properties (Busch et al. 2013). Incorporating inert filler material, such as lipids, can influence saltiness perception by distributing salt in a nonhomogeneous manner and increasing sodium concentration in the aqueous phase. Modifying food matrix structure and textural properties can influence sodium mobility in the food matrix (Boisard et al. 2013), and how foods break down and release sodium during mastication (Busch et al. 2013; Kuo and Lee 2014a; Kuo and Lee 2014b). In lipoproteic emulsion gels, it has been found that gel texture can be influenced by varying formulation parameters (Kuo and Lee 2014b) and fat distribution (Dickinson 2012; Kuo and Lee 2014b), but the relationship between formulation, processing, and sensory properties needs further exploration.

Sodium behavior properties have been previously related with sensory saltiness in protein-based food materials. Boisard et al. (2014) found that many sodium mobility and binding properties determined by ^{23}Na nuclear magnetic resonance (NMR) spectroscopy correlated with saltiness perception in model cheeses. Saltiness showed significant positive correlation with metrics for free sodium, sodium mobility, and decreasing structural order, and negative correlation with work at maximal deformation. In a study on protein matrices, Mosca et al. (2015) found that sodium binding and mobility were influenced by protein interactions. Mosca et al. found that matrix rheological properties had a more significant influence on salty taste than sodium mobility and binding, but suggested that modulating sodium binding could still be useful for influencing saltiness perception.

The objective of this study was to correlate sodium mobility and rheological properties of lipoproteic emulsion gels to sensory properties to characterize the effects of varying formulation and processing parameters. The properties of model lipoproteic emulsion gels with varying whey protein isolate and anhydrous milkfat content prepared under different homogenization pressures were analyzed. Sodium mobility and binding were characterized by ^{23}Na NMR spectroscopy, and intrinsic rheological properties were determined from small deformation oscillatory rheometry, creep compliance rheometry, and mechanical modeling. Sensory taste and texture properties were obtained from quantitative descriptive analysis (QDA) data collected by Kuo (2016). Correlation and principle component analyses were performed on the measured properties to explore the relationship between formulation, processing, sodium availability, and saltiness perception. It was hypothesized that saltiness would correlate positively with sodium mobility, and negatively with sodium binding and gel firmness.

5.3 Materials and Methods

Emulsion gel preparation

The model gel formulation and preparation procedures were adapted from the method developed by Kuo and Lee (2014). Whey protein isolate (WPI, Hilmar 9000) was donated by Hilmar Ingredients (Hilmar, CA), anhydrous milkfat (AMF) was purchased from Danish Maid Butter Company (Chicago, IL), and sodium chloride (NaCl, Crystalline/Certified ACS) was purchased from Fisher Scientific (Fair Lawn, NJ). Table 5.1 lists the formulation and homogenization pressures used for each emulsion gel, which were selected for overlap with sensory analysis performed by Kuo (2016). Samples were coded by their formulation and homogenization pressures in the format of: [Protein (% w/w)]-[Fat (% w/w)]-[NaCl (% w/w)]-[Homogenization pressure (MPa)]. For example, a sample containing 8% protein, 11% fat, and 1.5% NaCl homogenized at 55 MPa would have the code 8-11-1.5-55.

The procedures for preparing lipoproteic emulsion gel samples for ^{23}Na NMR spectroscopy and rheological analyses are detailed in Chapters 3 and 4, respectively. The procedure for preparing samples for sensory analysis has been previously described by Kuo (2016). Samples prepared for each experiment were subjected to compatible homogenization, temperature change, and storage conditions.

Instrumental and sensory data collection

Sample dry matter content was determined by adding together the protein and fat content (% w/w). The ^{23}Na NMR spectroscopy methodology is described in Chapter 3, and the methodologies for the rheometry experiments are presented in Chapter 4. ^{23}Na NMR experiment results (T_1, single quantum (SQ) longitudinal relaxation time; T_2, SQ transverse relaxation time;

τ_{opt}, double quantum (DQ) creation time; A_{DQ}/A_{SQ}, relative 'bound' sodium fraction) can be found in Chapter 3 (Table 3.2), and rheometry experiment results (J_0, instantaneous compliance; J_1, retarded compliance; τ, retardation time; η_N, Newtonian viscosity; G', shear storage modulus; G'', shear loss modulus) can be found in Chapter 4 (Tables 4.3 and 4.4).

For the sensory data collection, the panelist recruitment procedures, training protocols, and quantitative descriptive analysis methodology and results have been previously reported by Kuo (2016). 12 panelists rated lipoproteic emulsion samples on a 15-point scale for 21 attributes across 5 modalities. For this study, 8 attributes from the taste (salty) and texture (fracturable, crumbly, gelatinous, gritty, fibrous, syneresis, squeaky) modalities were selected for correlation analysis based on their relationship to saltiness perception or hypothesized relationship with instrumental measurements, matrix structure, and mastication behavior. Table 5.2 shows the relevant definitions and references for the selected attributes, and Table 5.3 shows the QDA panel data for sample formulations that were common to the ^{23}Na NMR and rheometry experiments.

Statistical analysis

Statistical analysis was performed using OriginPro 2016 (OriginLab Corporation, Northampton, MA). Pearson's correlation analysis was performed for comparisons between measured properties, and significant correlations were determined by comparing the associated *p*-values with type I error significance levels (α) of 0.05, 0.01, and 0.001. Principal component analysis (PCA) was performed on the measured properties with 4 principal components retained. Hierarchical cluster analysis (HCA) was performed on the sample formulations by the measured

properties with 4 clusters selected. Data was standardized to equal variance prior to PCA and HCA to adjust for the differences in units and scales of the analyzed data.

5.4 Results and Discussion

Correlation with salty taste

Table 5.4 lists the Pearson's correlation coefficients (r) for comparisons between the formulation, instrumental, and sensory parameters. In terms of saltiness perception, salty taste had significant correlation with many of the measured properties in the lipoproteic emulsion gels. Comparing with sodium mobility and binding data, salty taste correlated positively with total sodium mobility (T_2, $r = 0.83$) and creation time (τ_{opt}, $r = 0.76$) and negatively with relative 'bound' sodium fraction (A_{DQ}/A_{SQ}, $r =$ -0.95). Across comparisons with all other parameters, salty taste had the strongest correlation with A_{DQ}/A_{SQ} ($p = 0.00002$). Samples with higher total sodium mobility or lower relative 'bound' sodium tended to be rated as having higher salty taste, which agrees with the hypothesis that increased intrinsic availability of sodium ions would contribute to higher perceived saltiness. These results were consistent with past research that found decreased 'free' sodium (or increased 'bound' sodium) contributed to decreased saltiness perception (Boisard et al. 2014; Mosca et al. 2015). Mosca et al. also found that sensory saltiness decreased and firmness increased as protein matrix viscosity increased, which was consistent with the trends observed in this study of salty taste correlating negatively with increasing viscosity (η_N, $r =$ -0.72) and firmness (G', $r =$ -0.75). Salty taste increased with increasing elastic compliance (J_0, $r = 0.68$; J_1, $r = 0.67$), which could be due to elastic character affecting mastication behavior and matrix breakdown.

The correlations with dry matter content (DM, protein + fat) indicated trends between formulation parameters and sodium behavior which may contribute to the observed saltiness perception trends. DM correlated negatively with T_2 (r = -0.88) and τ_{opt} (r = -0.67), and positively with A_{DQ}/A_{SQ} (r = 0.89). Dry matter (as protein) provides potential binding sites for sodium ions via negatively charged groups on the protein molecules (Mosca et al. 2015). This was consistent with the trends of decreasing mobility and increasing relative 'bound' sodium fraction with increasing DM. Beyond potential ionic interactions, dry matter can additionally affect viscosity and texture. As discussed in Chapter 3, increasing the amount of dry matter may also decrease sodium mobility by increasing three-dimensional structure around 'bound' sodium (which is indicated by a smaller τ_{opt} value). This would agree with the observed trends of DM correlating negatively with J_0 (r = -0.82) and J_1 (r = -0.81) and positively with η_N (r = 0.79) and G' (r = 0.81). Lower elastic compliance and higher viscosity and storage modulus values indicate a firmer, less elastic gel, which could be due to the increased dry matter resulting in increased protein interactions. Texture may affect saltiness perception by influencing sodium mobility, cross-modal texture-taste interactions, or matrix breakdown and sodium release (Mosca et al. 2015).

Although sodium release properties were not directly explored in this study, the QDA syneresis texture may be related to in-mouth sodium and serum release. Syneresis was defined as "Expulsion of liquid with chews" (Table 5.2), and Kuo (2016) found significant correlation between syneresis texture and salty taste, porosity, and instrumentally measured sodium and serum release. In this study, syneresis correlated positively with salty taste (r = 0.92) and T_2 (r = 0.86) and negatively with DM (r = -0.93) and A_{DQ}/A_{SQ} (r = -0.99). Samples with higher syneresis ratings had relatively higher sodium mobility and lower relative 'bound' sodium,

which could be due to the lower relative dry matter (and more relative water) in the sample formulations. Water would be the liquid released during mastication resulting in a higher syneresis score, and released water may carry aqueous sodium for saltiness perception. With respect to structure and texture, syneresis correlated positively with τ_{opt} ($r = 0.71$), J_0 ($r = 0.72$) and J_1 ($r = 0.71$) and negatively with η_N ($r =$ -0.82) and G' ($r =$ -0.84), and G'' ($r =$ -0.85). These results indicate a potential relationship between texture and saltiness, as samples with higher syneresis tended to have less ordered structure, more elasticity, or lower viscosity or firmness. The variations in texture may have resulted in different fracturing or mastication patterns, affecting serum and sodium release.

Correlation with other sensory texture properties

DM correlated positively with fracturable ($r = 0.73$) and crumbly ($r = 0.83$) textures and negatively with fibrous texture ($r =$ -0.79). The definitions for the fracturable and crumbly texture terms were related to how the sample responded to biting, and the trends between DM and these properties suggest that formulation can influence mastication behavior. The negative correlation between DM and fibrous may be due to higher DM resulting in a denser matrix with more three-dimensional structure, compared to a lower density structure for gels with lower DM. Under this hypothesis, a denser matrix would break under stress into smaller pieces, which would agree with the positive correlation between DM and crumbly. A less dense matrix would be comprised of more water, with water released during chewing and the solid content compacting over time and perceived as fibrous texture. This is supported by syneresis correlating negatively with fracturable ($r =$ -0.77) and crumbly ($r =$ -0.81) and positively with fibrous ($r =$

0.88), as samples with increasing fibrous character had increased perception of releasing liquid during chewing.

A_{DQ}/A_{SQ} correlated positively with fracturable ($r = 0.75$), crumbly ($r = 0.75$), and gelatinous ($r = 0.73$) textures, and negatively with fibrous ($r =$ -0.89) and squeaky ($r =$ -0.63) textures. As discussed above, increasing ratings for fracturable and crumbly textures could be related to a denser sample matrix, which would be consistent with the trend of increasing A_{DQ}/A_{SQ} (relatively more sodium exhibiting restricted mobility). The negative correlation between A_{DQ}/A_{SQ} and squeaky could be due to the samples with less fat tending to have higher squeaky ratings. The samples formulated with less fat would have more water and matrices with less density and firmness, which would explain why they would have relatively less 'bound' sodium.

PCA of lipoproteic emulsion gel samples

Figure 5.1 shows the principal component biplot and associated hierarchical cluster analysis dendrogram of the lipoproteic emulsion gel samples by formulation, sodium mobility and binding, rheology, and sensory properties. PC I and PC II explained 61.2% and 22.0% of the total variance, respectively. Salty, syneresis , T_2, J_0, and J_1 are arrayed on the positive side of PC I, while DM, A_{DQ}/A_{SQ}, η_N, G', and G'' were arrayed along the negative side of PC I. Non-fat samples were found on the positive side of PC I, with the 8-0-1.5-xx sample cluster more closely aligned with salty taste than the 16-0-1.5-xx sample cluster. The fat containing samples were found on the negative side of PC I and aligned closer with DM and A_{DQ}/A_{SQ} as dry matter content increased.

The high saltiness of the non-fat samples may be explained by the negative correlation between salty and DM. The non-fat samples had lower dry matter content, which also correlated with increased total sodium mobility (T_2) and decreased relative 'bound' sodium. The non-fat samples had less dry matter to contribute to three-dimensional structural order relative to the fat-containing samples. As discussed in Chapters 3 and 4, the dispersed lipid droplets are emulsified by protein molecules and therefore may behave as active fillers which contribute to matrix structure and gel strength. Dry matter as protein may also bind sodium ions (via negatively charged groups on the protein) and reduce sodium availability for saltiness perception. This is supported by the 16-0-1.5-xx sample cluster being less aligned with salty and T_2 than the 8-0-1.5-xx sample cluster. Also, the 16-11-1.5-xx and 8-22-1.5-xx samples were formulated with comparable amounts of dry matter (27% and 30% w/w, respectively), but the 16-11-1.5-xx samples were less aligned with salty than the corresponding 8-22-1.5-14 samples. This could be due to the increased protein content contributing to increased sodium binding or three dimensional structure via increased intermolecular interactions.

With regards to homogenization pressure, the fat-containing samples prepared under higher homogenization pressure tended to be less aligned with salty taste and more aligned with A_{DQ}/A_{SQ}. As discussed in Chapters 3 and 4, this could be due to the increased homogenization pressure increasing protein interactions by increasing interfacial surface area (via decreased particle size). Samples treated with higher homogenization pressure also were more aligned with the parameters associated with gel thickness (η_N, G', G'') and less aligned with parameters corresponding to elasticity, suggesting that homogenization pressure may influence gel firmness which may then influence mastication behavior and saltiness perception. However, it should be noted that in the original sensory study Kuo only found one pair of samples with the same

formulation and different homogenization pressures to have significantly different saltiness ratings (16-11-1.5-55 had significantly lower salty taste than 16-11-1.5-14). Methods such as varying homogenization pressure can influence properties which correlate with salty taste (i.e. sodium mobility and texture), but the magnitude of the ultimate effect on saltiness perception may be matrix-dependent.

5.5 Conclusions

Sensory saltiness and texture were correlated with sodium mobility and rheology properties for lipoproteic emulsion gels prepared with varying formulation and processing conditions. Sodium mobility and binding showed significant correlation with sensory saltiness, and A_{DQ}/A_{SQ} exhibited the strongest correlation with salty taste out of all the analyzed properties. Syneresis texture correlated positively with salty taste, sodium mobility, and elasticity, and negatively with dry matter content, relative 'bound' sodium, and gel firmness, indicating that sodium availability may be related to serum release and mastication behavior. PCA indicated an association between salty taste, sodium mobility, and elasticity properties, and another association between dry matter, sodium binding, and firmness in the opposite direction with respect to the principle components explaining the most variation. PCA also indicated that samples treated with higher homogenization pressure tended to have firmer gel character and associate less with salty taste. Sample formulation and dry matter content influence several properties that may affect saltiness perception (including sodium mobility, sodium binding, and sample texture), and processing methods such as homogenization may also be useful for modulating molecular interactions, microstructure, and sodium availability.

5.6 Literature Cited

Boisard L, Andriot I, Arnould C, Achilleos C, Salles C, Guichard E. 2013. Structure and composition of model cheeses influence sodium NMR mobility, kinetics of sodium release and sodium partition coefficients. Food Chem. 136(2):1070–1077.

Boisard L, Andriot I, Martin C, Septier C, Boissard V, Salles C, Guichard E. 2014. The salt and lipid composition of model cheeses modifies in-mouth flavour release and perception related to the free sodium ion content. Food Chem. 145:437–444.

Busch JLHC, Yong FYS, Goh SM. 2013. Sodium reduction: Optimizing product composition and structure towards increasing saltiness perception. Trends Food Sci. Technol. 29(1):21–34.

de Wardener H, MacGregor G. 2002. Harmful effects of dietary salt in addition to hypertension. J. Hum. Hypertens. 16(4):213–223.

Dickinson E. 2012. Emulsion gels: The structuring of soft solids with protein-stabilized oil droplets. Food Hydrocoll. 28(1):224–241.

Dietary Guidelines Advisory Committee. 2010. Report of the Dietary Guidelines Advisory Committee on the Dietary Guidelines for Americans, 2010. Washington, DC: United States Department of Agriculture.

Kuo W-Y. 2016. Relating structural properties to saltiness perception of model lipoproteic gels. Doctoral dissertation. University of Illinois at Urbana-Champaign.

Kuo W-Y, Lee Y. 2014a. Effect of Food Matrix on Saltiness Perception-Implications for Sodium Reduction. Compr. Rev. Food Sci. Food Saf. 13(5):906–923.

Kuo W-Y, Lee Y. 2014b. Temporal Sodium Release Related to Gel Microstructural Properties — Implications for Sodium Reduction. J.Food Sci. 79(11):2245–2252.

Mosca AC, Andriot I, Guichard E, Salles C. 2015. Binding of Na^+ ions to proteins: Effect on taste perception. Food Hydrocoll. 51:33–40.

National Cancer Institute. 2016. Sources of Sodium among the U.S. Population, 2005-06. http://epi.grants.cancer.gov/diet/foodsources/sodium/. Accessed 2016 May 9.

Panouillé M, Saint-Eve A, de Loubens C, Déléris I, Souchon I. 2011. Understanding of the influence of composition, structure and texture on salty perception in model dairy products. Food Hydrocoll. 25(4):716–723.

5.7 Tables and Figures

Table 5.1 Formulation and homogenization pressure sample matrix for correlation analysis.

PROTEIN (% w/w)	FAT (% w/w)	NaCl (% w/w)	PRESSURE (MPa)	SAMPLE CODE
8	0	1.5	14	8-0-1.5-14
			55	8-0-1.5-55
	11	1.5	14	8-11-1.5-14
			55	8-11-1.5-55
	22	1.5	14	8-22-1.5-14
			55	8-22-1.5-55
16	0	1.5	14	16-0-1.5-14
			55	16-0-1.5-55
	11	1.5	14	16-11-1.5-14
			55	16-11-1.5-55

Table 5.2 Selected QDA attributes for emulsion gel samples and the associated references and definitions.

Modality	Attribute	Reference		Definition
		Item	Score	
Taste	Salty	0.4% NaCl 0.3% NaCl	10.2 4.0	The salty taste (peak intensity) of NaCl solution
Texture	Fracturable	Firm tofu	8.0	Easiness of first bite to fracture (into two or more pieces)
	Crumbly	Feta cheese	9.7	Readily breaks into small pieces with chewing
	Gelatinous	Jell-O	10.7	Firm and moist
	Gritty	Grits	10.8	Feeling of coarse particles like grits during chewing
	Fibrous	Pineapple core	13.3	Lasting fibrous feeling during chewing
	Syneresis	Fresh mozzarella balls	8.3	Expulsion of liquid with chews
	Squeaky	Exploded egg	8.0	The squeaky sounds with chews

(Kuo 2016)

Table 5.3 Summary of taste and texture properties collected by QDA.

Sample	Salty	Fracturable	Crumbly	Syneresis	Gelatinous	Gritty	Fibrous	Squeaky
8-0-1.5-14	11.9 ± 3.2	5.4 ± 2.7	6.4 ± 2.9	13.8 ± 1.6	7.0 ± 2.5	7.0 ± 3.1	11.2 ± 2.3	7.2 ± 4.0
8-0-1.5-55	11.9 ± 2.7	4.8 ± 3.4	6.3 ± 3.3	13.8 ± 1.8	5.8 ± 2.0	6.8 ± 2.6	11.3 ± 3.7	6.2 ± 3.6
8-11-1.5-14	8.9 ± 3.1	9.0 ± 2.3	7.3 ± 2.5	9.7 ± 2.5	10.5 ± 2.9	4.9 ± 2.3	2.5 ± 2.5	4.6 ± 2.9
8-11-1.5-55	9.2 ± 2.3	10.5 ± 2.7	8.6 ± 2.3	9.2 ± 1.8	11.0 ± 2.4	6.7 ± 1.8	2.9 ± 2.4	5.3 ± 2.4
8-22-1.5-14	9.3 ± 2.6	9.5 ± 2.2	8.6 ± 2.3	8.3 ± 1.6	9.8 ± 2.6	6.3 ± 2.3	2.8 ± 2.7	4.1 ± 2.7
8-22-1.5-55	9.3 ± 2.4	10.2 ± 2.2	9.5 ± 2.3	6.8 ± 2.6	8.7 ± 2.7	8.8 ± 2.7	3.4 ± 2.8	4.0 ± 2.4
16-0-1.5-14	11.1 ± 2.3	5.4 ± 2.6	6.9 ± 2.8	12.5 ± 1.9	6.7 ± 2.2	7.6 ± 3.2	11.2 ± 3.2	12.0 ± 2.9
16-0-1.5-55	10.9 ± 2.8	4.8 ± 2.2	6.2 ± 2.8	12.8 ± 2.1	5.5 ± 2.2	9.1 ± 3.2	11.5 ± 3.2	10.2 ± 4.3
16-11-1.5-14	8.4 ± 2.9	8.0 ± 2.0	8.0 ± 2.0	7.0 ± 1.9	9.9 ± 2.8	6.5 ± 2.3	4.8 ± 3.6	5.1 ± 2.9
16-11-1.5-55	6.2 ± 2.4	7.6 ± 2.5	7.7 ± 2.3	5.8 ± 2.2	8.2 ± 2.5	7.5 ± 2.2	3.3 ± 2.7	5.3 ± 3.0

Sample code represents [Protein (% w/w)]-[Fat (% w/w)]-[NaCl (% w/w)]-[Homogenization pressure (MPa)]. Results are expressed as mean ± standard deviation (n = 24; 12 panelists, 2 replicates each) (Kuo 2016).

Table 5.4 Pearson's correlation coefficients between formulation, ^{23}Na NMR, rheometry, and QDA properties.

	DM	T_1	T_2	τ_{opt}	A_{DQ}/A_{SQ}	J_0	J_1	τ	η_N	G'	G''	Salty	Fracturable	Crumbly	Syneresis	Gelatinous	Gritty	Fibrous
T_1	-0.56																	
T_2	-0.88 ***	0.77 **																
τ_{opt}	-0.67 *	0.91 ***	0.74 *															
A_{DQ}/A_{SQ}	0.89 ***	-0.58	-0.88 ***	-0.74 *														
J_0	-0.82 **	0.74 *	0.96 ***	0.63	-0.73 *													
J_1	-0.81 **	0.73 *	0.94 ***	0.62	-0.72 *	0.98 ***												
τ	0.25	0.42	-0.01	0.24	0.27	0.11	0.15											
η_N	0.79 **	-0.54	-0.65 *	-0.73 *	0.74 *	-0.60	-0.59	-0.15										
G'	0.81 **	-0.57	-0.69 *	-0.76 *	0.77 **	-0.63	-0.62	-0.13	1.00 ***									
G''	0.81 **	-0.59	-0.69 *	-0.77 **	0.78 **	-0.63 *	-0.63	-0.14	1.00 ***	1.00 ***								
Salty	-0.78 **	0.61	0.83 **	0.76 *	-0.95 ***	0.68 *	0.67 *	-0.16	-0.72 *	-0.75 *	-0.77 **							
Fracturable	0.73 *	-0.01	-0.63	-0.14	0.75 *	-0.56	-0.54	0.56	0.45	0.47	0.46	-0.62						
Crumbly	0.83 **	-0.14	-0.65 *	-0.29	0.75 *	-0.62	-0.61	0.39	0.66 *	0.68 *	0.66 *	-0.58	0.92 ***					
Syneresis	-0.93 ***	0.53	0.86 **	0.71 *	-0.99 ***	0.72 *	0.71 *	-0.25	-0.82 **	-0.84 **	-0.85 **	0.92 ***	-0.77 **	-0.81 **				
Gelatinous	0.59	-0.05	-0.60	-0.14	0.73 *	-0.47	-0.43	0.66 *	0.20	0.24	0.23	-0.61	0.91 ***	0.72 *	-0.69 *			
Gritty	0.06	-0.27	-0.02	-0.23	-0.16	-0.19	-0.18	-0.70 *	0.42	0.40	0.39	0.15	-0.30	0.00	0.07	-0.60		
Fibrous	-0.79 **	0.19	0.72	0.34	-0.89 ***	0.60	0.58	-0.55	-0.52	-0.55	-0.54	0.82 **	-0.94 ***	-0.82 **	0.88 ***	-0.90 ***	0.40	
Squeaky	-0.53	-0.21	0.26	0.11	-0.63 *	0.08	0.10	-0.71 *	-0.38	-0.38	-0.37	0.55	-0.75 *	-0.65 *	0.66 *	-0.70 *	0.44	0.80 **

Correlation coefficients denoted with *, **, and *** are significant at $\alpha = 0.05$, 0.01, and 0.001, respectively. DM, dry matter content (protein + fat); T_1, single quantum (SQ) longitudinal relaxation time; T_2, SQ transverse relaxation time; τ_{opt}, double quantum (DQ) creation time; A_{DQ}/A_{SQ}, relative 'bound' sodium fraction; J_0, instantaneous compliance; J_1, retarded compliance; τ, retardation time; η_N, Newtonian viscosity; G', shear storage modulus; G'', shear loss modulus

Figure 5.1 Principal component biplot and cluster analysis dendrogram of lipoproteic emulsion gel samples by formulation, ^{23}Na NMR, rheometry, and QDA properties.

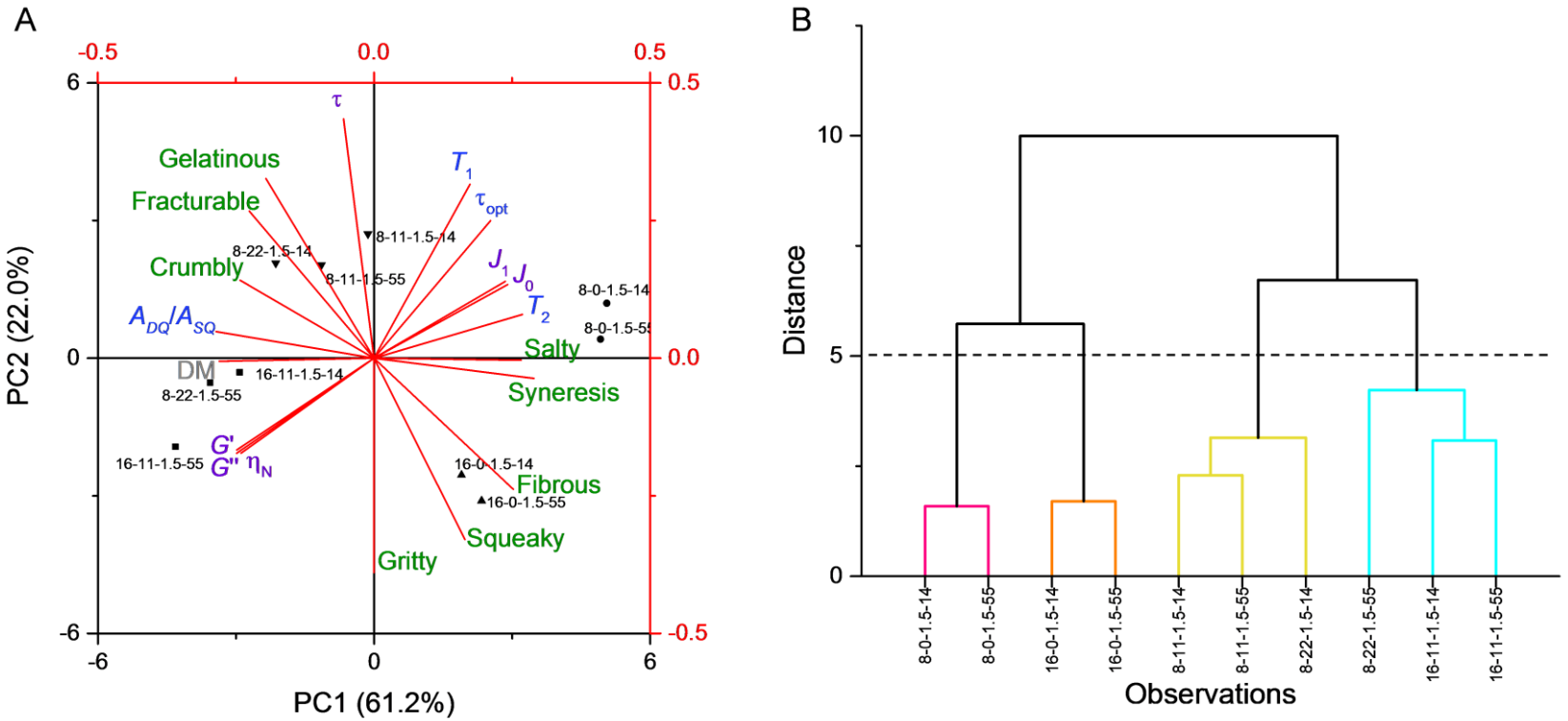

(A) Principal component biplot by PC I and II of sample formulation (grey), sodium mobility and binding (blue), rheology (purple), and sensory (green) properties and sample score points. Score points designated by the same shape share a cluster by hierarchical cluster analysis. The top and right axes correspond to the loading vectors (red); the left and bottom axes correspond to the score points (black). (B) Dendrogram for the corresponding hierarchical cluster analysis; samples designated by the same branch color share a cluster. Sample code represents [Protein (% w/w)]-[Fat (% w/w)]-[NaCl (% w/w)]-[Homogenization pressure (MPa)]. DM, dry matter content (protein + fat); T_1, single quantum (SQ) longitudinal relaxation time; T_2, SQ transverse relaxation time; τ_{opt}, double quantum (DQ) creation time; A_{DQ}/A_{SQ}, relative 'bound' sodium fraction; J_0, instantaneous compliance; J_1, retarded compliance; τ, retardation time; η_N, Newtonian viscosity; G', shear storage modulus; G'', shear loss modulus.

Chapter 6. Summary

This study characterized the effects of formulation and processing parameters on sodium availability and saltiness perception in a model lipoproteic emulsion food system. The overall conclusion is that factors contributing to increased intermolecular interactions result in decreased sodium availability and saltiness perception. The findings of this study suggest that mechanisms resulting in increased sodium availability for taste perception can be optimized for purposes of sodium reduction.

Model lipoproteic emulsion gels were prepared with varying amounts of whey protein isolate, anhydrous milkfat, and salt, and subjected to different levels of higher pressure homogenization. Sodium mobility and binding were characterized by ^{23}Na nuclear magnetic resonance spectroscopy, and rheological properties were characterized by small amplitude oscillatory rheometry, creep compliance rheometry, and mechanical modeling. Instrumental data were correlated with previously collected sensory taste and texture data.

Sodium binding increased with increasing protein content, fat content, or homogenization pressure. This was attributed to increased molecular interactions within the food matrix, including binding between sodium ions and protein groups and network interactions contributing to matrix structural order. Increasing homogenization pressure decreased the particle size of the dispersed lipid droplets, increasing the protein-stabilized interfacial surface area, the dispersion of active filler particles, and matrix strength. Increasing protein, fat, or salt content or homogenization pressure increased firmness and decreased elasticity.

Saltiness perception had significant positive correlation with sodium mobility and matrix elasticity, and significant negative correlation with dry matter content, sodium binding, and matrix firmness. These properties had similar correlations with syneresis texture, indicating that

saltiness perception may be closely related to serum release and factors affecting aqueous sodium distribution and mastication. Principle component analysis indicated that fat-containing samples prepared with the same formulation but increased homogenization pressure showed trends of increased firmness and relative 'bound' sodium and decreased salty taste and elasticity. While cluster analysis indicated that formulation may have a more significant effect than homogenization pressure in determining saltiness perception, adjusting processing variables such as homogenization pressure may be a useful tool to alter matrix interactions in conjunction with formulation changes.

Future research could explore competitive binding between sodium ions and other introduced species. Relative 'bound' sodium was found to have a significant negative correlation with salty taste for samples with the same total sodium content, suggesting that reducing the 'bound' sodium fraction may result in increased salty taste. This could be achieved by introducing other ionic species to interact with the matrix in lieu of sodium, resulting in more 'free' sodium. The 'bound' components may be less available for sensory perception, so salt replacers with less desirable sensory properties could have their detrimental impact reduced. Optimizing temporal salt introduction into the matrix could also be explored, such as by introducing portions of salt into the system after the bulk of the matrix network has already been established. This may allow for relatively more 'free' sodium that does not have mobility reduced by entrapment within the network structure, as well as a more heterogeneous sodium distribution with elevated sodium concentrations in some regions.

Modifying the composition and processing parameters of lipoproteic food products influences molecular interactions, matrix structure, and sensory properties. This area of research

may provide effective methods for reducing sodium content to reduce health risks while satisfying consumer quality expectations.

Appendix A. ^{23}Na NMR Spectroscopy Protocol for Model Gel Analysis

Adapted from Defnet (2015)

‘_____’ = type and hit Return on keyboard
[_____] = click button with mouse
(_____) = notes/comments about command

- Insert sample
    - Log in to ChemFOM using username and password on login computer
    - Walk back to NMR computer
    - Insert NMR tube into plastic casing
        - *Make sure sample is centered in opening (will affect tuning)
    - ‘e’ (ejects sample, shouldn’t be a sample already in there)
    - Insert NMR tube in plastic casing in NMR
    - ‘i’ (insert) (wait for click)
    - ‘logon’
    - ‘directory name’ (don’t actually type ‘directory name’ – type whatever yours actually is)
- Tune (^{1}H first, then ^{23}Na)
    - [Main Menu]
    - [Setup]
    - [Nuc, Solv]
    - [H1]
    - [D2O] (even if there isn’t D2O in sample)
    - [Acqi]
    - [Lock]
    - [Off] (because there isn’t any D2O in the sample – D2O locks the magnetic field, so if no D2O, record Z0 and turn off lock; Best to use at least 10% D2O if possible to stabilize chemical shifts; should also use at least a little H2O so can autoshim – otherwise have to shim manually)
    - [Close]
    - ‘su’
    - Follow instructions on diagram for which cables to move where
        - Disconnect 1H cable, connect end attached to NMR to PROBE TUNE INTERFACE
        - Disconnect cable connected to OUTPUT and connect to TUNE OUTPUT
        - Press + button to change channel from 0 to 1 on the TUNE INTERFACE
        - Use red tune and match knobs on NMR probe to reduce reflected power number to 0 (or at least under 5)
        - Press the – button to change channel from 1 to 0
        - Reattach cables to initial positions
        - Move cable attached to OUTPUT on left-hand side to TUNE OUTPUT
    - ‘autotune’
    - ‘Na23’
    - Hit Return key on keyboard again

    - Wait for the message in the command line of VNMR to say ‘Ok… ‘ to indicate tuning is complete
        - X-channel autotune cables will change, creating a whirring sound – watch to make sure cables don’t fall out, and tell someone if they do
    - If the TUNE INTERFACE light is still on (it probably will be), push + button to change to channel 1, then push the – button to change it back to 0 (the light should go off)
    - Move cable back to original position
- To collect ^{1}H spectrum
    - ‘gain=’n’’
    - ‘ga’
    - Wait until you hear a beep, indicating the experiment has finished
    - ‘wft’ (weighted fourier transform)
    - ‘aph’ (autophase)
    - Use middle mouse key to autoscale
    - ‘nl’ (nearest line)
    - ‘dres’ (to determine linewidth at half height)
    - Record linewidth at half height
    - ‘svf(‘_____’)’ (to save file)
- To collect ^{23}Na spectrum
    - ‘jexp2’ (jump to experiment 2)
    - [Setup]
    - [Nuc, Solv]
    - [Other]
    - ‘Na23’
    - [D2O] (even if there isn’t D2O in sample)
    - ‘gain=’n’’
    - ‘ga’
    - Wait for experiment to finish
    - ‘aph’
    - ‘gain?’
    - Note the gain value used, but subtract 4 from it for next run
    - ‘gain=____’ (4 minus whatever the autogain number was)
    - ‘array’
    - ‘pw’
    - ‘10’
    - ‘56’
    - ‘1’
    - ‘pw[1]=15’
    - ‘d1=0.2’
    - ‘at=0.4’
    - ‘go’
    - Wait for experiment to finish
    - ‘wft’
    - ‘ai’
    - ‘aph’

- ‘da’
- ‘dssh’ (look where the peaks switch from negative to positive, estimate pw (closer to one with larger peak) – if all peaks are positive, re-do array with lower initial value (e.g. use 52 instead of 56))
- Record pw90 value
- ‘pw90=___/4’
- ‘pw=pw90’
- ‘gain=’n’’
- ‘go’
- Wait for experiment to finish
- ‘gain?’
- Set gain to 4 less than the auto gain value
- ‘gain=___’ (Use this value for all future experiments)
- ‘go’
- Wait for experiment to finish
- ‘wft’
- ‘nl’
- ‘dres’
- Record linewidth at half height

- To find T_1
  - ‘jexp3’
  - ‘mf(2,3)’ (Make sure gain and pw90 are the same from exp 2)
  - ‘dot1’
  - ‘0.001’
  - ‘0.5’
  - ‘1’
  - ‘gos(‘_____’) (Fill in blank with file name) (This command is go and save combined)
  - ‘wft’
  - ‘aph’
  - ‘dssh’ (should have negative peaks, then positive peaks)
  - ‘dll’
  - ‘fpdc’
  - ‘t1’ (record T1 value and error)
  - Repeat procedure two more times for triplicate T_1 measurements

  OR (If you have already measured this parameter using other samples)
  - ‘jexp3’
  - [Main Menu]
  - [File] (Find a previous T1 data file, click on that file)
  - [Load]
  - ‘wft’
  - ‘pw90=____/4’ (use same value as exp 2)
  - ‘pw=pw90’
  - ‘gain=_____’ (use same value from exp 2)
  - ‘gos(‘_____’) (Fill in blank with file name) (This command is go and save combined)

- ‘wft’
- ‘aph’
- ‘dssh’ (should have negative peaks, then positive peaks)
- ‘dll’
- ‘fpdc’
- ‘t1’ (record T1 value and error)
- Repeat procedure two more times for triplicate T_1 measurements

- To find T_2
  - ‘jexp4’
  - ‘mf(2,4)’ (Make sure gain and pw90 are the same from exp 2 and 3)
  - ‘doT2’
  - ‘d2=0.0002’
  - ‘nt=1’
  - ‘bt=0.000375, 0.0005, 0.0075, 0.0009, 0.0015, 0.0022, 0.003, 0.0045, 0.006, 0.008, 0.01, 0.012, 0.015, 0.018, 0.021, 0.024, 0.028, 0.032, 0.036, 0.04, 0.048, 0.058, 0.068, 0.078, 0.088, 0.096, 0.015, 0.0192, 0.0384, 0.0768, 1.536’
  - ‘gos(‘_____’)’ (put whatever you want the file name to be in the blank)
  - ‘aph’
  - ‘dssh’ (when finished – should look like decay curve)
  - ‘ds(1)’
  - [Th] (make sure line is only going through one peak)
  - ‘dll’
  - ‘fpdc’
  - ‘t2’ (record T2 value and error)
  - Repeat procedure two more times for triplicate T_2 measurements

  OR (If you have already measured this parameter using other samples)
  - ‘jexp4’
  - [Main Menu]
  - [File] (Find a previous T2 data file, click on that file)
  - [Load]
  - ‘wft’
  - ‘pw90=____/4’ (use same value as exp 2 and 3)
  - ‘pw=pw90’
  - ‘gain=_____’ (use same value from exp 2 and 3)
  - ‘gos(‘_____’) (Fill in blank with desired file name) (This command is go and save combined)
  - ‘aph’
  - ‘dssh’ (when finished – should look like decay curve)
  - ‘ds(1)’
  - [Th] (make sure line is only going through one peak)
  - ‘dll’
  - ‘fpdc’
  - ‘t2’ (record T2 value and error)
  - Repeat procedure two more times for triplicate T_2 measurements
- To array tau (in order to calculate tau opt)

- ‘jexp5’
- ‘mf(2,5)’
- ‘dqft2’
- ‘delta=10’
- ‘array’
- ‘tau’
- ‘25’ (or however many tau values you want to array)
- ‘0.0001’ (starting value)
- ‘0.002’ (increment)
- ‘il=’y’’
- ‘nt=256’
- ‘gos(‘_____’) (insert desired file name into blank)

OR (If you have already measured this parameter using other samples)

- ‘jexp5’
- [Main Menu]
- [File] (Find a previous data file, click on that file)
- [Load]
- ‘wft’
- ‘pw90=____/4’ (use same value as exp 2 and 3)
- ‘pw=pw90’
- ‘gain=_____’ (use same value from exp 2 and 3)
- ‘gos(‘_____’) (insert desired file name into blank)

- Set up 3 replicates of sodium spectrum (while tau opt is running)
  - ‘jexp2’
  - ‘nt=1024’
  - ‘gos(‘_____’) (fill in blank with desired file name)
  - ‘jexp6’
  - ‘mf(2,6)’
  - ‘gos(‘_____’)’
  - ‘jexp7’
  - ‘mf(2,7)’
  - ‘gos(‘_____’)’
- Set up 3 replicates for dqft2 peak (While waiting for tau array to finish, you can look at the tau array and estimate the optimum tau value – look at highest peak and up to two values around it that could also be the optimum)
  - ‘jexp5’
  - ‘wft’
  - ‘dssh’
  - ‘da’
  - ‘dssl’ (once all peaks are collected, look at which peak is highest)
  - ‘jexp8’
  - ‘mf(5,8)’
  - ‘tau=_____, _____, _____’
  - ‘nt=1024’ (make sure this matches the nt value for the sodium spectra)
  - ‘il=’n’’
  - ‘gos(‘_____’)’

    - ‘jexp9’
    - ‘mf(8,9)’
    - ‘gos(‘_____’)’
    - ‘jexp10’
    - ‘mf(8,10)’
    - ‘gos(‘_____’)’
- Once all experiments are complete:
    - ‘e’ (ejects sample)
    - ‘i’ (don’t have to insert another sample)
    - ‘logoff’
    - Log off of ChemFOM computer

Literature Cited

Defnet E. 2015. Investigation of sodium binding through implementation and application of single- and double-quantum filtered 23Na NMR spectroscopy. University of Illinois at Urbana-Champaign, Urbana, Illinois.

Appendix B. Particle Size Analysis Data

Table B.1 Dispersed particle size (d_{43}) for emulsion samples**.**

Sample	d_{43} (nm)	
8-11-1.5-14	845.7 ± 16.0	ab
8-11-1.5-55	381.9 ± 12.0	d
8-11-3.5-14	876.2 ± 32.2	a
8-11-3.5-55	342.9 ± 17.7	d
8-22-1.5-14	791.7 ± 20.8	c
8-22-1.5-55	360.7 ± 5.3	d
8-22-3.5-14	848.4 ± 21.9	ab
8-22-3.5-55	354.4 ± 9.0	d
16-11-1.5-14	784.3 ± 32.2	c
16-11-1.5-55	204.3 ± 7.7	e
16-11-3.5-14	805.9 ± 65.7	bc
16-11-3.5-55	219.3 ± 5.9	e

Sample code represents [Protein (% w/w)]-[Fat (% w/w)]-[NaCl (% w/w)]-[Homogenization pressure (MPa)]. Results are expressed as mean ± standard deviation (n = 3). Values denoted with different letters were significantly different ($\alpha = 0.05$).

Appendix C Rheometer Protocol for Model Gel Analysis

'XXX' → 'YYY' → 'ZZZ' = File/tab/command paths in TRIOS software

- Start up
  - Open compressed air lines
  - Turn on ARES-G2 rheometer
    - Set air flow to Peltier system to 5 L/min.
  - Set environmental controls
    - Turn on circulating bath and set to 25.0 °C
    - Using ARES-G2 touchscreen, select 'Temp Control'
    - Click 'Temp Enable'
    - Temperature = 25.0 °C
    - Click 'Set Temp'
  - Turn on computer, log in, open TRIOS software
- Install sample geometry
  - Install lower parallel plate and thermocouple
  - Install upper 25 mm stainless steel
  - 'File Manager' → 'Geometries'
    - Select '25mm parallel plate, Stainless steel, serrated'
    - Otherwise use the 'Add New Geometry' wizard function to install the desired probe geometry
  - In the 'Geometries' subsection, verify or enter:
    - Diameter = **25** mm
    - Gap = **0.5** mm
    - Loading gap = **15.0** mm
    - Trim gap offset = **0.025** mm
    - Material = **Stainless steel, serrated**
  - Zero the fixture
- Load the sample
  - Click the 'Go to Loading Gap' icon in the probe menu
  - Center the gel sample on the lower parallel plate
  - Click the 'Go to Trim Gap' icon, verify the sample is centered, and trim excess sample from around the top sample plate
  - Click the 'Go to Sample Gap' icon
- Conduct Amplitude Sweep and verify Linear Viscoelastic Region
  - 'File Manager' → 'Experiments' → 'Sample'
    - Under 'Name' enter a unique sample/experiment name
  - 'File Manager' → 'Experiments' → 'Geometry'
    - Verify geometry information entered previously
  - 'File Manager' → 'Experiments' → 'Procedure'
    - If running a previously established experiment, use the 'Open Procedure file' icon to load the experiment.
    - Otherwise, use the 'Append Default Step' to add steps until there are 2 total steps and edit each step as follows:
      - Step 1: Conditioning Sample

        - Temperature = **25** °C
        - Soak Time = **180.0** s
        - Wait For Temperature = ☑
      - Step 2: Oscillation Amplitude
        - Temperature = **25** °C
        - Soak Time = **0.0** s
        - Frequency = **1.0** Hz
        - Sweep = **Logarithmic sweep**
        - Strain % = **0.01** to **10.0**%
        - Points per decade = **10**
    - Click the 'Start' icon in the 'Experiment' tab
    - When experiment is done identify Strain % and Stress
      - 'File Manager' → 'Results' → 'Amplitude – 1'
      - Double click the variable label on the y-axis
        - X1 = $\hat{\gamma}$ (%)
        - Y1 = η^* (Pa.s)
        - Y2 = $\hat{\sigma}$ (Pa)
      - Select LVR Strain % (%) and LVR Stress (Pa) within the linear viscoelastic range (<10% deviation of η^*)
- Conduct Creep Compliance/Recovery test
  - 'File Manager' → 'Experiments' → 'Sample'
    - Under 'Name' enter a unique sample/experiment name
  - 'File Manager' → 'Experiments' → 'Geometry'
    - Verify geometry information entered previously
  - 'File Manager' → 'Experiments' → 'Procedure'
    - If running a previously established experiment, use the 'Open Procedure file' icon to load the experiment.
    - Otherwise, use the 'Append Default Step' to add steps until there are 5 total steps and edit each step as follows:
      - Step 1: Conditioning Sample
        - Temperature = **25** °C
        - Soak Time = **180.0** s
        - Wait For Temperature = ☑
      - Step 2: Conditioning Transducer
        - Motor State/Equilibration Delay = ☑
        - Motor State = **Locked**
        - Equilibration time = **300.0** s
      - Step 3: Conditioning Stress Control
        - Run and Calculate = ⊙
        - Temperature = **25** °C
        - Soak Time = **0.0** s
        - Strain % = **[Insert LVR Strain % from Amplitude Sweep]**
        - Save stress control PID file = ☑
        - Stress control PID file path = **[Insert a unique sample/experiment file path]**
      - Step 4: Step (Transient) Creep

    - Temperature = **25** °C
    - Soak Time = **60.0** s
    - Wait For Temperature = ☑
    - Duration = **180.0** s
    - Stress = **[Insert LVR Stress from Amplitude Sweep]**
    - Sampling = **Linear**
    - Sampling rate = **1.0** pts/s
- Step 5: Step (Transient) Creep
    - Temperature = **25** °C
    - Soak time = **0.0** s
    - Duration = **300.0** s
    - Stress = **0.0** Pa
    - Sampling = **Linear**
    - Sampling rate = **1.0** pts/s